*In Hypertension do smaller holes in arterial internal elastic lamina lead to fewer routes for myoendothelial junctions and hence less EDHF response?*

**Claire Hamill**

*A thesis submitted for the degree of Ph.D. (November 2009)*


**UNIVERSITY *of* GLASGOW**

Division of Integrated Biology
Faculty of Biomedical & Life Sciences

University of Glasgow
Glasgow, Scotland.
G12 8QQ

## Abstract

The work presented in this thesis describes the influence of the endothelium on smooth muscle cells, and how the structure of the internal elastic lamina (IEL) affects this relationship in mesenteric and saphenous arteries. This was enabled by the study of functional and confocal microscopy dye transfer experiments. Normotensive (WKY) and hypertensive (SHR) rats of 12 weeks and 6 months of age were used to assess the effect of hypertension and ageing on endothelial and smooth muscle cell communication.

The endothelium-derived hyperpolarising factor (EDHF) response in mesenteric arteries was investigated using wire myography, and the involvement of myoendothelial gap junctions (MEGJs) was assessed using the putative gap junction inhibitor carbenoxolone. Carbenoxolone attenuated the EDHF response in the WKY, suggestive of the involvement of myoendothelial gap junctions in EDHF. In the saphenous artery, incubation with L-NAME and indomethacin abolished the relaxation to ACh, indicating that there was no EDHF response in this artery.

Dye transfer experiments using luminally loaded calcein-AM and the gap junction blocking peptides (GJi) $^{37,43}$Gap27 and $^{40}$Gap27 in mesenteric arteries demonstrated that the dye moved from endothelial cells to smooth muscle cells by means of gap junctional transfer in the WKY. In the SHR, calcein staining in the smooth muscle showed a significant reduction to that observed in the WKY at both age points (with endothelial cell staining remaining constant between strains), and GJi incubation did not reduce smooth muscle cell staining from that of the control. Dye transfer was correlated with the EDHF function of the vessels, and was consistent with the increasing evidence supporting the role of MEGJS in the EDHF response. No conclusive evidence could be obtained from saphenous artery imaging of dye transfer or fenestrae area due to its unsuitability for this approach. However, functional experiments illustrated this artery (reported to have a lack of MEGJs) to be devoid of an EDHF response, thereby making it a potential control artery for the mesenteric artery.

Differences in the organisation of elastin in the IEL were assessed by measurement of fenestrations in the IEL, which are the only points through

which endothelial and smooth muscle cells can connect. In WKY, the fenestrae appeared to fuse with age, causing a parallel increase in fenestrae area and decrease in fenestrae number which was not apparent in the SHR due to the inability of fenestrae to fuse in this strain. The smaller fenestrae area in the 6 month old SHR is thought contribute to the reduced EDHF response compared with WKY.

Collectively, the results of this study imply that there is a relationship between the EDHF response and myoendothelial coupling within an artery. EDHF response and smooth muscle cell staining following luminal calcein-AM application were reduced in the 6 month old SHR compared with aged-matched WKY. The smaller fenestrae in the IEL of the 6 month old SHR is a possible explanation as to why there is reduced cellular coupling, as this would restrict the passage of substances or charge between the endothelium and smooth muscle, be it by gap-junctional transfer or by diffusion.

# Table of Contents

## List of Tables

## List of Figures

## Acknowledgements

I would like to thank Professor McGrath for the opportunity to work in his lab and making my PhD a brilliant experience. You've been a great supervisor and always been interested in what I've had to say.

I've thoroughly enjoyed my time in the lab and thanks to Laura, Joyce, Anne and Melissa (as well as Arnold, Steve and Molly), it has been a welcoming place to work. Anne, I've liked our early morning blethers and your one-liners; and you never fail to point me in the direction of any free food going in the building. Thanks to Laura (my in house agony aunt), for being so positive, never losing the rag at my daily questioning, and dragging my backside to circuits on a Tuesday night. I'm grateful to Joyce for always going out of her way to help- her years of lab experience means she knows *everything*, and her enthusiasm for science and work is totally infectious. I'm so glad you don't know how to retire properly; it wouldn't have been the same without you (and biscuits). Thanks also go to Dr Daly for introducing me to the delights of the confocal microscope, on which I spent many a happy hour!

Big thanks go to my friends for being the nicest bunch of people you could meet and always being about for a cuppa tea or a drink. Cheers to Holly for plonking me in the sea or on a bike at weekends and plying me with the odd haggis supper. John Martin, I won't embarrass you but you deserve a mention *snooklehoneypiesugarbun* (kidding!). Ellen, it's been great meeting up for well needed lunchtime rants and laughs.

My mum deserves a big hug for all she's put up with and done for me over the years (and has unwittingly learnt an abnormal amount about the cardiovascular system for a middle-aged woman!); and my wee sisters too for looking after me in their own "special" ways. And in memory of my dad- one of the cleverest people I've met… bet you never thought that helping me out with sums and reading stories would lead to a PhD- I wouldn't have been to Uni without the encouragement you gave me to try hard and do something I like ☺.

Finally, I would like to acknowledge the financial support of the British Heart Foundation.

## Author's Declaration

I hereby declare that this thesis has been composed by myself, and that the work of which it is a record has been done by myself, except where specifically acknowledged. I also confirm that it has not been submitted in any previous application for a higher degree and that all sources of information have been specifically acknowledged by means of references.

Some of the results contained in this thesis have been published in peer-reviewed journals as follows:

Hamill C, González JM, Methven L, Daly CJ, McGrath JC. Approaches to visualising myoendothelial connections using laser scanning confocal microscopy. *J Vasc Res* 2008; **45** suppl. 1:8

Hamill C, González JM, Methven L, Daly CJ, McGrath JC. Approaches to visualising myoendothelial connections using laser scanning confocal microscopy. *Basic Clin. Pharmacol. Toxicol* 2008; **102**, S5-4, 15

## Abbreviations

| | |
|---|---|
| ACh | Acetylcholine |
| ANOVA | Analysis of variance |
| ATP | Adenosin triphosphate |
| $Ba^{2+}$ | Barium |
| BP | Blood pressure |
| CCRC | Cumulative concentration response curve |
| COX | Cyclo-oxygenase |
| Cx | Connexin |
| Da | Daltons |
| EC | Endothelial cell |
| CYP | Cytochrome P450 |
| DAB | 3,3'-diaminobenzidine |
| DAPI | 4',6-diamidino-2-phenylindole, dihydrochloride |
| EC | Endothelial cell |
| EDCF | Endothelium derived contractile factor |
| EETs | Epoxyeicosatrienoic acids |
| EDHF | Endothelium derived hyperpolarising factor |
| ELWD | Extra long working distance objective |

| | |
|---|---|
| $E_m$ | Excitation maximum |
| GJi | Gap junction inhibitor |
| $H_2O_2$ | Hydrogen peroxide |
| IEL | Internal elastic lamina |
| $IK_{Ca}$/KCa3.1 | Intermediate conductance calcium-activated potassium channels |
| $K^+$ | Potassium ion |
| KCl | Potassium chloride |
| L-NAME | Nω-Nitro-L-arginine-methyl ester |
| LSCM | Laser scanning confocal microscopy |
| MCA | Middle cerebral artery |
| MEGJ | Myoendothelial gap junction |
| MRA | Mesenteric resistance artery |
| mM | Millimolar |
| MOPS | 3-morpholinopropanesulphonic acid |
| nM | Nanomolar |
| NO | Nitric oxide |
| NOS | Nitric oxide synthase |
| PBS | Phosphate buffer solution |
| PE | Phenylephrine |

| | |
|---|---|
| $pEC_{50}$ | Negative value of log concentration of agonist producing a half-maximal response |
| PSS | Physiological salt solution |
| SEM | Standard error of the mean |
| SHR | Spontaneously hypertensive rats |
| $SK_{Ca}$/KCa2.1 | Small conductance calcium-activated potassium channels |
| SMC | Smooth muscle cell |
| TEA | Tetraethylammonium |
| TRAM-34 | 1-[(2-Chlorophenyl)diphenylmethyl]-1H-pyrazole |
| TRPV4 | Transient receptor potential vanilloid subtype 4 channel |
| WKY | Wistar Kyoto rats |
| µM | Micromolar |

# Chapter 1 General Introduction

## 1.1 Endothelial and smooth muscle cell communication

Endothelial cells connect with smooth muscle cells through fenestrae in the internal elastic lamina (IEL), which is an elastic membrane that separates the two vascular layers. These myoendothelial connections are thought to contribute to the endothelial control of the smooth muscle cells and hence dilation of the vessel. In spontaneously hypertensive rats (SHR) the mesenteric resistance arteries have been found to have smaller fenestrae in the IEL compared with the WKY normotensive strain (Briones *et al.*, 2003; Gonzalez *et al.*, 2006). It is hypothesised that in the SHR the decreased fenestrae size limits the number of myoendothelial connections able to form, therefore limiting dilation of the resistance arteries and causing an increase in blood pressure.

### *1.1.1 Endothelium-Derived Relaxation Factor (EDRF)*

It had long been known that the tone of vascular smooth muscle could be influenced by circulating hormones in the bloodstream such as adrenaline, angiotensin or vasopressin; or by release of mediators from nerve terminals in the arterial wall before it was appreciated that factors released from endothelial cells themselves could regulate vessel tone. Prostacyclin was the first of these mediators to be found during the study of arachadonic acid metabolism in the artery wall (Moncada *et al.*, 1976). The subsequent discovery of endothelium-derived relaxation factor (EDRF) in 1980 by Furchgott and Zawadzki (Furchgott & Zawadzki, 1980) gave the endothelium an important role in vascular physiology, and illustrated that it was not just a passive barrier between the plasma and the vessel wall. They found that the endothelium was essential in the relaxation of arterial smooth muscle by acetylcholine (ACh), and proposed that ACh acted on muscarinic receptors on the endothelial cells to stimulate the release of a substance that caused relaxation of the vascular smooth muscle. The later discovery that EDRF was nitric oxide (NO) (Palmer *et al.*, 1987) is now fundamental to our understanding of blood vessel function with the idea that NO release influences blood vessel tone and opposes vasoconstriction. Constitutive NO release has been shown to occur in certain vascular beds (Martin *et al.*, 1986).

The biological precursor of NO was established as L-arginine (Palmer *et al.*, 1988a), an amino acid usually present in excess in the endothelial cytoplasm. An

understanding of the NO pathway made it possible to develop inhibitors of its enzymatic generation (Palmer *et al.*, 1988b; Rees *et al.*, 1989; Rees *et al.*, 1990), including L-NAME and L-NMMA which have come to be commonly used experimental tools for excluding nitric oxide synthase (NOS)-derived NO from a preparation.

### *1.1.2 Mechanism of NO relaxation*

The action of relaxatory substances such as ACh, bradykinin, or substance P on receptors on the endothelium causes an increase in intracellular calcium which can bind calmodulin to form a calcium-calmodulin complex. This complex is capable of converting the nitric oxide synthase (NOS) enzyme from its inactive to its active form (Busse & Mulsch, 1990), which converts L-arginine to citrulline plus NO in the presence of molecular oxygen and NADPH. The NO produced in the endothelial cell then diffuses to the smooth muscle where it binds the haem moiety of the basal soluble guanylate cyclase enzyme. This converts the soluble guanylate cyclase enzyme to its activated form, which in turn converts GTP to cGMP, resulting in relaxation of the smooth muscle (Rapport & Murad, 1983). An increase in cGMP in the smooth muscle can result in relaxation by: inhibiting calcium entry to the cell, thereby reducing intracellular calcium concentration; activating potassium channels causing hyperpolarisation and relaxation; or stimulating a cGMP-dependent protein kinase that activates myosin light chain phosphatise (Carvajal *et al.*, 2000).

ACh has been demonstrated to hyperpolarise and relax vascular smooth muscle in guinea pig uterine arteries (Tare *et al.*, 1990). This relaxation and hyperpolarisation observed was decreased in the presence of L-NAME, which showed that NO was capable of hyperpolarising the smooth muscle in this artery. In rat middle cerebral arteries, hyperpolarisations to ACh were sensitive to glibenclamide, which inhibits ATP-sensitive potassium ($K_{ATP}$) channels (Standen *et al.*, 1989). In the rat mesenteric artery, Garland and McPherson showed that NO could produce hyperpolarisation which was abolished by glibenclamide, and that this was a different mechanism from the hyperpolarising response to ACh, which was blocked by a combination of apamin and charybdotoxin (Garland & McPherson, 1992). This suggested that the $K_{ATP}$ channels located on the smooth

muscle cells were responsible for the NO-induced hyperpolarisation of the vascular smooth muscle.

### *1.1.3 Endothelium-Derived Hyperpolarising Factor (EDHF)*

The finding that the muscarinic agonist carbachol could hyperpolarise the smooth muscle cells of guinea pig mesenteric artery, only when the endothelial layer was present, led to the hypothesis that there was a factor released from the endothelial cells which had the property of hyperpolarising the smooth muscle cells (Bolton *et al.*, 1984). In these experiments the membrane potential was recorded in the smooth muscle cells of the small mesenteric artery from guinea pig, and changes in artery length were measured on helical strips of artery. Carbachol inhibited the shortening of helical strips by noradrenaline or raising extracellular potassium concentration, and removal of the endothelium abolished this inhibitory effect of carbachol. Removal of the endothelium also changed the hyperpolarising response to carbachol observed during control conditions to a depolarisation. The hyperpolarisation observed by Bolton and colleagues was endothelium-derived, however the phrase endothelium-derived hyperpolarising factor was not coined until a later date (Taylor & Weston, 1988).

It was later found that when NO and prostacyclin production were blocked pharmacologically, stimulation of the endothelium by ACh or bradykinin could still cause a hyperpolarisation and hence relaxation of vascular myocytes (Chen *et al.*, 1988; Taylor & Weston, 1988; Garland & McPherson, 1992). This observation provided evidence for the existence of another endothelium-dependent relaxation factor, distinct from NO and prostacylin, christened endothelium-derived hyperpolarising factor (EDHF) due to its hyperpolarising effect on the membrane. The cause of this hyperpolarisation which is transmitted to the smooth muscle cells from the endothelium has yet to be classified, despite extensive research since its discovery, but has been termed generally as endothelium-derived hyperpolarising factor (EDHF). There are many candidates for EDHF including: potassium ions; hydrogen peroxide; metabolites of arachadonic acid; or products of lipoxygenases, to name only a few, but agreement over its nature has not been reached and it is now thought that a universal EDHF is unlikely.

## *1.1.4 EDHF Candidates*

### 1.1.4.1 Potassium ions

It has been proposed that $K^+$ efflux through $IK_{Ca}$ or $SK_{Ca}$ during endothelial hyperpolarisation can act directly on adjacent smooth muscle as EDHF and cause relaxation, meaning $K^+$ itself is EDHF. Edwards and colleagues demonstrated that EDHF hyperpolarisation of smooth muscle and the subsequent relaxation of small resistance arteries (hepatic and mesenteric) in rats were inhibited by a combination of ouabain and barium ($Ba^{2+}$) (Edwards *et al.*, 1998). Ouabain blocks the $Na^+/K^+$ ATPase, and $Ba^{2+}$ blocks inwardly rectifying $K^+$ channels ($K_{IR}$) present on the smooth muscle cells. The fact that ouabain and $Ba^{2+}$ abolish relaxations to EDHF and $K^+$ in rat hepatic artery; and antagonise, but do not abolish, the relaxations to EDHF and $K^+$ in rat mesenteric arteries, supports the theory that $K^+$ is an EDHF in rat arteries. The presence of myoendothelial gap junctions (MEGJs) is thought to account for the fact that relaxations were not completely abolished in rat mesentery by oubain and $Ba^{2+}$. The maximum $K^+$-induced relaxation of endothelium-denuded segments of mesenteric artery in the presence of oubain and $Ba^{2+}$ was less than when the endothelium was intact, probably due to the contribution of MEGJs when the endothelium is intact. The mechanism of hyperpolarisation was thought to be related to the opening of inwardly rectifying $K^+$ channels, $K_{IR,}$ (sensitive to $Ba^{2+}$) and activating a $NA^+/ K^+$-ATPase (sensitive to ouabain). However, contrasting data to this theory was found when the EDHF-induced hyperpolarisation of guinea pig internal carotid and porcine coronary arteries was not inhibited by a combination of $Ba^{2+}$ and ouabain (Quignard *et al.*, 1999). Nevertheless, a common feature of the EDHF response in all these arteries was its antagonism by the toxin mixture of apamin and charybdotoxin. It was found that incubation of the guinea pig internal carotid artery with carbenoxolone, a putative gap junction inhibitor, abolished the hyperpolarisation to ACh in this artery. This suggested that electronic propagation via MEGJs could be the only mechanism underlying the EDHF response in the guinea pig internal carotid artery (Edwards *et al.*, 1999), confirming that $K^+$ was not a universal EDHF in all arteries.

### 1.1.4.2 Hydrogen Peroxide

Hydrogen peroxide ($H_2O_2$) has been shown to be an EDHF in certain vascular beds. Catalase, a specific inhibitor of $H_2O_2$, inhibits EDHF-mediated relaxations and hyperpolarisations in mice mesenteric arteries (Matoba *et al.*, 2000). Endothelial Cu,Zn-superoxide (SOD) dismutase plays an important role in the synthesis of $H_2O_2$ in mesenteric arteries of mice (Faraci & Didion, 2004). It has been shown that in Cu,Zn-SOD knockout mice, the EDHF-mediated relaxations and hyperpolarisations are reduced in mesenteric arteries and coronary microvessels compared with control mice, without a change in the vasodilator properties of the smooth muscle (Morikawa *et al.*, 2003). In addition, supplements of the SOD mimetic Tempol restored the EDHF-mediated responses in these Cu,Zn-SOD knockout mice. Conversely, in isolated guinea-pig carotid artery it was found that hyperpolarisation of the vascular smooth muscle was not affected by catalase, indicating that hydrogen peroxide is unlikely to contribute to EDHF in this artery (Gluais *et al.*, 2005).

### 1.1.4.3 Epoxyeicosatrienoic acids

Epoxyeicosatrienoic acids (EETs) are arachadonic-acid-derived products of cytochrome P450 (CYP) epoxygenases which increase the open-state probability of $BK_{Ca}$. Most evidence for EETs as EDHF has been obtained from bovine, porcine, canine and human *coronary* arteries (Flemming & Busse, 2006). In bovine coronary arteries it was found that the CYP inhibitors SKF 525A and miconazole inhibited relaxations and hyperpolarisations to methacholine (Campbell *et al.*, 1996). These relaxations and hyperpolarisations to methacholine were also inhibited by tetraethylammonium (TEA), an inhibitor of calcium-activated potassium channels, and by high potassium (20mM). Arachadonic acid relaxed precontracted coronary arteries and this was blocked by TEA, charybdotoxin and high potassium. 14,15-EET, 11,12-EET, 8,9-EET, and 5,6-EET relaxed precontracted coronary arteries and relaxations were attenuated by TEA, charybdotoxin and high potassium (Campbell *et al.*, 1996). A canine *in-vivo* study demonstrated that the epicardial coronary artery dilation induced by ACh or arachadonic acid was abolished by a combination of clotrimazole (an inhibitor of several isoforms of cytochrome P450 mono-oxygenases) and the nitric oxide synthase inhibitor L-NNA, indicating that EETs were an EDHF in this artery *in-*

*vivo*. However, EETs are not an EDHF in all arteries; for instance it has been shown that EETs are not an EDHF in the rat hepatic artery (Zygmunt *et al.*, 1996). In these experiments extracellularly-applied EETs did not produce relaxation, and 17-Octadecynoic acid (a suicide-substrate inhibitor of the cytochrome P450 mono-oxygenases) had no effect on the relaxations mediated by EDHF, causing the authors to conclude that EDHF is not an EET in the rat hepatic artery.

### *1.1.5 Mechanism of EDHF relaxation*

The application of a muscarinic agonist to the endothelium causes a rise in endothelial calcium ions ($Ca^{2+}$) (Peach *et al.*, 1987) and thus hyperpolarisation due to the opening of calcium-activated potassium channels of small ($SK_{Ca}$) and intermediate ($IK_{Ca}$) conductance, and efflux of positively charged potassium ions from the cell (Edwards *et al.*, 1998). This hyperpolarisation generated in the endothelium spreads to the underlying smooth muscle cell layer, by an unknown means, and causes dilation of the artery (Busse *et al.*, 2002).

Voltage sensitive $Ca^{2+}$ channels (VSCCs) open during *depolarisation* of vascular smooth muscle and allow entry of extracellular $Ca^{2+}$, which subsequently causes contraction. *Hyperpolarisation* of the vascular smooth muscle reduces the probability of the voltage-gated $Ca^{2+}$ channels being in the open state, thus causing a fall in cytoplasmic free $Ca^{2+}$ levels, leading to reduced contractility of the smooth muscle and hence relaxation (Nelson *et al.*, 1990). It is by these means that EDHF causes relaxation of the artery. The endothelium also releases a contractile peptide, endothelin, which initiates the opening of voltage-dependent $Ca^{2+}$ channels (Neylon, 1999); therefore EDHF and endothelin may operate as physiological antagonists.

The method by which the EDHF is transmitted from the endothelium to the smooth muscle cells is debatable and several methods have been proposed:

- Direct cell to cell contact between the endothelial and smooth muscle cells exists, through which ions and small molecules (<1 kDa in size) can pass. This allows electrical or chemical signals to pass between the coupled cells.

- A substance is released from the endothelial cells, which diffuses to the smooth muscle cells.

The evidence supporting each of these pathways for relaxation varies in each part of the vasculature. However, a common feature of an EDHF response is the ability to block it with inhibitors of the calcium-activated potassium channels located on the endothelial cells ($SK_{Ca}$ and $IK_{Ca}$); such as apamin in combination with charybdotoxin or TRAM-34 (Garland & McPherson, 1992).

Apamin is a toxic octadecapeptide that was first isolated from bee venom and has been shown to selectively block the $SK_{Ca}$ channel (Habermann, 1984). Charybdotoxin is a 37 amino acid peptide isolated from the venom of scorpion and can inhibit both the intermediate and large conductance calcium-activated potassium channels (Garcia *et al.*, 2001). The more recently synthesised TRAM-34 is a drug that was designed to be a selective inhibitor of $IK_{Ca}$ channels (Wulff *et al.*, 2000), and is now commonly used in place of charybdotoxin to block these channels.

Stimulation of only a small number of endothelial cells by microionophoresis application of ACh caused the whole length of the artery to dilate in the hamster cheek pouch microcirculation *in vivo* (Duling & Berne, 1970), and it has been proposed that the mechanism for this phenomenon is the rapid spread of current through gap junctions (which is capable of spreading upstream against the direction of flow). The increase in intracellular calcium $[Ca^{2+}]_i$ in the endothelium occurs only in the area stimulated by ACh, whereas the cells along the whole arterial length hyperpolarize causing dilation of the entire vessel (Dora *et al.*, 2003b; Takano *et al.*, 2004). The spread of this hyperpolarisation was not caused by a diffusible factor since: it could be prevented by cutting the vessel (Takano *et al.*, 2004); and the time course of spread was at a rate much greater than diffusion or other movement of an agent could account for (Duling & Berne, 1970). This is suggestive of the propagation being electrical in nature.

### *1.1.6 Importance of EDHF increases as vessel size decreases*

Several findings have suggested that communication via gap junctions may be most important in vessels where the endothelial: smooth muscle ratio is high

(Berman *et al.*, 2002; Shimokawa *et al.*, 1996a). It has been found that the gap-junction-dependent component of relaxation is greater in the small mesenteric artery relative to aorta (Chaytor, 1998). This would fit physiologically since the smaller vessels such as mesenteric resistance arteries are important in controlling the total peripheral resistance and hence blood pressure. Furthermore, the greater the role of EDHF in vasodilatation of small vessels as compared with large vessels raises the possibility that release of EDHF may be important in the maintenance of blood pressure. This has been established by the findings that $SK_{Ca}$ and $IK_{Ca}$ knockout mice are hypertensive (Taylor *et al.*, 2003; SI *et al.*, 2006). In hypertension where there is a loss of EDHF function (Goto *et al.*, 2000), the most important sites of loss are at the resistance arteries, as this is where a loss of EDHF would be so detrimental to BP control.

### *1.1.7 Endothelium-Derived Contractile Factor (EDCF)*

In contrast to NO and EDHF whereby the endothelium exerts a relaxatory effect on the underlying smooth muscle cells, the endothelium also releases an unknown contractile factor in certain vascular beds (Vanhoutte & Tang, 2008). The first observation of EDCF was in isolated *veins* of the dog, in which endothelial cells caused the surrounding smooth muscle to contract in response to arachidonic acid and thrombin. This contrasted to the *arteries* of the same preparation where endothelial cells caused a vascular relaxation (De Mey & Vanhoutte, 1982). EDCF was also observed in the aorta of the SHR (Luscher & Vanhoutte, 1986), in which ACh caused a concentration-dependent increase in tone.

EDCF release is triggered by increases in intracellular calcium, sheer stress, muscarinic agonists, and serotonin. The release of EDCF increases in hypertension whilst the release of EDHF decreases and this contributes to endothelial dysfunction, that is, an upset in the balance of EDHF and EDCF (Vanhoutte *et al.*, 2005). EDCF is a product of arachadonic acid metabolism by the COX enzyme which is blocked by indomethacin, and has been reported to be prostaglandin H2 ($PGH_2$) and prostacyclin acting on the thromboxane-prostanoid (TP) receptors on the vascular smooth muscle cells (Vanhoutte & Tang, 2008).

## 1.2 Myoendothelial Gap Junctions

Points of direct cell to cell contact between the endothelial and smooth muscle cells coupled by a gap junction are termed myoendothelial gap junctions (MEGJs). These MEGJs are formed when projections from endothelial cells extend through fenestrations in the internal elastic lamina (IEL) and come into contact with vascular smooth muscle cells; or less commonly smooth muscle cells protrude through the IEL and come into contact with endothelial cells. Proteins in the adjacent membranes then connect to form a gap junction. The IEL is a layer of elastic tissue that acts as a barrier between the intima and media of the vessel, and the fenestrae can be likened to windows through which the two cell layers can connect. A myoendothelial bridge (or connection) means that the membrane of the endothelial and smooth muscle cell are in close apposition but does not strictly mean that the cytoplasm of the cells are coupled by a gap junction. It is for this reason that the terminology of myoendothelial connections/bridges must not be confused with MEGJs, with the prior meaning the protrusion of one cell type through the IEL, and the latter meaning the coupling of an EC and SMC via the pore of the gap junction.

Thoma first found myoendothelial bridges in coronary arteries in 1921, which led to the subsequent discovery of myoendothelial bridges in other arteries (Thoma, 1921). Prior to the identification of gap junctions on myoendothelial bridges it was thought that the points of contact between the endothelium and smooth muscle might only have provided a structural means of attaching the endothelium to the underlying vascular smooth muscle. Spagnoli and colleagues (1982) first demonstrated that myoendothelial bridges contained gap junctions: cytoplasmic bridges passing through the fenestrae of the IEL of rabbit carotid artery were imaged by electron microscopy and it was found that these bridges connected the endothelium to the first row of underlying smooth muscle in the media of the vessel. Lanthanum hydroxide (an electron dense tracer) permeated junctional areas causing pentalaminar patterns that were consistent with gap junctional structure (Spagnoli *et al.*, 1982). It was later found that heterocellualar junctions formed between cultured layers of aortic endothelial and smooth muscle cells, and that cells pre-labelled with [3H]uridine would transfer this nucleotide across the heterocellular attachment to the other cell population (Davies *et al.*, 1985). Further early evidence supporting the coupling

of EC and SMCs was provided by dye studies, whereby dye was shown to transfer from the endothelial to the smooth muscle cell following dye injection by microiontophoresis (Little et al., 1995).

Gap junctions on these myoendothelial projections are termed myoendothelial gap junctions and can also be termed heterocellular gap junctions since they join two different cell types. Similarly, homocellular gap junctions occur between cells of the same type, that is, connecting two endothelial cells or two smooth muscle cells (Figueroa & Duling, 2009). The vessel wall contains gap junctional communication both within and across the vascular layers, which may have a significant role in the co-ordination of conducted vasomotion and vascular tone (de Wit *et al.*, 2006).

### *1.2.1 Anatomical Evidence of MEGJs*

At the ultrastructural level gap junctions can be identified by an electron-dense pentalaminar structure of approximately 10nm in diameter. These ultrastructurally identified gap junctions are composed of clusters of gap junction channels, varying from a few to thousands of channels in size, and are often referred to as gap junctional plaques when viewed with freeze fracture techniques or immunohistochemistry (Rummery & Hill, 2009). Anatomical evidence for MEGJs is limited, probably due to the small size of these junctions and the difficulty in preserving them for analysis.

MEGJs have recently been observed in mouse mesenteric arteries and it was found that all of the MEGJs were located on projections that originated from the endothelial cells (Dora *et al.*, 2003a). There is other anatomical evidence of MEGJs in different vascular beds including: rat retinal arterioles (Lesson, 1979); rat glomerular arterioles (Taugner *et al.*, 1984); rat mesentery (Sandow *et al.*, 2002; Hill *et al.*, 2002); hamster feed arteries (Sandow *et al.*, 2003; Emerson & Segal, 2000); and rat middle cerebral arteries (Sokoya *et al.*, 2006).

Controversy exists over whether or not electron microscopy images show convincing evidence of gap junctions. It is however obvious that cellular projections pass through holes in the IEL and come into close apposition with the other cell type. It could be argued that even if gap junctions were not present

then the fact that these projections traverse the IEL is important in communication between the endothelial and smooth muscle layers.

### *1.2.2 Gap junction formation: connexins and connexons*

Gap junctions are formed by the docking of two hemichannels (called connexons) at points of cell to cell contact. Each hemichannel is composed of six connexin protein subunits and the interdigitation of the extracellular loops of opposing connexons creates an aqueous central pore that allows diffusion of ions and signalling molecules less than 1 kDa in size between cells (Kumar & Gilula, 1996). The connexin structure consists of four $\alpha$-helical membrane-spanning domains (M1-M4) with two extracellular loops (E1 and E2). These extracellular loops contain highly conserved cysteine residues, which are essential for the docking of the two hemichannels (Brink, 1998). Each connexin is named after its molecular weight in kDa. There are four connexins (Cx) expressed in the walls of blood vessels, namely: Cx37, Cx40, Cx43 and Cx45, and their expression varies according to vessel location and species (Figueroa & Duling, 2009).

Connexins have a half-life of between 1 and 5 hours in cultured cells, meaning cellular communication can be modulated by an up- or down-regulation of synthesis, assembly, trafficking and degradation (Segretain & Falk, 2004). This process can be likened to that of a cell surface receptor's lifecycle, whereby the responsiveness to an agonist can be modulated by receptor up- or down-regulation or internalisation. The lifetime of a gap junctional plaque may be longer than that of the channels of which it is composed (in which the connexons have a half life of only 1-5 hours) and new channels have been shown to be added to the edges of the plaques whilst old channels are removed from central areas (Jordan *et al.*, 2001).

## 1.3 Evidence for MEGJs transmitting EDHF

There is a growing body of evidence suggesting that MEGJs are at least partly, if not fully, responsible for transmitting EDHF in certain vascular beds. In order to assess the effects of gap junctions on the EDHF response, the building blocks of the gap junctions, the connexins, can be disrupted. There are two ways in which this can be done: either by using mice in which the gene for a specific connexin

has been knocked out; or by interrupting the gap junction by means of a gap junction inhibitor.

In connexin knockout mice there is a possibility of long-term compensatory mechanisms or neonatal lethality, whereas with short term connexin block these problems are avoided. However, there are difficulties with gap junction inhibitors in that the exact mechanism by which the junction is inhibited is unknown and other non-junctional effects have been reported. The putative gap junction inhibitor heptanol has been shown to cause hyperpolarisation, a decrease in intracellular calcium concentration and a decrease in tension in rat mesenteric arteries at low concentrations, and a depolarisation at high concentrations, in addition to gap junction inhibition (Matchkov *et al.*, 2004).

The fact that inhibition of gap junctions results in reduced endothelium-dependent vasodilatation (Taylor *et al.*, 1998; Goto *et al.*, 2002), coupled with the fact that hypertensive mice express a decrease in connexins (Rummery & Hill, 2004), and Cx40 knockout mice are hypertensive (de Wit *et al.*, 2000), strongly implies that gap junctions are involved in the EDHF response. Also, studies examining the incidence of MEGJs in relation to the importance of EDHF in a particular vessel have shown that there is a correlation between the two (Berman *et al.*, 2002; Shimokawa *et al.*, 1996).

### *1.3.1 The EDHF response is dependent on the presence of MEGJs in certain vascular beds*

In sandwich preparations, the SMC layer of aorta was separated from the underlying endothelium, thus removing any viable MEGJs that may have been present. It was found that in this preparation, ACh-induced relaxations of rabbit aorta and small mesenteric artery were completely abolished by L-NAME alone and no residual relaxation was present, illustrating that the relaxation was mediated exclusively by NO (Chaytor *et al.*, 1998a). This preparation demonstrates that if the endothelium and smooth muscle are parted, and the smooth muscle is then opposed with another sheet of endothelium, that only the NO mediated relaxation from the endothelium prevails and EDHF can no longer be detected. If EDHF diffused extracellularly then it should transfer from the

endothelium to the smooth muscle in sandwich preparations as NO does. This is strongly suggestive of EDHF being transmitted by MEGJs.

It was demonstrated that in the saphenous artery of juvenile WKY rats, where MEGJs were abundant, that ACh evoked a hyperpolarisation and relaxation in the presence of L-NAME and idomethacin. However, in the adult rat saphenous artery, MEGJs were found to be rare, EDHF-mediated relaxation was absent and hyperpolarisations were unstable (Sandow *et al.*, 2004). This would suggest that MEGJs have an important role in the saphenous artery in development but are not necessary in the adult saphenous artery. It also raises the question as to how these gap junctions that were present in the juvenile saphenous artery are no longer present in the same artery of the adult.

Results from the porcine coronary artery showed that non-NO and non-prostanoid-mediated endothelium-dependent relaxation required functionally intact myoendothelial junctions (Kühberger *et al.*, 1994).

In rat mesentery (where MEGJs are present) the EDHF-mediated relaxation is prominent, and in adult rat femoral artery (where no MEGJs are present) there is no EDHF-mediated relaxation (Sandow *et al.*, 2002). In this study, stimulation of rat mesentery with ACh caused hyperpolarisation of both the endothelial cells (EC) and smooth muscle cells (SMC) and pentalaminar MEGJs were found to connect the two vascular layers. Conversely, in the femoral artery, stimulation by ACh only evoked hyperpolarisation in ECs and not in SMCs, also no MEGJs were found to be present (Sandow *et al.*, 2002). In adult rat femoral and saphenous arteries only non-junctional projections were present, that is, the endothelial cells projected through fenestrae in the IEL but no gap junction was present between the membranes of the opposing endothelial and smooth muscle cells; and there was a large difference in resting membrane potential of ECs and SMCs suggesting an absence of electrical connectivity between the cell layers. The endothelial dependent relaxation observed in the femoral artery appeared to rely entirely on diffusable NO. Similar resting membrane potentials in ECs and SMCs in the mesenteric arteries were thought to be due to the transmission of electrical responses by MEGJs.

### *1.3.2 Gap junction inhibition*

Further evidence for a role of MEGJs in transmitting EDHF has been provided by studies using gap junction inhibitors such as Gap 27 and 18$\alpha$-glycyrrhetinic acid (Chaytor *et al.*, 2001; Taylor *et al.*, 1998), whereby inhibition of gap junctions has been shown to either significantly reduce or completely abolish the EDHF mediated component of relaxation. Gap 27 is a peptide that has sequence homology with the extracellular loop 2 of connexin 43 and disrupts gap junction function by an unknown mechanism.

This peptide was found to inhibit relaxation to ACh by around 40% in aorta and small mesenteric artery of the rabbit, and also attenuated the endothelium-dependent component of relaxations to ATP in aorta that were insensitive to L-NAME. In preparations of denuded endothelium, Gap 27 had no effect on the NO-mediated relaxation induced by sodium nitroprusside, thus showing that the peptide does not interfere with NO-induced relaxation. From these results it was concluded that direct cell to cell contact between endothelium and smooth muscle contributes to endothelium-dependent relaxations (Chaytor et al, 1998).

The lack of action of Gap 27 against ACh-induced relaxations in sandwich preparations showed that this peptide did not inhibit the synthesis or release of NO by the endothelium. These findings suggest that electrical coupling or diffusion of a low molecular weight mediator through the MEGJs account for the NO-independent component of relaxation, rather than the more traditional view of extracellular diffusion of an EDHF (Hutcheson *et al.*, 1999).

In rabbit iliac artery it has been shown that in the presence of indomethacin, L-NAME causes a 60-70% reduction in relaxations induced by ACh and cyclopiazonic acid (CPA). The L-NAME-insensitive component of relaxations to ACh and CPA was attenuated by 18-$\alpha$ glycyrrhetinic acid (18$\alpha$-GA), an inhibitor of gap junctional communication, suggesting that gap junctions are involved in the EDHF response in rabbit iliac arteries (Taylor *et al.*, 1998).

More recent studies have looked at the effects of the gap blocking peptides, small peptides designed to interfere with a specific extracellular loop of a connexin. Mather at al 2005 developed a new method that loaded connexin-

specific inhibitory molecules into endothelial cells within pressurised mesenteric arteries of the rat. This method relied on endocytosis and was achieved by changing luminal solution independently of the bathing solution in cycles of hypertonic and hypotonic solution. Loading otherwise cell-impermeant fluorescent dyes into the endothelial cells via the luminal surface validated this technique by demonstrating that uptake did not disrupt the tissue. This method of targeting MEGJs by loading putative gap junction blockers through the endothelium of intact vessels provided a more precise route for MEGJ blockade that did not alter the gap junctional communication within the smooth muscle layer. Using this technique in arteries maximally stimulated with phenylephrine it was found that the EDHF response was significantly reduced with antibodies and mimetic peptides directed against intracellular regions of Cx40 but not Cx37 or Cx43 (Mather *et al.*, 2005).

Gap peptides have recently been assessed in human resistance arteries (Lang *et al.*, 2007). These resistance arteries were obtained from subcutaneous fat biopsies of healthy pregnant women undergoing caesarean. It was found that L-NAME plus indomethacin reduced the maximal relaxation to bradykinin by approximately 50%; and the combination of L-NAME plus indomethacin plus three connexin mimetic peptides ($^{37,43}$Gap27, $^{40}$Gap27 and $^{43}$Gap26) almost abolished relaxations to bradykinin. It should be noted that each gap peptide is homologous to a region of the extracellular loop of the connexin whose number(s) is denoted by the superscript of its name, and hence this is the connexin it "blocks". In arteries incubated with L-NAME and indomethacin neither $^{37,43}$Gap27 or $^{40}$Gap27 alone had a significant effect on bradykinin-induced relaxation, whereas $^{43}$Gap26 caused marked inhibition that was similar to that of the triple combination of connexin mimetic peptides. It was concluded that in pregnant women, EDHF-mediated relaxation of subcutaneous resistance arteries was dependent on Cx43 and gap junctions. Immunohistochemistry demonstrated Cx37, Cx40 and Cx43 expression in the endothelial and vascular smooth muscle cells of these human resistance arteries.

Gap junction blockers added to an organ bath permits them to act on all of the specific connexins that they are directed against in the vessel; irrespective of whether these connexins are part of a homocellular or heterocellular gap junction. This results in a big assumption in that the effects observed are due to

the blockade of these connexins *only* at the MEGJ (Chaytor *et al.*, 1998a; Dora *et al.*, 1999). The gap junction blocker may be exerting effects on the endothelial-endothelial cell or the smooth muscle cell-smooth muscle cell gap junctions and this possibility is not always highlighted in papers using such drugs. In ignoring this possibility, authors are inadvertently implying that homocellular coupling is not important.

## 1.4 Hypertension

Hypertension is defined as a repeatedly elevated blood pressure exceeding 140mmHg systolic pressure and 90mmHg diastolic pressure in man (Chobanian *et al.*, 2003). It is a risk factor for strokes, heart attacks and arterial aneurysims and is a "silent" condition, meaning that symptoms can go unnoticed until a major event such as these occur. Around 90-95% of hypertensive patients have essential or idiopathic hypertension, which has no known cause. The other less commonly diagnosed type of hypertension is secondary hypertension, where high blood pressure is a consequence of another condition such as kidney disease or an adrenal medulla tumor. Treatment of essential hypertension is symptomatic, therefore it is aimed at lowering blood pressure and does not treat the underlying cause of the elevated blood pressure. Commonly used drug treatments for hypertension include: angiotensin-converting-enzyme inhibitors; angiotensin II receptor antagonists; calcium channel blockers; and diuretics (Chobanian *et al.*, 2003).

## 1.5 Role of gap junctions in hypertension

Little is known about the role of gap junctions in hypertension. However, from their role in the normal physiology of blood vessels it can be postulated that their function alters in the hypertensive state, either as a prerequisite to elevated blood pressure or as a consequence of elevated pressure. There is limited data on the connexin expression in the media of resistance arteries during hypertension, however, it has been found that expression of endothelial connexons is significantly reduced in SHR caudal and mesenteric arteries as compared with the normotensive control rats (Rummery & Hill, 2004). This would imply that the limited endothelial connexins in hypertension contributes to the elevated pressure.

Genetically modified mice with deletion of specific connexins often die or exhibit a compensatory change in the remaining connexins. However, Cx40 knockout mice have been successfully bred and have been found to be hypertensive (de Wit *et al.*, 2000).

In SHR caudal arteries the density of Cx40 decreases, and in mesenteric arteries the density of Cx37 decreases (Kansui *et al.*, 2004; Goto *et al.*, 2000). Treatment of high blood pressure with the angiotensin-II receptor antagonist candesartan has been found to restore endothelial connexin expression (Kansui *et al.*, 2004).

In mice, neither the deletion of the gene encoding endothelial NOS (eNOS) or the inhibition of NOS attenuates agonist-induced vasodilator responses *in-vivo* and *in-vitro* (in perfused hindlimb) (Brandes *et al.*, 2000), meaning that another mechanism must compensate for the lack of NO. eNOS knockout mice were shown to be hypertensive compared with wild type controls (Brandes *et al.*, 2000; Huang *et al.*, 1995), however, the dose dependent decrease in mean arterial pressure in response to bradykinin was not significantly different between the wild type and eNOS knockout mice (Brandes *et al.*, 2000). It has been argued that in mice, EDHF mediated relaxations are equally if not more important than endothelium-derived NO in responses to agonist-induced endothelium-dependent vasodilatation in resistance arteries (Busse *et al.*, 2002).

## 1.6 Structure of the Internal Elastic Lamina

The IEL of the SHR mesenteric arteries has been found to differ significantly from that of the normotensive WKY strain, with the SHR having smaller fenestrae in the IEL in adult rats (Gonzalez *et al.*, 2006). It has also been shown that spontaneously hypertensive stroke prone rats (SHRSP) have smaller fenestrae in the IEL of the carotid artery compared with normotensive controls, due to vascular remodelling (Briones *et al.*, 2003). Whether or not this remodelling is a consequence of hypertension or is already present and predisposes the SHR to be hypertensive remains debatable. It is postulated in this study that the smaller fenestrae in the SHR mesenteric arteries restricts the possibility of communication of the EDHF, be it electrical or chemical, from the endothelial cells to the vascular smooth muscle cells. The myoendothelial bridges may not

be able to traverse the smaller fenestrae and this would lead to a smaller number of MEGJs being formed in the SHR, as the fenestrae decrease in size with age. This therefore seems a reasonable explanation as to why EDHF function decreases with age in the SHR.

The fenestrae in the IEL have also been studied in rabbit arteries and these data show that the IEL was fenestrated at all ages (from 3 to 23 weeks) and the size of the fenestrae increased dramatically during postnatal development. The estimated number of fenestrae increased per vessel, however fenestrae per $mm^2$ decreased by 26%, possibly due to fusing of adjacent fenestrae as they increased in size with age (Wong & Langille, 1996). It is thought that the very small fenestrae in the immature IEL act as a protective mechanism to counteract the high endothelial permeability during development, seen as the IEL presents a barrier to transport of substances from the blood and intima to the arterial media. Also, the enlargement of the fenestrae during development allows for more contact between the endothelium and smooth muscle which is thought to cause growth arrest of endothelial cells (Wong & Langille, 1996).

### *1.6.1 Influence of Elastin on Vessel Mechanical Properties*

The main constituent of the IEL is elastin. In small arteries such as mesenteric artery, elastin is a minor component and is present only in the IEL and discrete parts of the media and adventitia. Due to the fact that elastin is scarce in the resistance arteries compared with the large conductance vessels, it has been misconstrued that elastin has no major role in the small resistance vessels. In rat mesenteric resistance arteries the intrinsic stiffness of the vessel has been found to decrease with age, and digestion of elastin with pancreatic elastase has been found to greatly increase intrinsic wall stiffness since elastin is an important determinant of arterial wall distensibility (Briones *et al.*, 2003). Normally elastin is only synthesised in embryonic and rapidly developing postnatal tissues. In embryonic development, after the mesenchymal cells surrounding the endothelial tube differentiate into smooth muscle cells, elastin appears in the extracellular matrix between cell layers (Nakamura, 1995). Elastic fibre formation then begins with the arrangement of an extracellular microfibrillar scaffold where the soluble elastin monomers tropoelastin are deposited (Daga-Gordini *et al.*, 1987). It has been shown that in rat blood vessels elastin

increases from the tenth day to the first month of life, and that by 6 months there is no further increase in elastin content (Gonzalez *et al.*, 2005). Collagen content was also quantified to assess if changes in this caused the decreased stiffness of mesenteric arteries with age and it was found that collagen content was not modified between one and six months of age in the adventitia or the media. These findings led to the conclusion that the decreased intrinsic stiffness of the mesenteric arteries between one and six months was not due to a change in content of the structural proteins collagen or elastin, but is more likely to be due to a reorganization of the arterial wall structure. This same study found that in rat MRA the IEL remodelled with age, giving rise to a gradual reduction in the thickness of the IEL and a parallel increase in the area occupied by fenestrae. These results are consistent with those found in the rabbit carotid artery during postnatal development (Wong & Langille, 1996) and suggest that the reorganisation of the IEL in rat MRA may be related to a decrease in stiffness with age.

A comparison between the middle cerebral artery (MCA) and mesenteric resistance artery, both of which have a similar size of around 250μm internal diameter, demonstrates that the differences in elastic properties between these arteries is most probably due to their different physiological roles (Briones *et al.*, 2003). The media of MCA constricts or relaxes to carefully regulate pressure, whereas the mesenteric vessels have a lower degree of myogenic constriction and the elasticity of the vessel is more important in regulating vessel dimensions. From these observations it is suggested that in resistance arteries, the way in which elastin is organised in the IEL may be an important factor in the elastic properties of the vessel. It is clear that elastin is an important component in determining vessel distensibility, therefore any differences in its structural organisation between normotensive and hypertensive rats is a worthwhile aspect to study.

## 1.7 Relationship between Fenestrae, Myoendothelial Bridges and Myoendothelial Gap Junctions

The studies examining fenestrae in the IEL have not analysed the myoendotheilal bridges passing through them. Fenestrae in the IEL are only potential sites for MEGJs; therefore assumptions cannot be made about the existence of MEGJs on

projections passing through these fenestrae without physical evidence of the junctions themselves. Early electron microscopic studies showing the protrusion of either an endothelial cell or smooth muscle cell through the IEL only stain for the presence of gap junctions but provide no insight into which connexins make up the gap junctional channel (Lesson, 1979; Taugner *et al.*, 1984). A more recent study (Sandow *et al.*, 2006b) provided evidence of connexins near the sites of fenestrae in the IEL by imaging connexin antibodies using confocal microscopy. This combined approach of visualising connexins by antibody staining and visualising fenestrae by means of elastin autofluorescence simultaneously using confocal microscopy provides a more useful way of studying the relationship between fenestrae and gap junctions. When compared at different age points for both normotensive and SHR strains, it would be possible to compare differences in both fenestrae size and connexin expression to assess if there is a change in these parameters with age or between strains.

As yet, the size of the fenestrae through which the myoendothelial bridges pass remains a fairly neglected concept. The smaller size of fenestrae shown to be present in the SHR mesenteric arteries as compared with the normotensive strain is likely to have functional consequences, whereby it affects the formation of connections between the endothelium and smooth muscle cell. This would lead to a reduced capacity for the endothelium to hyperpolarize the underlying smooth muscle, if the EDHF is indeed transmitted through MEGJs. The aim of this study is to establish the correlation between fenestrae size and age in both hypertensive (SHR) and normotensive (WKY) rats, to establish if the smaller fenestrae size found in the SHR could be a mechanism of reduced EDHF.

Although the fenestrae in the IEL and the MEGJs have been studied individually, very few studies have analysed the relationship between the two structures. It is unknown if the projections from the endothelial cell (or very rarely the smooth muscle cell) are able to fit through any size of gap in the IEL, or if a smaller size of fenestration would prevent the interaction of the two vascular layers.

The turnover of myoendothelial connections is an important concept about which very little is known. A study using dog coronary artery showed that myoendothelial contacts decreased with age, with 5.17±0.50, 1.94±0.17, and 0.33±0.09 contacts observed per 100μm inner circumference of coronary artery

for foetuses, newborns and adults respectively (Kristek & Gerova, 1997). However it must be noted that this study quantified only the myoendothelial connections and not the myoendothelial gap junctions. It is careless to assume that MEGJs are present for every myoendothelial "connection". However, clearly if the myoendothelial bridges are not present then there is no possibility of MEGJs forming since MEGJ formation requires the membranes of the endothelial and smooth muscle cell to be in close apposition.

It would be interesting to assess the effect that stress on the artery has on these myoendothelial bridges, i.e. does a higher pressure cause the bridges to be destroyed. If a vessel was visualised live using confocal microscopy and pressure myography then it is feasible that an individual bridge could be examined as the pressure was increased, and the resulting fate of the bridge observed.

To conclude, much work has been done in the field of myoendothelial bridges, their associated gap junctions and their involvement in EDHF. However, to date, there is a poor understanding of the formation/ lifecycle/ breakage of these bridges and their relationship with the fenestrae through which they pass. It is postulated that the smaller fenestrae in the IEL of the small mesenteric resistance vessels in SHRs may be related to the reduced EDHF in this strain, if EDHF is indeed transmitted by MEGJs. This study hopes to contribute to the current literature by using both WKY and SHR rats at different age points to establish the incidence of myoendothelial bridges and fenestrae size throughout development. From this information, inferences can be made about whether a loss of EDHF in the SHR with age can be attributed to a decrease in myoendothelial connections due to the already known decrease in fenestrae size with hypertension.

## 1.8 Aims

The main objectives of this research were:

(i) To establish whether differences in WKY and SHR internal elastic lamina structure exist by analysing fenestrae area and number.

(ii) To compare the contractile and relaxant responses in mesenteric and saphenous arteries of WKY and SHR rats.

(iii) To establish whether there was a relaxant response to ACh which persisted following blockade of NO and prostaglandin production in mesenteric and saphenous arteries; and to characterise this relaxation as an EDHF response using a combination of endothelial cell calcium-activated $K^+$ channel blockers.

(iv) To investigate the effect of the putative gap junction inhibitor carbenoxolone on the EDHF response.

(v) To study heterocellular dye transfer on pressure myograph-mounted vessels and to assess if this transfer was impeded by gap junction blocking peptides.

(vi) To investigate connexin location in the mesenteric and saphenous arteries of WKY and SHR by means of immunohistochemistry.

# Chapter 2 General Methods

## 2.1 Animals used

Although the focus of this work was to highlight the functional and structural differences in the mesenteric vessels of SHR and WKY strains of male *rat*, mesenteric resistance arteries (MRA) were obtained from mice in preliminary experiments to test dye suitability and concentrations for confocal work; and to perfect the art of myograph mounting small resistance vessels for functional work. The mouse mesenteric arteries were obtained from wild type mice used by others working in the laboratory. First order mouse and third order rat mesenteric arteries were used, both with a similar diameter of around 250 microns (μm).

Mesenteric and saphenous arteries were obtained from 12 week old and 6 month old WKY (control) and SHR (hypertensive) animals (Table 2.1), killed by carbon dioxide overdose. The animals were obtained from Harlan Laboratories (UK) and housed in the University Central Research Facility for at least one week prior to sacrifice. Housing conditions were: 12 hour light/dark cycle; standard rat feed chow; humidity of 45-65%; and temperature 22-25°C.

**Table 2-1 Weight and number of animals used in entire project**

| | 12 week old | 6 month old |
|---|---|---|
| **WKY** | 287 ± 3 (n=24) | 367 ± 7 (n=16) |
| **SHR** | 283 ± 6 (n=18) | 350 ± 7 (n=12) |

**Expressed as mean ± SEM in grams**

## 2.2 Dissection

### *2.2.1 Mesenteric artery dissection*

The mesenteric arcade was removed after incision of the abdominal cavity to expose and open the overlying peritoneum. The gut wall was tied with thread at both ends to prevent the propulsion of gut contents into the Petri dish and so keep the dissection as clean as possible. The mesentery was then pinned out on a Petri dish in ice-cold physiological salt solution (PSS) buffer solution, with the gut wall outermost and the arcade branching towards the gut wall from the superior mesenteric artery to the third order branches. The first order arteries were located with a dissection microscope and identified as those branching directly from the superior mesenteric artery. The third order mesenteric vessels

were located as those between the gut wall and the second order vessels in the arcade. They were cleaned of surrounding fat with ultra fine forceps, removed with small spring scissors, and stored in PSS until use.

### *2.2.2 Saphenous artery dissection*

The saphenous vein and artery were identified as those extending distally from the femoral vessels branching towards the knee (Figure 2.1).

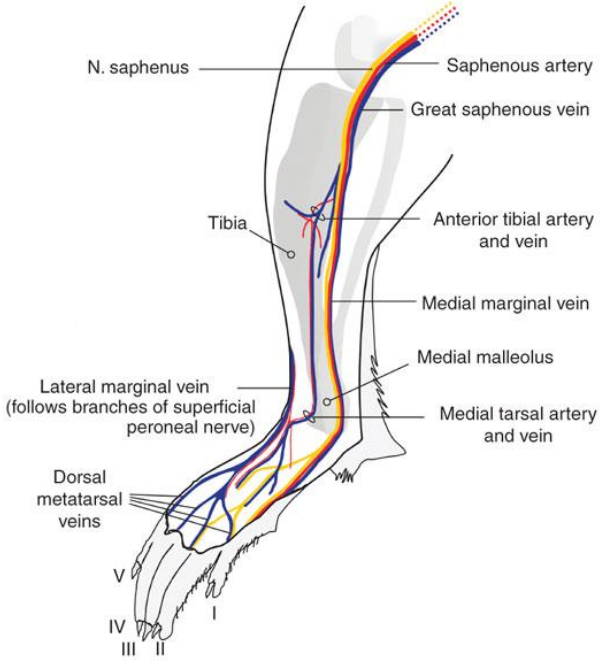


**Figure 2-1 Location of saphenous artery in rodent limb (Zimmermann *et al.*, 2009)**

These were removed from the limb together with the adjoining nerve and further dissection was performed under a microscope to remove the saphenous artery from this section. Care was taken to remove blood from the lumen of the arteries without damaging the delicate endothelium.

## 2.3 Wire Myography

Functional experiments to assess the responsiveness of vessels to various agonists were performed using a four chamber wire myograph (Danish Myotechnology, Aarhus, Denmark). Wire myography is a technique which was introduced to study vascular function *in-vitro* (Mulvany & Halpern, 1977). This advanced the study of vessels in organ baths where only larger vessels were used due to the mounting procedure not being a viable technique for small resistance

vessels. Wire myography allowed the functional responsiveness of small resistance vessels *in-vitro* to be measured, a technique used in Chapters 4 and 5.

### *2.3.1 Vessel mounting*

Following dissection, vessels were cut into 2mm segments and a 40µm stainless steel wire was carefully inserted through the vessel lumen using forceps. The vessel was then lifted with forceps, using the wire, into the myograph bath, and the jaws of the myograph brought together by adjustment of the micrometer to secure the wire in position. Metal screws anchored the wire in place and a second wire was then inserted through the vessel lumen and secured to the jaws in the same way. The fixed head of the myograph was connected to a force transducer which recorded the tension across the vessel wall under resting conditions and when challenged with various agonists (Figure 2.2).

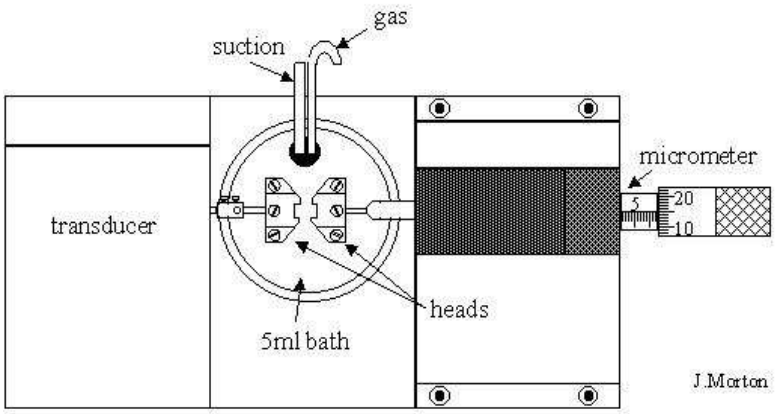


**Figure 2-2 Schematic diagram of myograph bath as viewed from above (reproduced with permission of J Morton, 2006 PhD thesis).**

A heating element on the base of the myograph warmed the baths to a constant temperature of 37°C, and baths were gassed with 95% oxygen/5% carbon dioxide. The baths were heated and twenty minutes after a temperature of 37 degrees was achieved, a resting tension of 0.25 grams force was applied to the arteries which were allowed to equilibrate for 30 minutes before the wake-up procedure was undertaken. A resting tension of 0.25 grams force was found to be optimal for both the third order mesenteric artery and the saphenous artery from previous normalisation experiments in the laboratory. Chart software (Version 5, ADInstruments, Chalgrove, UK) was used to record experiments and measure vessel responses.

### *2.3.2 Wire Myography Standard Experimental Protocols*

#### 2.3.2.1 Wake up Procedure

Vessels were equilibrated under tension for 30 minutes and then challenged with 10μM PE. The contractile response was allowed to plateau before washing with heated (37°C) PSS (three 5ml washes three times) over a 15 minute period. A second application of 10μM PE was administered 10 minutes after the end of the prior washout and a contraction similar in size to the first was obtained in viable vessels. To assess endothelial function, ACh was applied to the bath (10μM in saphenous, and 3μM in mesenteric) when the second contraction to PE had stabilised. Vessels that did not show a suitable relaxation to ACh were excluded from any further experimental protocol.

#### 2.3.2.2 Cumulative Concentration Response Curves

Cumulative concentration response curves (CCRCs) were obtained by adding concentrations of agonist to the bath in half-log molar increments. This was used as a standard protocol to assess the response to an agonist since a maximal response could be determined from this data. Also, it was possible to calculate the $pEC_{50}$ by means of spreadsheet calculations and so give an indication of the sensitivity of the tissue to the agonist.

#### 2.3.2.3 Time Control Curves

In experiments where more than one CCRC to an agonist was to be performed a time control experiment was run in parallel. The purpose of the time control was to ensure that a second CCRC to an agonist could be obtained which did not differ significantly from the first.

## 2.4 Pressure Myography

The pressure myograph system used was developed specifically for this project and was adapted for use on the confocal microscope. It was based on a model used by Dr Kim Dora, after a visit to her laboratory in the University of Bath. It consists of two stage-mounted micromanipulators with glass cannulae attached for vessel mounting. One of the glass cannulae has tubing connecting it to the inflow reservoir, with a small heater in series with the inflow cannula in order to warm the incoming solution. The flow and pressure were controlled by a Living

Systems peristaltic pump and pressure servo control. The outflow cannula was connected to tubing ending in a three way tap, which when closed permitted the maintenance of pressure within the system. The micromanipulators were directed into a Warner Instruments RC22 chamber (by use of the X, Y and Z axis adjusters), the base of which was a glass coverslip (number 1.5) for confocal use. Glass cannulae were made by pulling a thin walled glass cannula using a Kopf vertical pipette puller and heat from the metal filament in the puller split the cannula into two halves with fine tapered tips. These tips were then snapped to size under the microscope with forceps, using another tip to gauge size (around 150μm). To remove any ragged edges the tip was flamed with a lighter. Tip size was crucial since it had to be greater than 50% of vessel diameter under pressure to ensure that the vessel stayed on. Surgical suture was tied in loops and placed over the ends of the tips before vessel mounting to allow the vessel to be tightly secured (Figure 2.3). The bath was heated by a Warner Instruments heat controller, model TC-344B, and filled with MOPS buffer solution to keep pH constant at 7.4,  since the bath was not oxygenated.

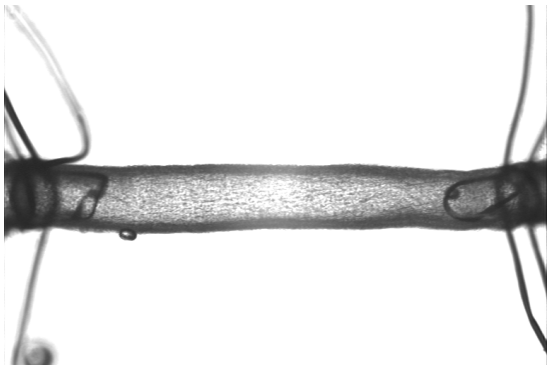

**Figure 2-3 Rat third order mesenteric vessel mounted on glass tips of pressure myograph, pressurised at 70mmHg**

The pressure myograph system previously used in the laboratory was designed so that the vessel was mounted on and level with the inflow and outflow cannulae. This system had a coverslip on top and once inverted, fitted on the confocal stage in a similar way to a slide, hence oil-immersion short working length objectives were suitable for use with this myograph. In developing the new system it was found that the short working length objectives (x20 oil WD=0.35mm, and x40 oil WD=0.16mm) were unsuitable, since the vessel could not be brought into focus without the objective pushing up the stage and breaking the glass cannulae on which the vessel was supported. This was due to

the fact that the glass cannulae approach the bath at an angle, meaning they could not come close to the coverslip (base of the bath) without breaking if there was any slight upward movement of the bath. To solve this problem new long working distance objectives were used (x20 ELWD WD 7.4mm, and x40 ELWD WD=3.7-2.7mm), which permitted a greater distance between the objective lens and the vessel (point of focus). Some other teething problems were encountered in developing this system, such as mastering the craft of making the glass cannulae, and ensuring that the system was free of any leaks.

There were several advantages to this new pressure system compared with the previous one, namely:

- Drugs could be added directly to the bath whilst pressure was maintained, allowing cumulative concentration response experiments to be conducted. This was not possible in the previous system since the bath was a sealed chamber.

- Vessels could be easily imaged before and after incubation of a dye, without the need to remove the coverslip before dye addition. This meant that progression of staining could be imaged easily, and addition of higher dye concentrations caused no disruption to the setup.

- The bath could be heated to a physiological temperature, especially useful when using dyes requiring esterase activity, such as calcein AM.

### *2.4.1 Pressure myograph vessel mounting*

Prior to vessel mounting the pressure lines were filled with room temperature MOPS buffer solution to ensure there were no air bubbles in the tubing. The vessel was then manoeuvred over the tip of the inflow glass cannula using ultra fine forceps and tied on securely with surgical suture. A flow 300 µL/min was applied briefly to the vessel to clear the lumen of any blood before the vessel was tied on to the outflow cannula. When the vessel was securely tied at both ends flow was passed through the system, with the tap at the outflow end open to allow the escape of fluid. The tap at the outflow end was then closed to allow pressure to be applied to the system and the peristaltic pump was switched from flow mode to pressure mode. Pressure was started at 10mmHg and was stepped up in 10mmHg intervals over a period of 30 minutes to 70mmHg. To avoid

buckling with increased pressure, the vessel length was adjusted using the micromanipulators if necessary without any additional stretching. After this equilibration period the vessel was ready for use in the protocol.

### *2.4.2 Pressure Fixing of Mesenteric Arteries*

In order to fix a vessel at pressure the vessel was firstly set up on the pressure myograph as detailed previously. After the equilibration period the vessel was set to the appropriate pressure at which it would be fixed at 37 $^{o}$C. The MOPS buffer was removed from the bath and replaced with 4% paraformaldehyde for one hour. The vessel was removed and stored in 4% paraformaldehyde in a refrigerator at 4$^{o}$C until use. This technique was used in Chapter 3.

To obtain cross sectional rings of pressure-fixed arteries the vessel was put on a slide with a drop of fixative fluid and was cut using a scalpel blade to a ring width of approximately 200 µm. A well for the vessel was prepared on another slide by an adhesive silicone spacer filled with glycerol. This was important to avoid crushing of the ring when the coverslip was applied, which would distort its shape. The cut ring was carefully placed inside the well on the slide and arranged to view the vessel as a cross-section when looking directly down on the slide. A cover slip was placed on top of the adhesive silicone spacer on the slide to create a sealed chamber containing the fixed ring.

## 2.5 Confocal Microscopy

Confocal microscopy was developed by Minsky in 1955 and later patented in 1957. It is based upon the principle that the first objective lens focused a point of light at the desired focal plane of the specimen and a second objective lens focused the light passing *through* the specimen with a pinhole at the same focus as the first objective lens' pinhole, hence both lenses were "confocal". This light passing through the specimen and subsequently through the second pinhole struck a low noise photomultiplier that generated a signal according to the brightness of the specimen. The second objective's pinhole had the purpose of preventing out of focus light from other parts of the specimen above or below the plane of interest from reaching the photomultiplier. By these means it was possible to collect serial optical sections from thick specimens without having to physically section the specimen. Thus structures such as blood vessels could be

imaged intact and a three dimensional image could be reconstructed using a Z-series (where focal planes are collected at given micron steps in the z-axis to collect optical xy “slices” that combine to form a 3D representation of the structure).

In the first confocal systems the beam was kept stationary and the specimen was moved on the stage. However, for most modern imaging it is necessary to keep the imaged specimen still (as in this work where the vessel was mounted on a pressure myograph) and thus more recent microscopes were developed so that the specimen remained stationary on the microscope stage and the beam scanned across the specimen: hence the name “Laser Scanning Confocal Microscopy” (LSCM).

The confocal microscope used in this study was a Bio-Rad Radience 2100, equipped with argon, HeNe and red diode lasers. The confocal objectives used in this study had a range of magnifications, numerical apertures (NA) and working distances (WD) to suit different experimental methods (Table 2.2). Numerical aperture is the most important characteristic defining the performance of an objective. The higher the numerical aperture of the objective, the higher the resolving power i.e. the power to recognise two discreet points (where the use of a lower numerical aperture objective may make these two points appear to be merged into one).

**Table 2-2 Numerical aperture and working distance of confocal objectives**

| | Numerical Aperture | Working Distance (mm) |
|---|---|---|
| **Nikon Plan Fluor ELWD 40x** | 0.45 | 8.1 - 7.0 |
| **Nikon Plan Fluor ELWD 20x** | 0.6 | 3.7 - 2.7 |
| **Nikon CFI Plan Fluor 20x oil/water** | 0.5 | 2.1 |
| **Nikon CFI Plan Fluor 40x oil** | 1.3 | 0.2 |

## *2.5.1 Principles of Fluorescence*

Fluorescence requires a source of excitation energy, which in the case of confocal microscopy is provided by lasers. Molecules capable of fluorescing are termed fluophores and require a wavelength of light near the excitation maximum ($E_m$) to induce fluorescence. The $E_m$ excites a higher proportion of fluophores than any other wavelength of light, and every dye has a characteristic range.

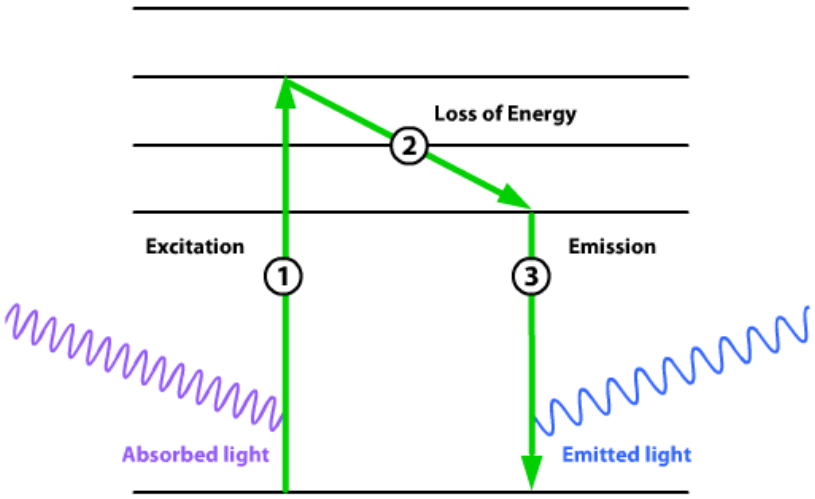


**Figure 2-4 Summary of fluorescence**
**(http://probes.invitrogen.com/resources/education/tutorials/1Intro/player.html)**

When the fluophore absorbs light energy of a particular wavelength the molecule reaches a higher energy (Figure 2.4), or excited, state [1]. The fluophore is unstable at this high energy state so it adopts its lowest high energy state which is more stable [2]. On return to the most stable "ground state" the fluophore releases energy in the form of emitted light [3]. This emitted light is always of a lower energy and hence a longer wavelength than the absorbed light due to the loss of energy between the higher and lower excited states.

## *2.5.2 Approaches to visualising myoendothelial connections using laser scanning confocal microscopy*

### 2.5.2.1 Technical problems

It was hoped that myoendothelial projections could be viewed in an intact vessel on the pressure myograph system using LSCM. Several technical problems were encountered in attempting this. Firstly, the oil immersion objectives were not compatible with the pressure myograph since the working distance was too small to accommodate the space between the vessel and objective. To overcome this problem new objectives were purchased with an "extra long working distance" (ELWD), allowing the live pressurised vessel to be viewed on the confocal microscope. However, at the zoom required to see the IEL in detail there was not sufficient definition to make the required measurements. Numerical

aperture had to be compromised for a greater working distance (Table 2.2), and this meant poorer resolution.

The membrane stain FM4-64 was used in live vessels on the pressure myograph in an attempt to depict the membrane stained projections traversing the IEL. The aim was to image a Z-series of the vessel and then use the 3D image analysis software Imaris (Bitplane Scientific Software, Zurich, Switzerland) to slice an orthogonal plane, on which the projections would be evident. This would advance the technique already established in rings cut from pressure fixed vessels (in which membrane stained cellular projections could be seen passing through fenestrae in the IEL) and be a more physiological alternative. In retrospect this was an ambitious approach to viewing these structures: it was found that the fenestrae could not be clearly visualised using the ELWD objectives; and that too much fluorescence due to the mass of SMC membranes dyed by FM4-64 caused the Z series to be saturated, making it impossible to identify defined cell membranes. All in, this approach was not successful and yielded no results.

The accurate measurement of fenestrae size and number on the live set up was not possible due to the lower numerical aperture of the ELWD lenses as compared with the oil immersion objectives. This meant that the resolution was lower in the ELWD lenses and consequently at the higher zoom needed to measure the fenestrae much definition was lost. To test that it was the objectives and not just the live set up that were the problem, a fixed vessel was slide-mounted and visualised using both the oil-immersion and the ELWD objectives. On the oil-immersion objectives clear sharp images were obtained, whereas the ELWD objectives gave a blurry undefined image. In light of the oil-immersion objectives not being suitable for use with the pressure system due to impractically small working distances, it was concluded that the fenestrae could not be measured on the live vessel as hoped. Instead of measuring fenestrae size on the live vessel as pressure was changed, pressure fixed arteries were mounted on a slide in order to measure fenestrae size (Chapter 3).

Another method was devised in an attempt to image the myoendothelial projections in the live vessel. Calcein-AM, a cell permeable dye which is taken up and converted to its cell impermeable fluorescent form by esterases (Griffith

*et al.*, 2002) was loaded luminally with the proposal of it being taken up by endothelial cells and transferred to the smooth muscle cells through MEGJs. Due to problems visualising the fenestrae on live vessels on the pressure system it was difficult to assess whether cellular projections traversed the fenestrations of the IEL. A possible way of solving this was attempted by applying dyes luminally in the live vessel and then pressure fixing the vessel after dye application to determine whether the dye and fenestrae could be visualised in the fixed vessel on a slide with the oil-immersion objective. It was necessary to stain the lamina with Alexa 633 hydrazide to view the fenestrae in combination with the calcein staining.

#### 2.5.2.2 Successful approach: Membrane-Stained Fixed Vascular Rings

It was possible to image cellular projections traversing the fenestrae of the IEL in cut rings from pressure fixed vessels (Figure 2.5). These images were obtained by taking a 10µm deep Z-series through a cut ring, and scanning the Z-series for the best plane to view a myoendothelial bridge. This technique was developed by Jose Maria Gonzalez (PhD thesis 2004), using the membrane stain FM1-43 FX, which has an emission in the same range as the autofluorescent IEL. This meant that fenestrae and bridges had to be imaged on separate vessels, with and without the membrane dye to view the bridges and lamina respectively. My development of this technique using the membrane dye FM4-64 FX allowed for simultaneous imaging of the lamina and the membrane stained projections on the same vessel (Figure 2.5). Pressure fixed vessels were incubated in a solution of 10µM FM4-64 FX in paraformaldehyde for 24 hours before a ring of the vessel was cut with a scalpel for imaging. Although this technique was effective for visualising the myoendothelial bridges, it gave no indication as to the function or the existence of MEGJs, therefore it was decided that dye transfer experiments using calcein-AM were more useful to explore the patency of the MEGJs.

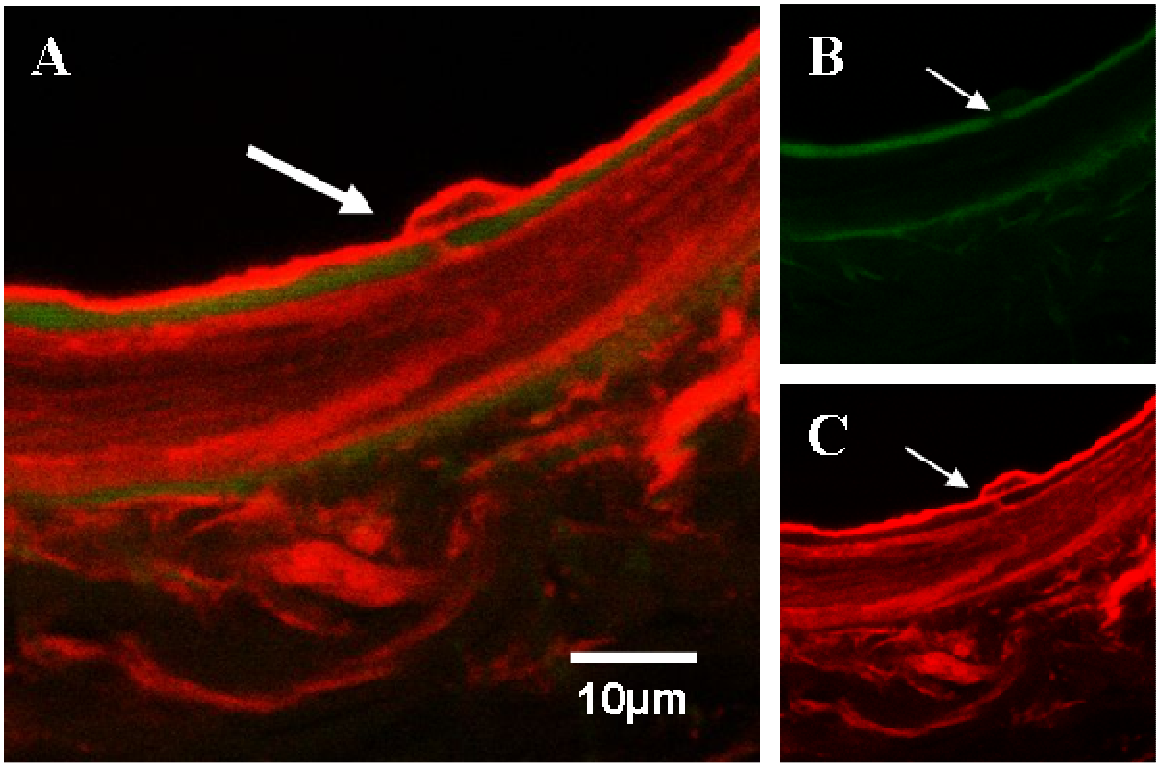


**Figure 2-5 High power view of arterial ring pressure fixed at 70mmHg (40x oil immersion objective, zoom 4.5) Image area 64µm x 64 µm. Auto fluorescent elastin is green (B), and membrane dye FM4-64 FX is red (C). Colour combine view demonstrates a myoendothelial projection traversing a fenestration in the internal elastic lamina (A).**

## 2.6 Immunohistochemistry

Thin (5µm) transverse sections of mesenteric or saphenous artery were cut using a cryostat and stained for the presence of connexins 37 and 43 using immunohistochemistry (see Chapter 7 for more detailed methodology). Unlabelled primary antibody reacts with the tissue antigen it is specific for, and a labelled secondary antibody then binds the primary antibody it is directed against. The secondary antibody must be raised against the immunoglobulin of the same animal species used in which the primary antibody has been made. Secondary antibody can be tagged with a fluophore to produce fluorescence on binding of the primary antibody; or it can be labelled with an enzyme such as horseradish peroxidise which reacts with 3,3'-diaminobenzidine (DAB) to produce a brown precipitate stain wherever the primary and secondary antibody are attached (Ramos-Vara, 2005). Both fluorescently labelled secondary antibodies and the DAB staining method were utilised in this study (Chapter 7). To assess the presence of Cx37 in the vessel, Cx37 mouse monoclonal primary antibody (1:200) was used with a goat anti-mouse conjugated alexa 488 secondary antibody. To assess the presence of Cx43 in the vessel, Cx43 rabbit

polyclonal primary antibody (1:100) was used with a goat anti-rabbit conjugated alexa 546 secondary antibody.

## 2.7 Data Analysis

### *2.7.1 Wire Myography Results*

The individual measurements from each bath were pooled to calculate the mean and standard error of the mean for each data set, where *n* denotes the number of animals used and *N* represents the total number of replicates.

Results were expressed in either grams tension (g), which is the value of the myograph response after subtraction of baseline tension; or as a percentage of a response. To calculate the $EC_{50}$, that is, the concentration of agonist required to obtain half the maximal response, it was necessary to express the data as a percentage of the response being assessed. In the case of PE, each response in the CCRC was expressed as a percentage of the maximum contraction in grams obtained during the curve.

In calculation of $pEC_{50}$ values for ACh the situation was more complex since the CCRC was performed on a stable preconstriction to PE, and the size of this preconstriction varied considerably between strains. In order to normalise for this difference in PE contraction, the ACh relaxation was expressed as a percentage of the PE preconstriction in grams rather than as a percentage of its own maximum relaxation in grams. A value of near 100% relaxation in this case would equate to almost a full reversal of the PE mediated contraction, and so this was more informative than simply expressing the points on the curve as a percentage of the maximal ACh induced relaxation in grams; since a value of 100% here would only indicate the greatest relaxation had been achieved but not necessarily a full reversal of the PE induced contraction.

### *2.7.2 Confocal Microscopy Results*

In an attempt to quantify observations made by eye from the images captured on the confocal microscope it was necessary to devise methods of quantitative analysis. Three imaging programs were used for this purpose, namely: Imaris (Version 5.1: Bitplane Scientific Software, Zurich, Switzerland); Amira (Version

3.2: Visage Imaging, Berlin, Germany); and Metamorph (Version 6.1: Molecular Devices, Wokingham, UK). Each image was composed of pixels, or in the case of three dimensional Z-series stacks- voxels. The brightness of these pixels or voxels lay on the 8 bit scale of 1 to 255; with 255 being the brightest value, and 1 the least intense. By differentiating voxels or pixels by brightness, it was possible in some cases to depict patterns in an image or to depict specific structures (in the case of fenestrations in the IEL which show up as dark patched against the bright auto-fluorescence of the IEL) and thresholding functions could be utilised. The method by which the images were analysed will be referred to in more detail in the appropriate confocal chapters.

### *2.7.3 Statistics*

All statistical analysis was performed using Graph Pad Prism software (Version 5). Two groups were compared using paired or unpaired Student's t-test. More than two groups with one variable were compared using one way analysis of variance (ANOVA). More than two groups with two variables were analysed using two way analysis of variance (ANOVA). If differences were detected by ANOVA, individual groups were compared with the use of Bonferroni post-tests for all pairwise comparisons. Statistical significance was classified as p values less than 0.05, as is standard practice in scientific papers. The number of animals used was denoted by *n*.

## 2.8 Solutions and Drugs

For wire myography experiments Physiological Salt Solution (PSS) of the following composition (mM) was used: NaCl 118.4, KCl 4.7, $CaCl_2$ 2.5, $KH_2PO_4$ 1.2, $MgSO_4$ 1.2, $NaHCO_3$ 25 and glucose 11.1, bubbled with 95% $O_2$/5% $O_2$ to pH 7.4 at $37^0$C.

For experiments on the pressure myograph, MOPS-buffer of the following composition (mM) was used: 145 NaCl, 4.7 KCl, 2.0 $CaCl_2 \cdot 2H_2O$, 1.17 $MgSO_4 \cdot 7H_2O$, 2.00 MOPS, 1.2 $NaH_2PO_4 \cdot H_2O$, 5.0 glucose, 2.0 pyruvate (Na salt), 0.02 EDTA free acid, 2.75 NaOH. This solution was adjusted to pH 7.4 ± 0.02 at 37°C by addition of 10M NaOH or HCl.

The drugs/compounds and method used to dissolve them are detailed (Table 2.3). Compounds dissolved in solvents were made at a higher concentration than required and diluted in distilled water or MOPS to minimise the effect of the solvent on the experiment.

**Table 2-3 Drugs/compounds, suppliers and solvents used to dissolve.**

| Drug/compound | Supplier | Solvent for stock |
|---|---|---|
| Phenylephrine hydrochloride | Sigma | Distilled water |
| Acetylcholine chloride | Sigma | Distilled water |
| L-NAME ($N^{\omega}$-nitro-L-arginine methylester) | Sigma | Distilled water |
| Indomethacin | Sigma | Ethanol (100%) |
| Carbenoxolone | Sigma | Distilled water |
| Apamin | Tocris | Distilled water |
| TRAM-34 | Tocris | DMSO |
| FM4-64 FX | Invitrogen | DMSO |
| Calcein-AM | Invitrogen/C300MP | 100mM in DMSO then dilution to 3µM in MOPS |
| $^{40}$Gap27 | Severn Biotech | Distilled water then dilution in MOPS |
| $^{37,43}$Gap27 | Severn Biotech | Distilled water then dilution in MOPS |
| Cx37 mouse monoclonal | Alpha Diagnostics | PBS (1 in 200) |
| Cx43 rabbit polyclonal | Millipore | PBS (1 in 100) |

# Chapter 3 Vessel Morphometry

## 3.1 Introduction

It is well established that the SHR blood vessel structure varies from that of the WKY; either as a consequence of or as a pre-requisite to elevated blood pressure (Heagerty *et al.*, 1993; Mulvany *et al.*, 1996; Gonzalez *et al.*, 2006; Arribas *et al.*, 1997), with a thickening of the media and alterations in elastin layout reported.

Elastin content and the layout of fenestrae have previously been studied in mesenteric arteries in our laboratory. It was found that there was no difference in elastin content between 1 and 6 month old WKY rats, but fenestrae area increased with age (Gonzalez *et al.*, 2005); and that SHR had an impairment of fenestrae enlargement throughout the first month of life, resulting in smaller fenestrae than those of the 1 month old WKY rats (Gonzalez *et al.*, 2006). There have been similar findings in the rabbit carotid artery in which fenestrae area increased with age from 3 to 23 weeks (Wong & Langille, 1996).

Since it was not possible to acquire blood pressure measurements from the animals used, one of the aims of this chapter was to assess the differences in arterial dimensions between the strains. This was intended to confirm that the SHR strain were indeed hypertensive since they would be expected to have an increased wall thickness compared with the WKY. Mesenteric arteries from SHR have been shown to have a thicker media than normotensive controls, without a significant increase in cross-sectional vessel area, thus implying that the increased wall thickness was a consequence of vascular remodelling (Mulvany *et al.*, 1985; Qiu *et al.*, 1995; Gonzalez *et al.*, 2006).

Fenestrae size and number was measured in each strain to correlate this with: previous work from the laboratory; the transfer of luminally loaded dye (Chapter 5); and the functional EDHF response (Chapters 3 and 4). Fenestrae area had been studied extensively in the previous papers from the laboratory therefore only a small sample size was assessed in this study.

### *3.1.1 Aims*

The aims of this chapter were:

- To compare arterial measurements in 12 week and 6 month old WKY and SHR to assess vascular remodelling with ageing or hypertension.

- To measure fenestrae size and number in 12 week and 6 month old WKY and SHR.

## 3.2 Methods

### *3.2.1 Arterial dimensions*

Measurements were made on live pressure myograph-mounted vessels (mounting procedure detailed in Chapter 2). Pressure diameter curves were obtained using Vediview software and a microscope-mounted camera to track the vessel walls (Figure 3.1). This allowed for inner and outer diameter; wall thickness; wall/lumen ratios; and cross sectional area to be calculated for each artery over intraluminal pressures ranging from 10 to 70mmHg. Intraluminal pressure was increased in 10mmHg steps at 5 minute intervals.

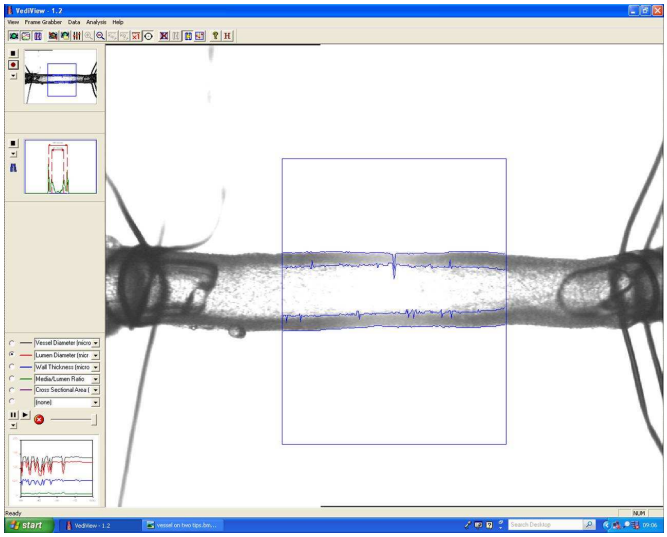

**Figure 3-1 Screenshot of Vediview software user interface tracking dimensions of 12 week old WKY pressurised mesenteric artery**

### *3.2.2 Fenestrae analysis*

Fenestrae were imaged from pressure-fixed (70mmHg) slide-mounted vessels. The protocol for pressure-fixing arteries was detailed in the General Methods chapter (Chapter 2). Pressure fixed vessels were viewed using a x40 oil immersion objective at a zoom of 4.5 (giving an image area of 64µm x64µm or 4096µm$^2$) and captured with a 3 frame Kalman. Elastin autofluorescence was

excited at 488 nm, and laser and gain settings were increased until fluorescence of the internal elastic lamina was at an optimal level. Metamorph imaging software (Version 6.1) was used to analyse the images. The original image underwent a 3x3 lowpass which was thresholded to select dark objects, i.e. the fenestrae (Figure 3.2). A size threshold range of between 0.5 and 300μm$^2$ for fenestrae area was implemented, to exclude any particularly small or large dark spots. Each of the green patches was counted as an object, with the orange patches included in the thresholding for dark objects but *excluded* from measurement by size. The number and area of fenestrae for each image were stored in a data log in Metamorph and exported to Excel (Microsoft Office 2003).

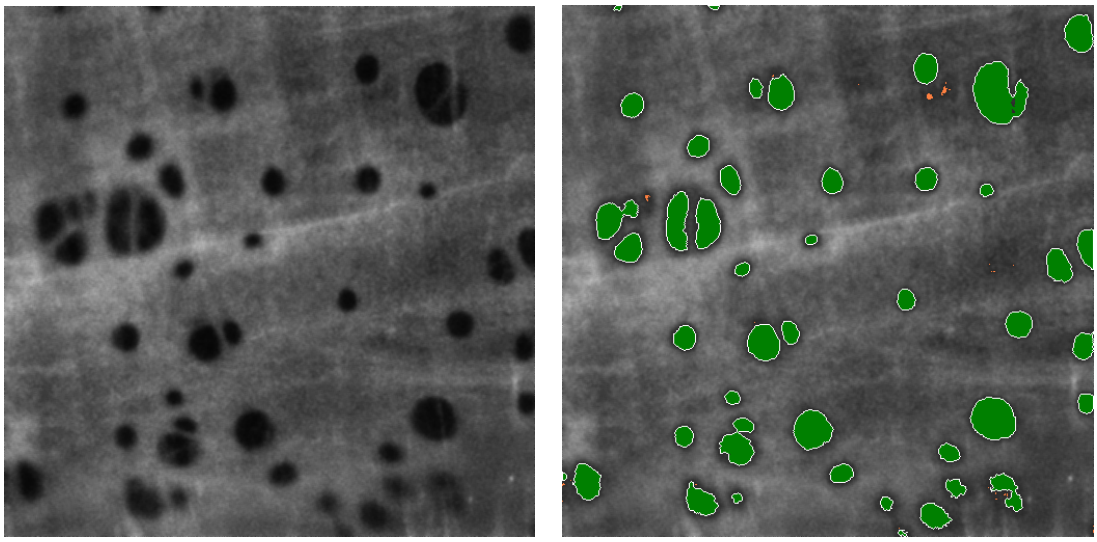

**Figure 3-2 Left hand pane showing original image, right hand pane showing thresholded measured objects on lowpass version of image (green included, orange excluded from count).**

Mean data for inner and outer diameter; wall thickness; wall/lumen ratios; and cross sectional area were compared between strains at each pressure using an unpaired t-test. Fenestrae area and number were compared between strains and ages using unpaired t-tests.

## 3.3 Results

### *3.3.1 Arterial dimensions*

Mesenteric vessel measurements showed that there was no significant difference in outer vessel diameter between age-matched WKY and SHR (Figures 3.3 and 3.4), and lumen diameter was not significantly different between age-matched WKY and SHR (Figures 3.5 and 3.6). Similarly, cross-sectional area did not vary

between WKY and SHR of the same age (Figure 3.8), with the exception of the 12 week old rats at 10mmHg (Figure 3.7). The 12 week old SHR had a significantly thicker wall than the 12 week old WKY at intraluminal pressures of 30, 60 and 70mmHg (Figure 3.7), and the 6 month old SHR had a significantly thicker wall than the age-matched WKY at 40 and 70mmHg (Figure 3.8). The wall: lumen ratio was significantly greater in the SHR compared with the WKY at: 50, 60 and 70mmHg in the 12 week old; and at 10, 30 and 70mmHg in the 6 month old animals (Figures 3.11 and 3.12).

In the WKY, outer vessel diameter increased significantly from the 12 week old to the 6 month old at pressures 10, 20 and 30mmHg ($P<0.05$). The SHR outer diameter did not vary with age at any intraluminal pressure. There were no significant increases in lumen diameter in either strain with age. Cross sectional area was significantly increased in the 6 month old WKY compared with the 12 week old WKY at intraluminal pressures 10, 20 and 30mmHg ($p<0.05$). In the SHR, the only significant increase in cross sectional area between the 12 week old and 6 month old was at 40mmHg ($p<0.05$). Wall thickness significantly increased with age in the WKY at intraluminal pressures of 60 and 70mmHg. SHR wall thickness significantly increased with age in the SHR at 10 and 70mmHg. The wall to lumen ratio did not differ significantly between the 12 week old and the 6 month old WKY. However, the wall to lumen ratio was increased in the 6 month old SHR compared with the 12 week old SHR at an intraluminal pressure of 70mmHg ($p<0.05$).

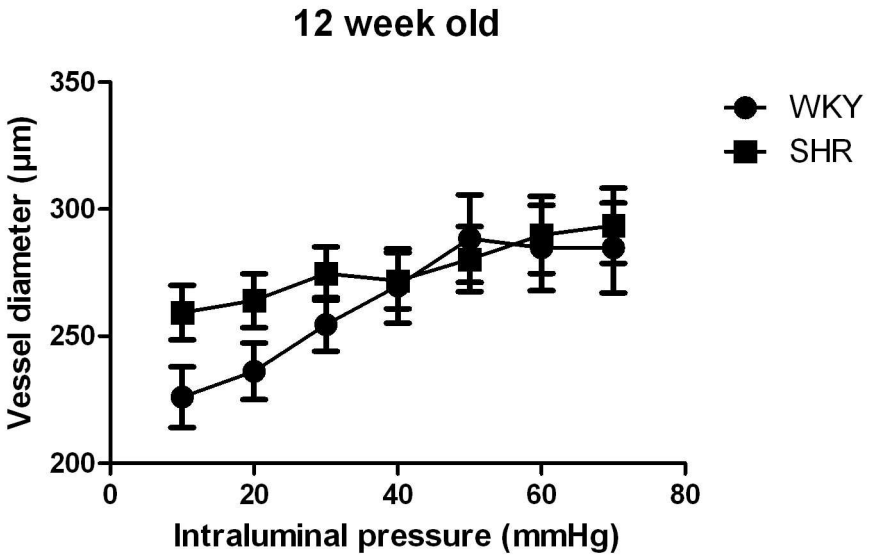


**Figure 3-3 Pressure diameter curve for outer vessel diameter at pressures ranging from 10 to 70 mmHg in 12 week old third order mesenteric arteries (n=6)**

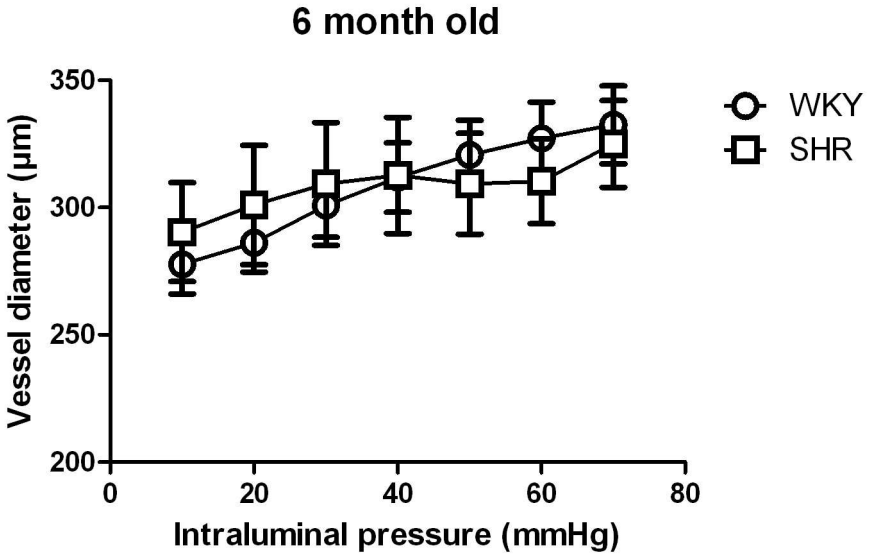


**Figure 3-4 Pressure diameter curve for outer vessel diameter at pressures ranging from 10 to 70 mmHg in 6 month old third order mesenteric arteries (WKY n=6, SHR n=3)**

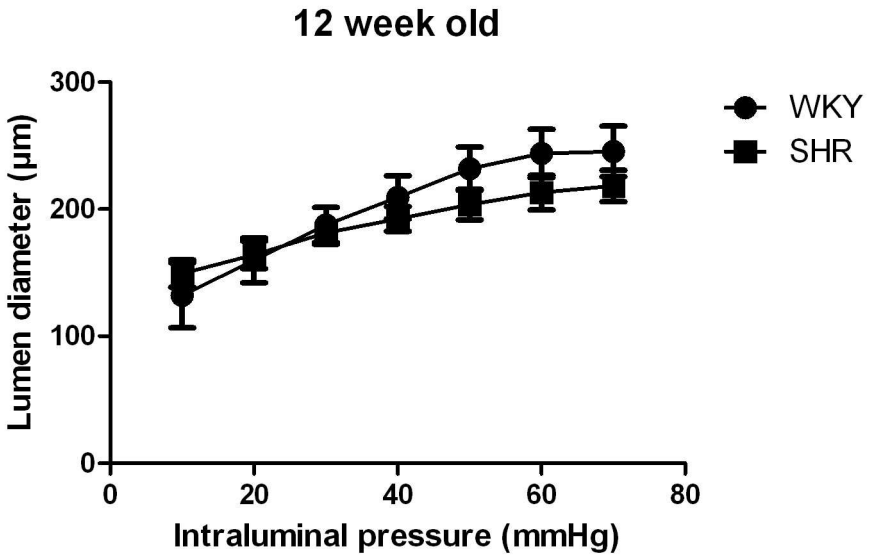


**Figure 3-5 Pressure diameter curve for lumen diameter at pressures ranging from 10 to 70 mmHg in 12 week old third order mesenteric arteries (n=6)**

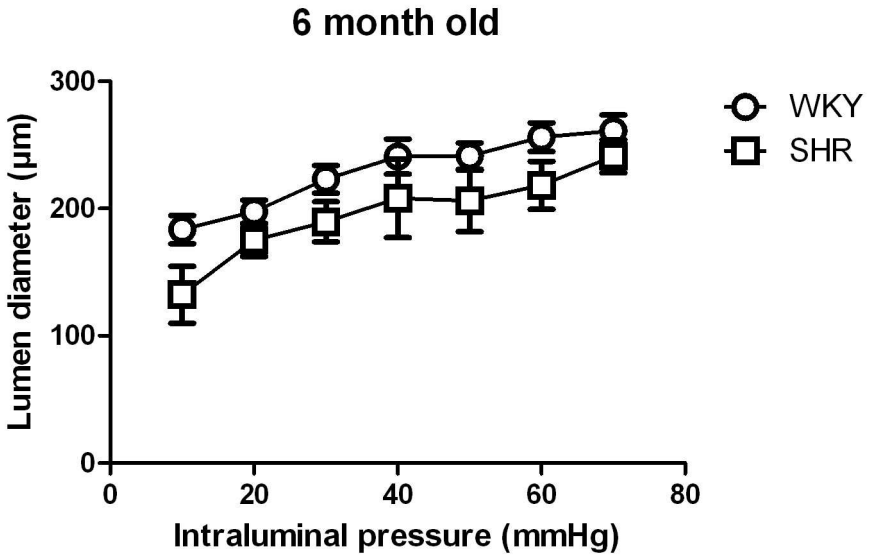


**Figure 3-6 Pressure diameter curve for lumen diameter at pressures ranging from 10 to 70 mmHg in third order mesenteric arteries (WKY n=6, SHR n=3)**

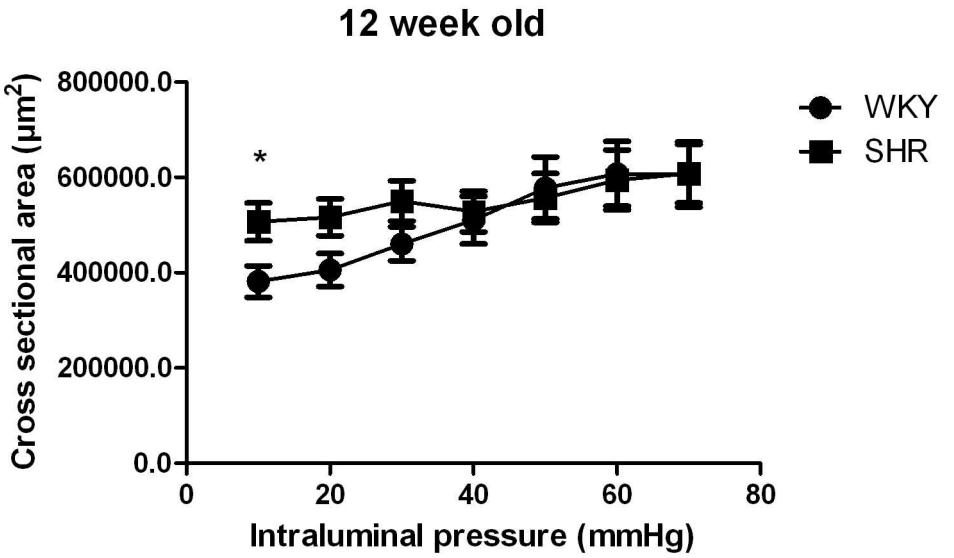


**Figure 3-7 Pressure curve for cross sectional area at pressures ranging from 10 to 70 mmHg in 12 week old third order mesenteric arteries (n=6). *p<0.05 compared with WKY**

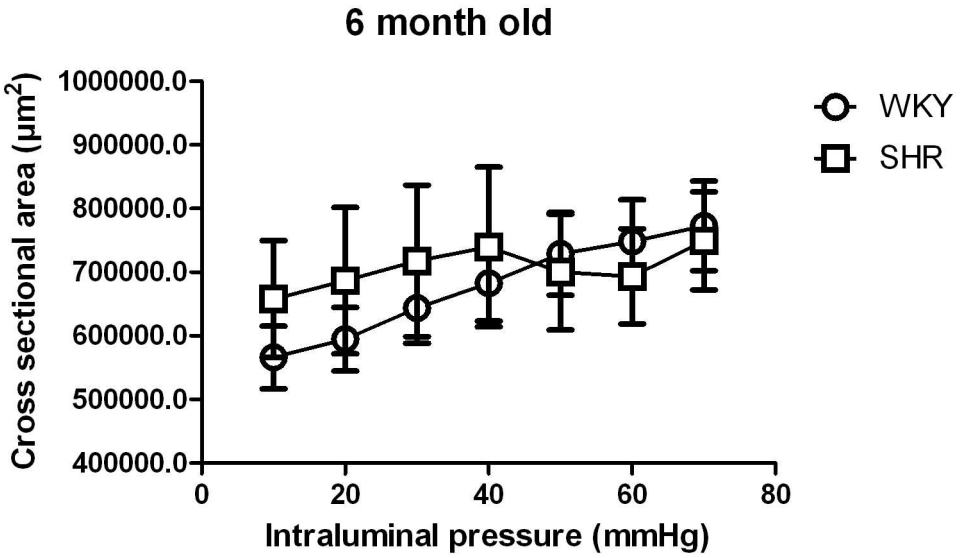


**Figure 3-8 Pressure curve for cross sectional area at pressures ranging from 10 to 70 mmHg in 6 month old third order mesenteric arteries (WKY n=6, SHR n=3).**

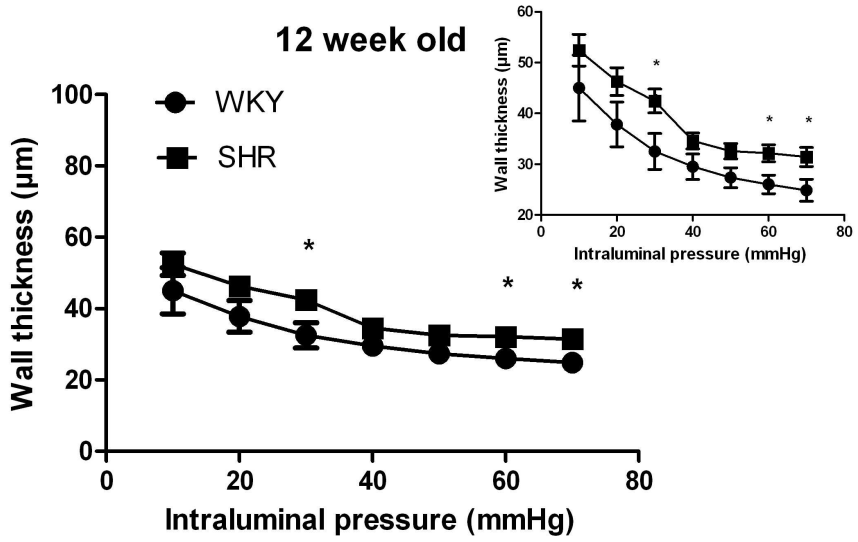


**Figure 3-9 Pressure curve for wall thickness at pressures ranging from 10 to 70 mmHg in 12 week old third order mesenteric arteries (n=6). *p<0.05 compared with WKY.**

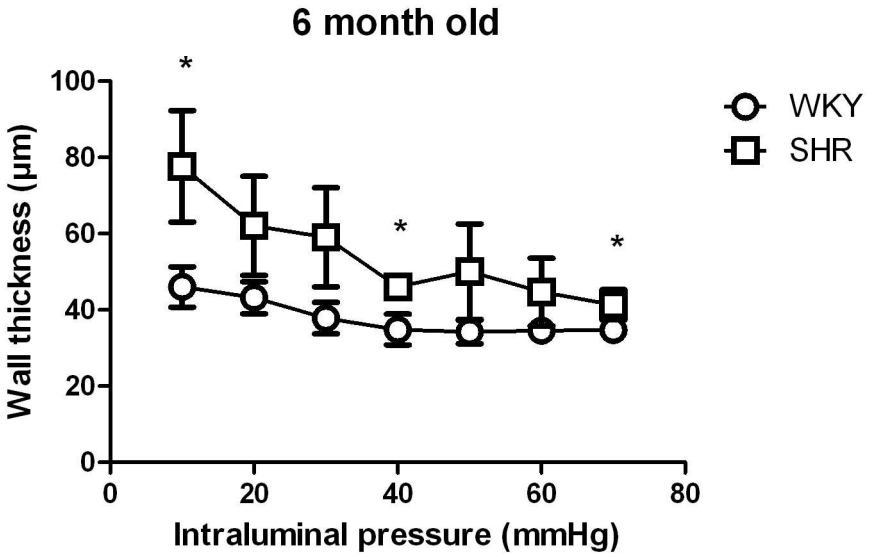


**Figure 3-10 Pressure curve for wall thickness at pressures ranging from 10 to 70 mmHg in 6 month old third order mesenteric arteries (WKY n=6, SHR n=3). * p<0.05 compared with WKY.**

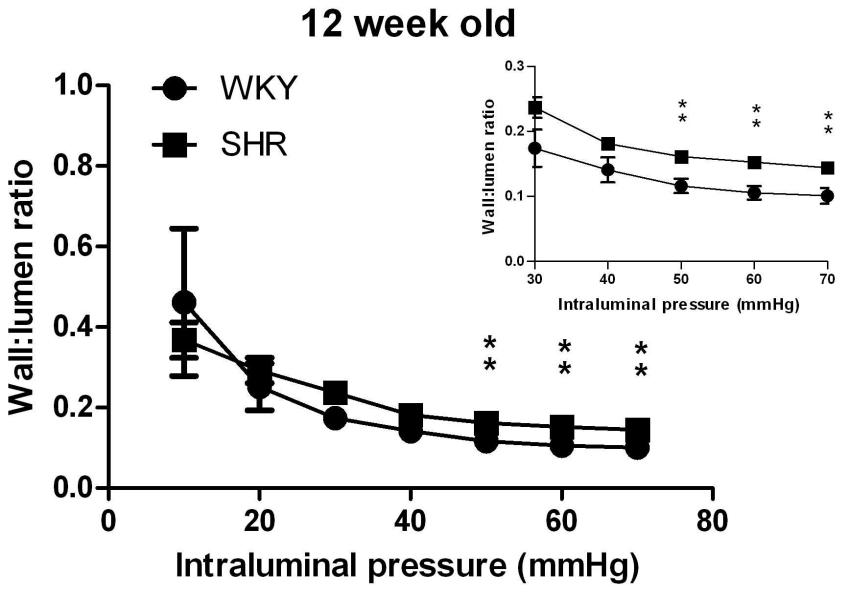


**Figure 3-11 Pressure curve for wall/lumen ratio at pressures ranging from 10 to 70 mmHg in 12 week old third order mesenteric arteries (n=2). **p<0.01 compared with WKY.**

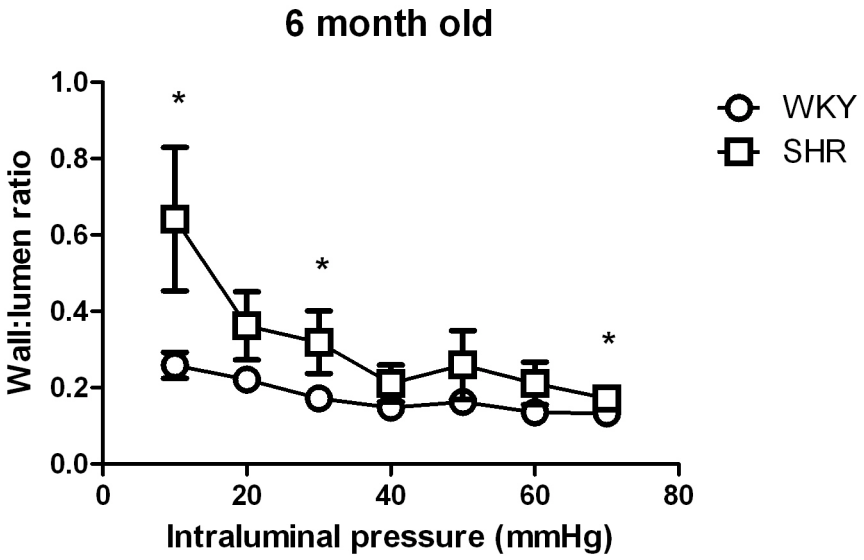


**Figure 3-12 Pressure curve for wall/lumen ratio at pressures ranging from 10 to 70 mmHg in 6 month old third order mesenteric arteries (WKY n=6, SHR n=3). *p<0.05 compared with WKY.**

### *3.3.2 Fenestrae analysis*

Images of fenestrae in the IEL of 12 week and 6 month old WKY and SHR are shown (Figures 3.13 and 3.14 respectively). Analysis of fenestrae area (Figure 3.15) showed that there was no significant difference between fenestrae area of the two strains at 12 weeks of age, but that the 6 month old WKY had significantly larger fenestrae than the 6 month old SHR. There was no significant increase in fenestrae area with age in the SHR, however, fenestrae area increased significantly between 12 weeks and 6 months in the WKY.

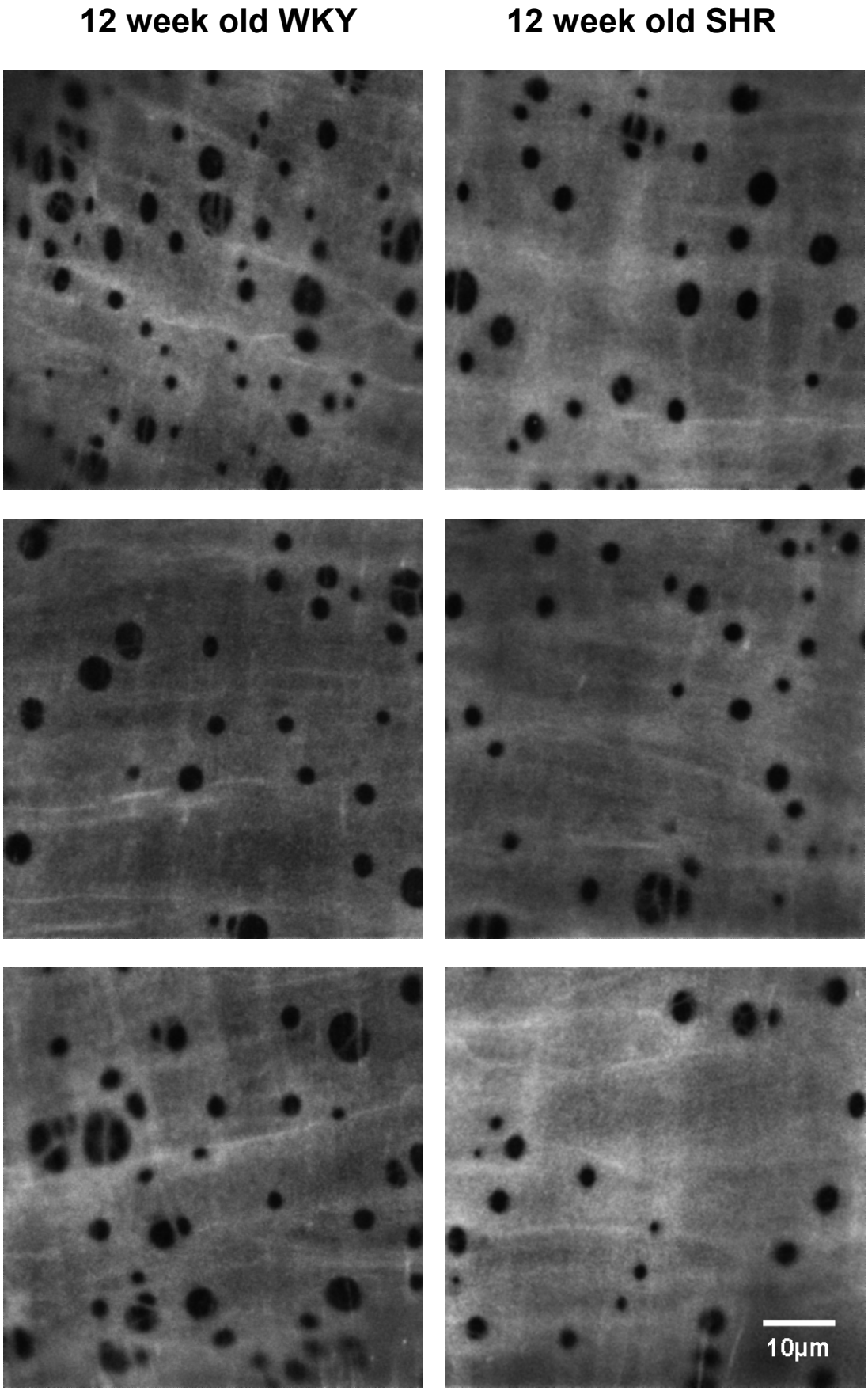


**Figure 3-13 Images of IEL from pressure fixed (70mmHg) arteries of 12 week old WKY (n=2, left hand pane) and SHR (n=2, right hand pane).**

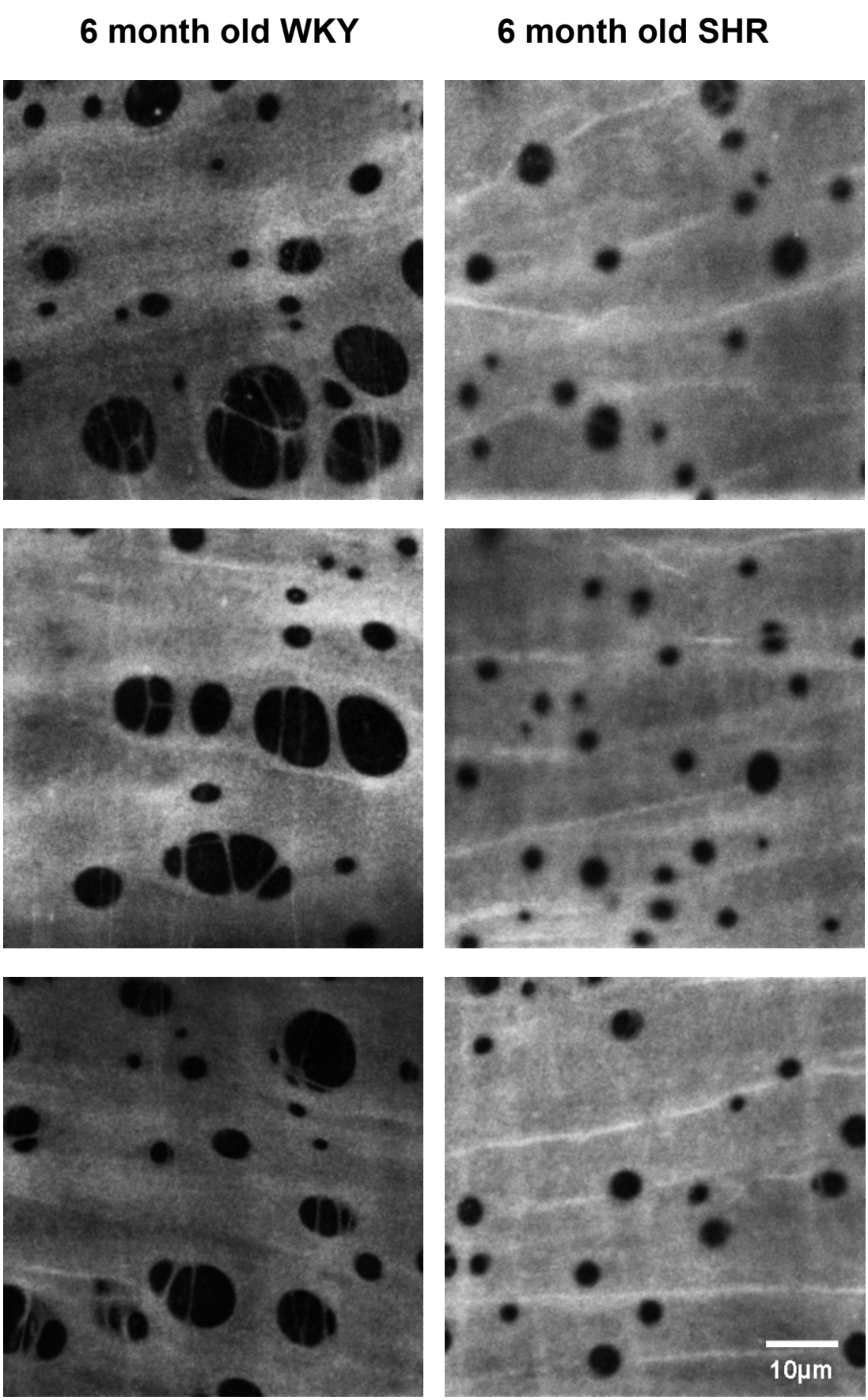


**Figure 3-14 Images of IEL from pressure fixed (70mmHg) arteries of 12 week old WKY (n=2, left hand pane) and SHR (n=2, right hand pane).**

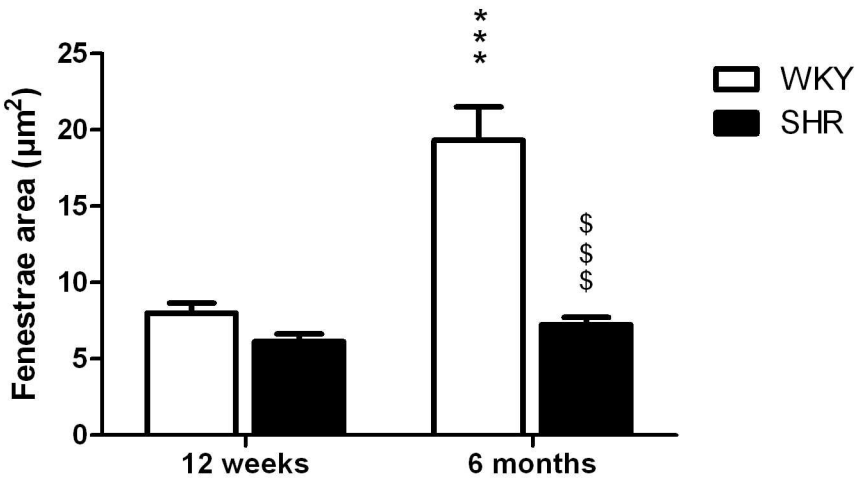


**Figure 3-15 Fenestrae area in 12 week and 6 month old WKY (n=2) and SHR (n=2) animals. Expressed as mean ± SEM. *** p<0.001 compared with 12 week old WKY, $$$ p<0.001 compared with 6 month old WKY.**

The 12 week old SHR had significantly less fenestrae than the 12 week old WKY, but there was no significant difference in fenestrae number between the strains at 6 months of age. The 6 month old WKY had significantly less fenestrae than the 12 week old WKY, however there was no significant difference in fenestrae number between the 12 week and 6 month old SHR (Figure 3.16)

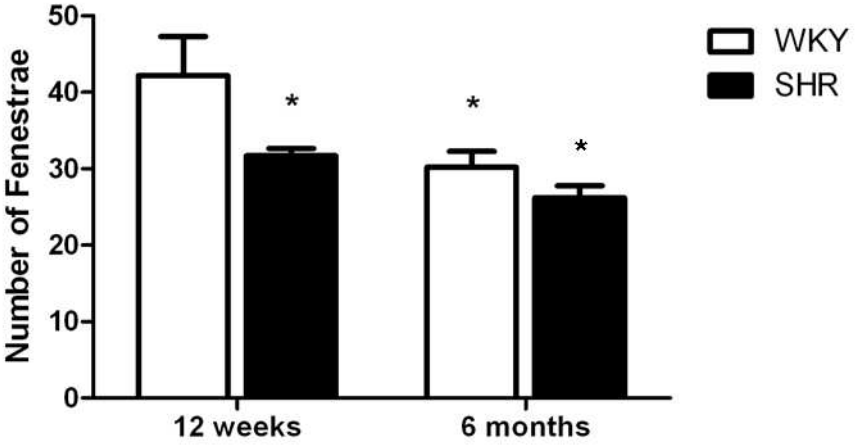


**Figure 3-16 Number of fenestrae in 12 week and 6 month old WKY (n=2) and SHR (n=2) animals. Expressed as mean ± SEM in µm². * p<0.05 compared with 12 week old WKY**

## 3.4 Discussion

There was no significant difference in outer vessel diameter between aged matched WKY and SHR, which implies that any differences observed in wall thickness or lumen diameter were a result of inward remodelling in the SHR. A

small sample size of only three for the 6 month old SHR may explain why some results did not reach statistical significance.

Since the vessels from the pressure diameter curves were later used in other protocols at 70mmHg they were not inflated above this pressure to avoid stretching. These data may have been more informative if the curves were continued to higher pressures where significant differences between the strains may have become apparent. Nevertheless, vessel dimensions at 6 months of age were analogous with those of Briones et al. (2003).

In the WKY, fenestrae number decreased with age, whilst fenestrae area increased. This was suggestive of the fusing of adjacent fenestrae during vessel growth. In the 6 month old WKY fenestrae do appear to be less distinct than those of the 6 month old SHR, with a slight "webbed" appearance which may be due to the joining of several smaller fenestrae to form a larger one. The appearance of the fenestrae was similar to that observed by Briones et al. (2003) in the 6 month old WKY and SHR. This theory of enlarging fenestrae was consistent with Wong and Langille (1996), where they state that fenestrae frequently fuse with neighbouring fenestrae in the rabbit carotid artery; and that fenestrae size increased with age between the 30 day old and the adult rabbit. In the SHR this fusing did not appear to occur, and indeed fenestrae area or number did not differ significantly with age in this strain. Fenestrae area of the 6 month old WKY and SHR in this study was comparable to Gonzalez et al. (2006). It may be that an inability of the fenestrae to fuse in the SHR strain could account for the decreased fenestrae area compared to the WKY at 6 months of age.

A study looking at the elastin *content* in small mesenteric arteries from 6 month old WKY and SHR rats showed that although fenestrae were smaller in the SHR, the amount of elastin did not differ between the strains (Briones *et al.*, 2003). It has also been shown that elastin content increased from the tenth day to the first month of life, with no further increase in the elastin content of the mesenteric arteries by 6 months of age (Gonzalez *et al.*, 2005). Elastin is reported to be synthesised only in embryonic and developing tissues, and in the vasculature the synthesis was at a maximum at the perinatal period (Davis, 1995). This was supported by the elastic laminae being completely formed by

four weeks of postnatal age in rat aorta (Gerrity & Cliff, 1975). Furthermore, elastin synthesis was found to be negligible in mature animals and mRNA levels for elastin were absent in the bovine aorta (Marriencheck *et al.*, 1995). In light of these data, the smaller fenestrae seen in the 6 month old SHR compared with the 6 month old WKY in the present study could be a result of the reorganisation of the elastin fibres rather than an increase in the production of elastin in the hypertensive strain. Gonzalez et al. (2006) also report a parallel reduction in IEL thickness and increase in fenestrae area with age in the WKY, which further suggests the elastin in the artery is able to adapt to changes in vessel diameter by remodelling. Vascular remodelling has been shown to involve either; an increase (hypertrophy); decrease (hypotrophy); or a rearrangement (eutrophy) of the vacular wall components (Mulvany *et al.*, 1996). In these terms, elastin eutrophy appears to contribute to vascular remodelling in the 6 month old SHR.

Vascular remodelling is associated with altered mechanical properties and SHR had greater intrinsic wall stiffness than WKY from 30 days onwards (Gonzalez *et al.*, 2006). It has been shown that elastase (which degraded elastin in a concentration dependent manner) incubation can abolish the structural and mechanical differences between the strains (Briones *et al.*, 2003) which suggests that the structural differences in elastin organisation are at least partly responsible for the increased wall stiffness in the SHR.

There was no significant difference between the strains in terms of fenestrae area at 12 weeks of age. However, at 6 months of age, SHR were shown to have smaller fenestrae than age-matched WKY. It is possible that if the SHR vessels are under higher pressure than WKY physiologically then fixing them at a higher pressure more representative of their physiological value would increase the fenestrae area to a size similar to that observed in the WKY. It would be interesting to pressure-fix SHR vessels at a higher pressure to determine how this affected fenestrae area and also the number of fenestrae observed per image, i.e. do the fenestrae become bigger and sparser if the artery expands.

Comparison of the fenestrae area in the literature varies, which is likely due to differences in the methodology of pressure fixing. Some papers have stated that vessels were dilated by the addition of compounds such as sodium nitrite or

sodium nitroprusside (Sandow *et al.*, 2009), or by the omission of calcium from the PSS (Briones *et al.*, 2003).

In addition to gap junctions, potassium channels have also been localised to fenestrae in the IEL of mesenteric vessels (Sandow *et al.*, 2006a; Dora *et al.*, 2008). This raises the possibility that there would be less opportunity for potassium channels to be involved in vasodilatation in the SHR, in which there are smaller fenestrae compared with WKY at 6 months of age. As yet, potassium channels at the IEL have not been studied in the SHR.

There was difficulty in obtaining images of the saphenous IEL due to thickness of the vessel wall. The pressure-fixed saphenous artery was sliced open with a scalpel and flattened on a slide in an attempt to obtain a better view of the IEL but the fenestrae were still unclear. In retrospect it may have been possible to image the IEL of this vessel whilst it was still mounted on the pressure myograph.

The presence of fenestrae was not always accompanied by a traversing cellular projection, however, the existence of the gap in the IEL may still be important in the diffusion of substances between endothelial and smooth muscle cell layers via a low resistance pathway. This has been studied previously in our laboratory (Gonzalez, unpublished) with results showing that 73% of fenestrae contained a projection in the WKY and only 40% in the SHR. This study imaged IEL and membrane projections separately due to fluorescence being in the same channel, therefore in the present study techniques were established to examine the cellular projections simultaneously to the fenestrae (Chapter 2, Figure 1.5), although this work was not pursued further due to time limitations.

A possible consequence of the reduced fenestrae area in the 6 month old SHR could be a restriction of the passage of cellular projections from the endothelial to smooth muscle cells, or conversely from smooth muscle to endothelial cells. If MEGJs located at the end of these cellular projections were to be involved in the EDHF response as reported (Chaytor *et al.*, 2001; Dora *et al.*, 2003a; Edwards *et al.*, 1999; Kühberger *et al.*, 1994) then this reduced fenestrae area in the 6 month old SHR as compared with the 6 month old WKY could account for the reduced EDHF response in the 6 month old SHR.

# Chapter 4

# Functional responses of third order mesenteric arteries from young and old WKY and SHR rats

## 4.1 Introduction

Third order mesenteric arteries (MRAs) in the rat are generally recognised as resistance arteries due to their small diameter of less than 400 microns, and their anatomical position at the end of a branching arcade which offers a high resistance pathway to the arterial blood passing through. EDHF is known to have an increasingly important role with decreasing vessel size (Chaytor *et al.*, 1998b; Shimokawa *et al.*, 1996b; Berman *et al.*, 2002; Berman *et al.*, 2002) and so rat third order MRAs were chosen in this study to establish EDHF function in the normotensive and hypertensive strains, to correlate this with the transfer of luminally loaded dye (Chapter 6). Additionally, the effect of age was studied since EDHF function is known to be impaired in ageing as well as in hypertension (Fujii *et al.*, 1993).

Much of the literature comparing WKY and SHR strains focuses surprisingly on larger vessels and not specifically on the resistance arteries which are thought to be most important in determining peripheral blood pressure. This may be due to the fact that organ baths were used to perform the experiments and the common usage of wire myographs, which are required for the study of very small resistance vessels, did not start until a later date, meaning that larger vessels were used due to a limitation of equipment available at the time.

It is well established that SHR has a greater contraction to adrenergic agonists than WKY (Mulvany & Halpern, 1977; Li *et al.*, 2007; Takata & Kato, 1995). This makes sense physiologically if an increased peripheral resistance occurs as a result of decreased lumen diameter and the SHR has a greater capacity for vascular constriction. However, the increased tone of SHR is not only due to the increased efficacy of adrenergic agonists, but is also a consequence of endothelial dysfunction (Vanhoutte, 1996). Jointly, this increase in contractility and decreased ability to relax is a major problem in blood pressure regulation in hypertension. The purpose of this chapter was to elucidate the vascular function of third order mesenteric vessels from young (12 week old) and old (6 month old) normotensive and hypertensive rats.

Arterial relaxations elicited by ACh are now known to involve different endothelium-derived factors. NO was established as an endothelium derived

relaxing factor by Moncada's group (Palmer *et al.*, 1987) following Furchgott and Zawadzki's observation that the endothelium was essential in ACh-mediated relaxations of isolated rabbit arteries (Furchgott & Zawadzki, 1980). Moncada's group also devised compounds inhibiting the synthesis of NO (Rees *et al.*, 1990), tools which consequently revealed NO was not the only factor causing an ACh-induced vascular relaxation in certain vessels. It was discovered that a factor other than NO was responsible for the hyperpolarisation to ACh in the rat small mesenteric artery (Garland & McPherson, 1992). Products of the cyclooxygenase (COX) pathway of arachadonic acid metabolism, for example, prostacyclin were also found to be involved in the relaxant response in certain vessels including bovine coronary artery and rabbit mesenteric artery (Bunting *et al.*, 1976; Dusting *et al.*, 1977).

In the presence of a combination of L-NAME and indomethacin (to block NO and prostacylin respectively), a relaxation to ACh still occurred. This factor released from the endothelium hyperpolarised the smooth muscle cells and so was termed EDHF. EDHF is known to be markedly reduced in the SHR mesenteric arteries compared with WKY controls (Fujii *et al.*, 1992), and in vessels such as third order mesenteric where the majority of the ACh-induced relaxation is accounted for by EDHF, this could be detrimental to blood pressure control. In addition to this, vessels from the SHR have been shown to release EDCF (Luscher & Vanhoutte, 1986; Rapoport & Williams, 1996; Luscher *et al.*, 1990). An imbalance in the release of EDHF and EDCF which act as physiological antagonists is thought to account for the endothelial dysfunction in this strain (Luscher, 1990; Vanhoutte, 1996).

The aim of this chapter was to assess the differing contribution of each of these endothelium-derived factors in response to ACh in third order vessels from young (12 weeks) and old (6 month) WKY and SHR rats. Since relaxations and *not* membrane potential was measured it was necessary to assume that a relaxation elicited by ACh in the presence of L-NAME and indomethacin was an EDHF response: even though the actual hyperpolarisation could not be measured, the relaxation observed was presumed to be a measure of the hyperpolarising effect on the vessel mechanics. This was further clarified by the use of a high potassium concentration to prevent the hyperpolarising response.

### *4.1.1 Aims*

The aims of this chapter were:

- To compare the PE and ACh response of 3rd order mesenteric arteries from normotensive and hypertensive rats and assess the effect of ageing on this response within strains.

- To compare the ACh response following incubation with L-NAME and indomethacin with that of the control in WKY and SHR at 12 weeks and 6 months of age.

- To assess the effect of the putative gap junction inhibitor carbenoxolone on the relaxation to ACh alone, and in combination with L-NAME and indomethacin.

- To establish if the ACh relaxant response observed following L-NAME and indomethacin incubation was representative of an EDHF response.

## 4.2 Methods

Third order mesenteric resistance vessels were myograph mounted as detailed in the General Methods (Chapter 2). Thirty minutes after the wake up procedure CCRCs to PE were constructed. After the return to baseline from washout of the PE curve a rest period of 30 minutes elapsed before an ACh CCRC was constructed. All ACh CCRCs were performed against a stable plateau of preconstriction of the artery with 10μM PE.

In a series of experiments examining the effects of endothelial factors, 100μM L-NAME and 10μM indomethacin; 10μM indomethacin; or 100μM carbenoxolone were incubated 40 minutes prior to the ACh CCRC. 30μM apamin and 1μM TRAM-34 were incubated for 1 hour prior to the ACh CCRC.

Mean data for PE-induced contraction and ACh-induced responses were compared using Student's t-tests or one-way ANOVA, with the use of Bonferroni post-tests for all pairwise comparisons.

# 4.3 Results

## *4.3.1 PE induced contraction*

Concentration dependent contractions were produced to PE in third order MRAs from WKY and SHR strains to assess the contractile responses. Representative traces of PE CCRCs are provided (Figures 4.1 and 4.2).

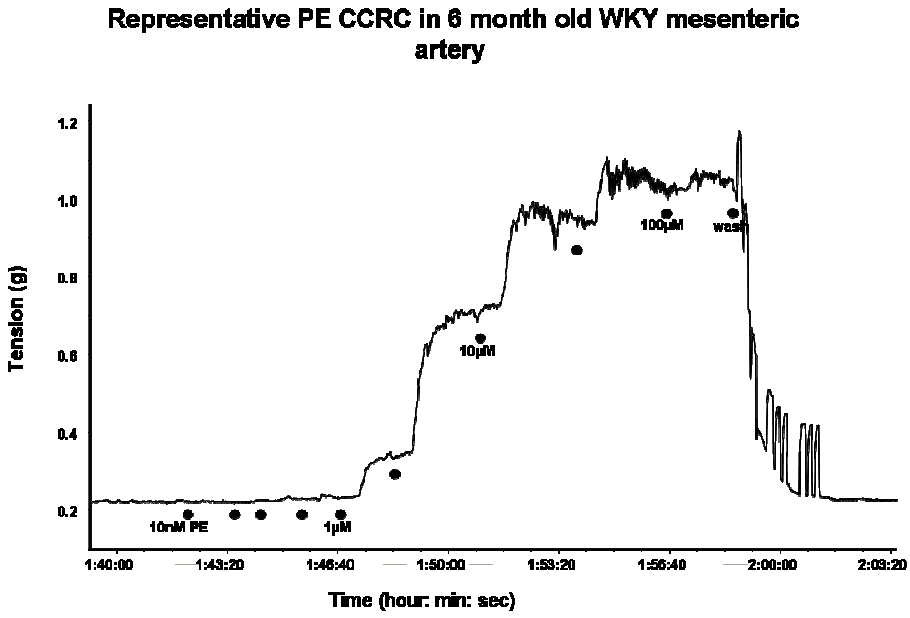


**Figure 4-1 Cumulative concentration response curve to PE in 3rd order MRA of 6 month old WKY (expressed in grams tension).**

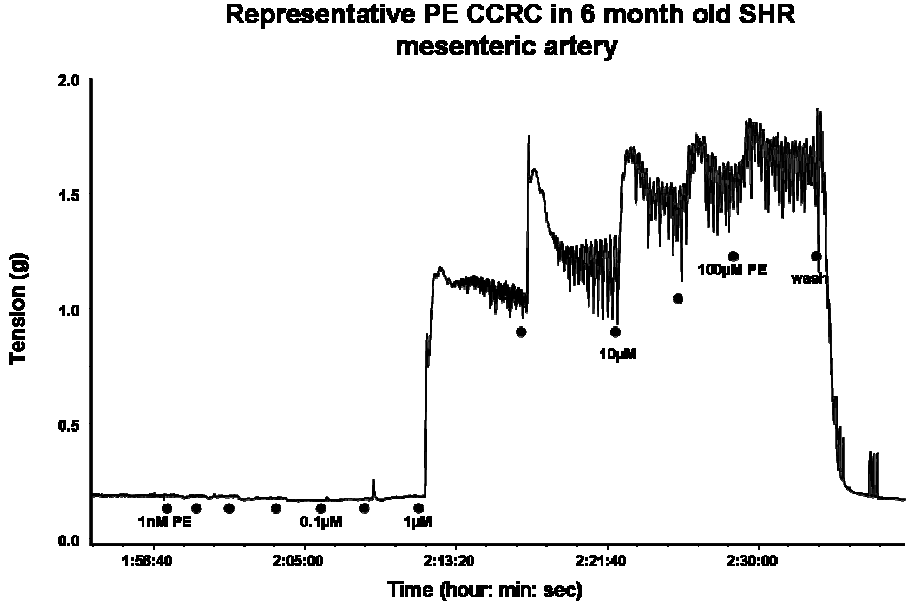


**Figure 4-2 Cumulative concentration response curve to PE in 3rd order MRA of 6 month old SHR (expressed in grams tension).**

At both age points the SHR had a significantly greater maximum response to PE than WKY. Also, for each strain, the maximum responses to PE were significantly

higher in the 6 month old than in the 12 week old animals (Figure 4.3 and Table 4.1). There was no significant difference in the $pEC_{50}$ values for PE between either of the strains or ages (Table 4.1), suggesting that the sensitivity to PE was the same in all the animals tested (Figure 4.4).

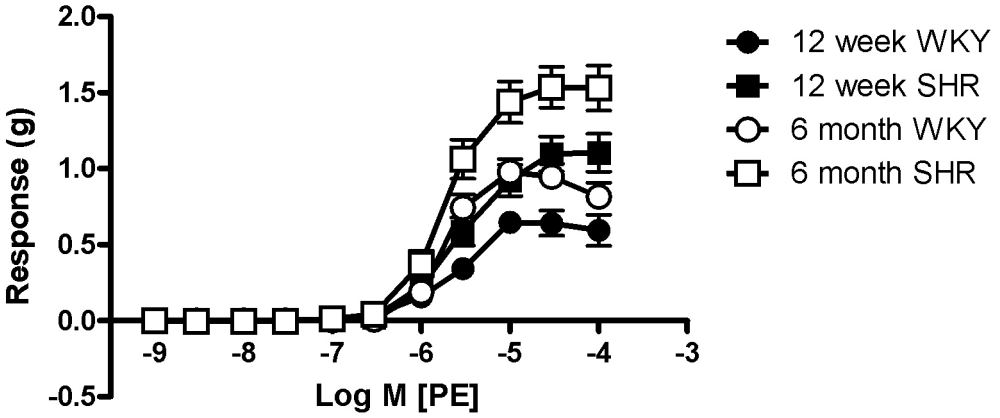


**Figure 4-3 Cumulative concentration response curves to PE in 3rd order MRAs of 12 week and 6 month old male WKY and SHR (12 week: WKY n=6; SHR n=8; and 6 month: WKY n=5, SHR n=6). Expressed as mean ± S.E.M in grams tension.**

**Table 4-1 Maximum response and $pEC_{50}$ of PE in 3rd order MRAs of 12 week and 6 month old WKY and SHR.**

| | WKY | | SHR | |
|---|---|---|---|---|
| PE | ***12 week*** | ***6 month*** | ***12 week*** | ***6 month*** |
| $E_{max}$ (g) | $0.75 \pm 0.07^{¥¥¥}$ | $1.01 \pm 0.08^{*}$ | $1.14 \pm 0.09^{**}$ | $1.57 \pm 0.14^{††¤}$ |
| $pEC_{50}$ | $5.65 \pm 0.11$ | $5.721 \pm 0.06$ | $5.70 \pm 0.08$ | $5.78 \pm 0.07$ |

**Expressed as mean ± S.E.M. (12 week: WKY n=6; SHR n=8; and 6 month: WKY n=5, SHR n=6).**

**$^{*}$ p<0.05; **p<0.01 compared with 12 week old WKY (unpaired t-test).**

**$^{††}$ p<0.01 compared with 6 month old WKY (unpaired t-test).**

**$^{¥¥¥}$ p<0.001 compared with 6 month old SHR (unpaired t-test).**

**¤ p<0.5 compared with 12 week old SHR (unpaired t-test).**

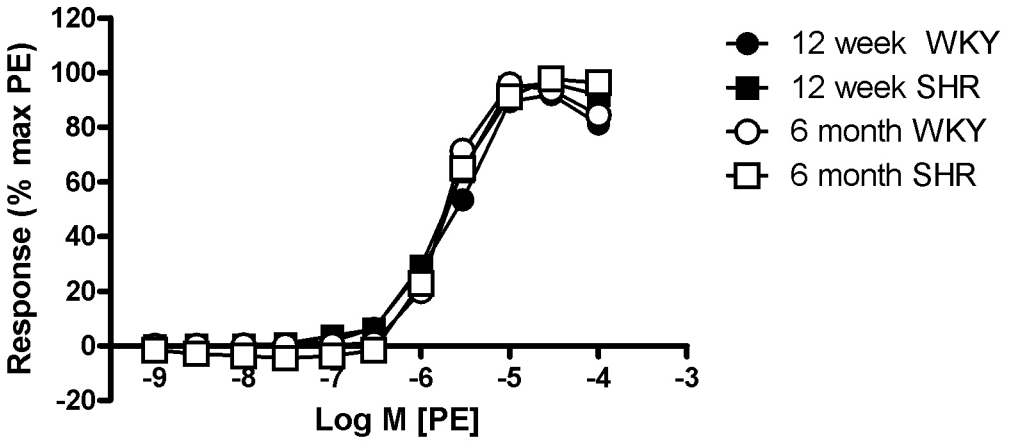


**Figure 4-4 Cumulative concentration response curves to PE in 3rd order MRAs of WKY and SHR (12 week: WKY n=6; SHR n=8; and 6 month: WKY n=5, SHR n=6). Expressed as a % of own maximum PE response obtained during CCRC, as mean ± S.E.M.**

### *4.3.2 ACh induced responses*

Responses to ACh were obtained by means of a concentration response curve following stable preconstriction with PE. Third order MRAs were precontracted with 10μM PE in order to establish a maintained constriction of the vessel upon which concentration dependent relaxations to ACh could be assessed. Representative traces of 12 week old WKY and SHR ACh CCRCs are provided (Figures 4.5 and 4.6 respectively).

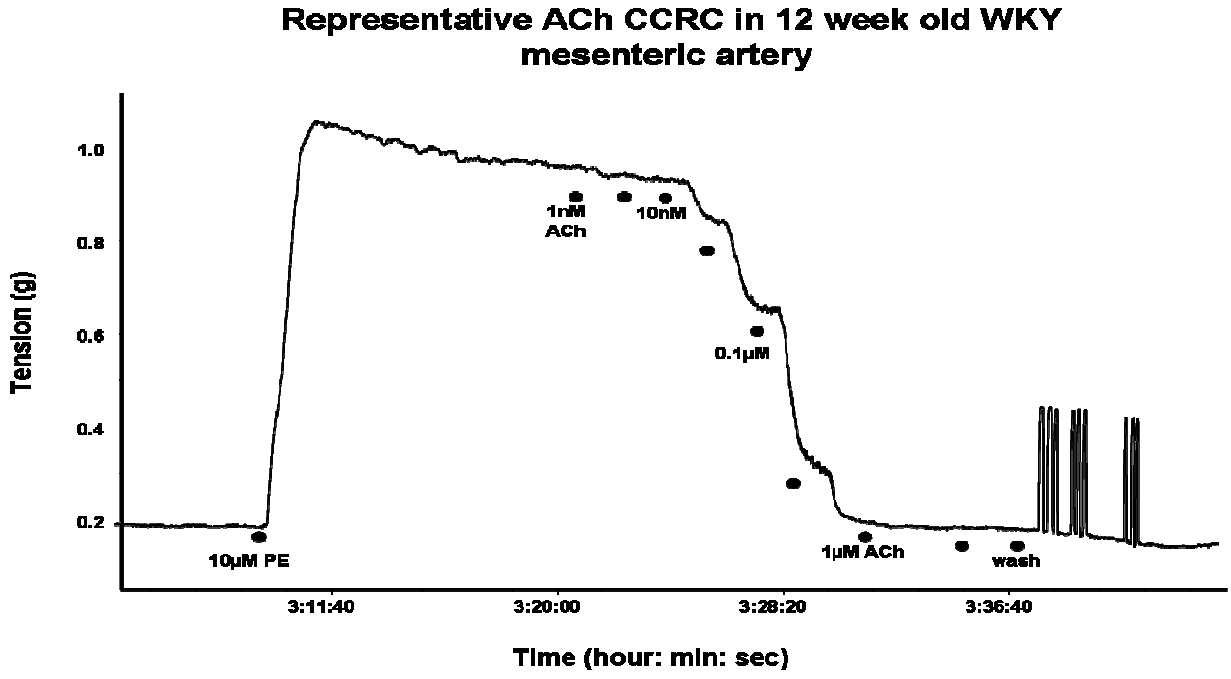


**Figure 4-5 Trace of 12 week old SHR contraction after application of 10μM PE and subsequent ACh CCRC (expressed in grams tension).**

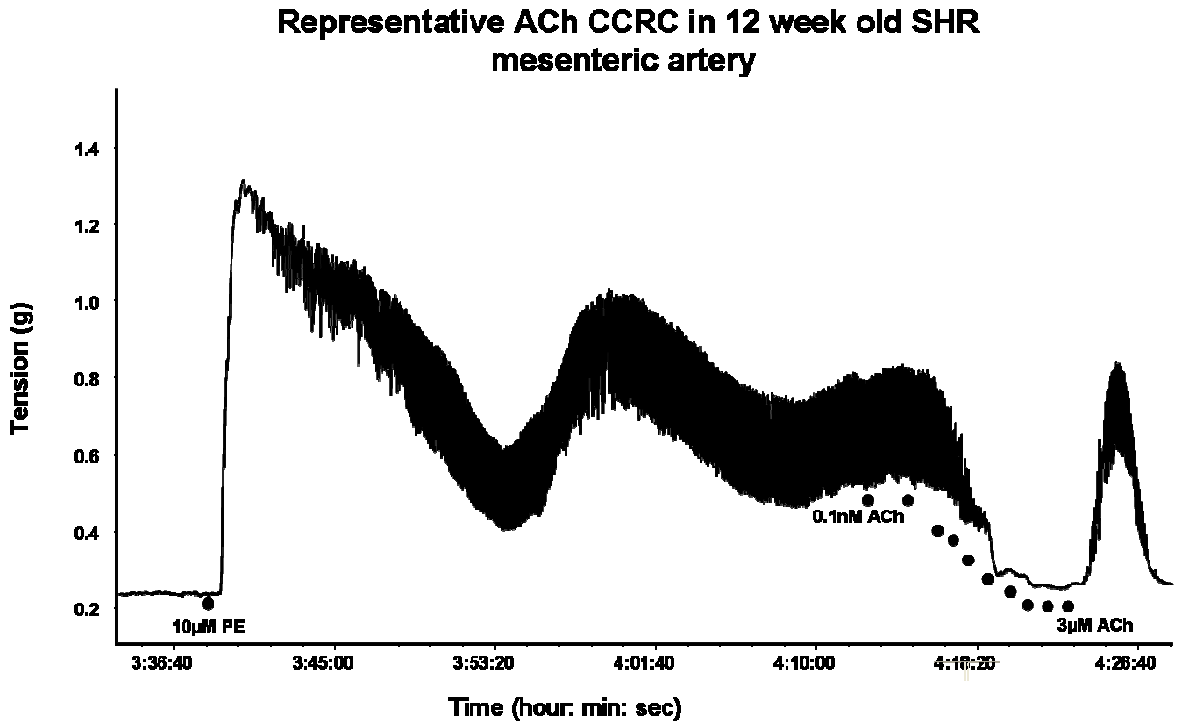


**Figure 4-6 Trace of 12 week old SHR contraction after application of 10µM PE and subsequent ACh CCRC. Representative of 4 out of 6 experiments (expressed in grams tension).**

Due to unstable PE preconstrictions in the 12 week SHR strain (Figure 4.5), there is a small sample size of only two animals for ACh induced relaxations. After a series of experiments challenging the 12 week old SHR mesenteric vessels with other agonists such as 5-HT and U-46619 in an attempt to gain a stable contractile baseline these preparations were discarded due to the spasmodic nature of the responses, since any relaxations produced by ACh could not be distinguished from the unstable nature of the pre-constriction. From six preparations tested (each with 4 replicates on the myograph) in the 12 week old SHR, a stable baseline could only be achieved in two of these experiments.

In order to make comparisons between the ACh responses in the two strains it was necessary to express the data as a percentage of the PE preconstriction, since the PE contractile responses in WKY and SHR differed (Table 4.1). Expressing the ACh relaxation as a percentage of PE-induced preconstriction is more indicative of the reversal of the PE induced tone than merely expressing it in grams, and it normalises the data between strains to take account of the greater PE response in the SHR.

For completeness the $pEC_{50}$ for ACh was expressed as a percentage of its own maximum relaxation (where 100% of its own response was always achieved) and

as a percentage of PE preconstriction (where a full reversal of the PE-induced tone was not necessarily achieved). It was shown that there was no significant difference in each group between $pEC_{50}$ values calculated by either method (Table 4.2), and for this reason any further $pEC_{50}$ values shown were calculated only as a percentage of the PE preconstriction.

**Table 4-2 Maximum relaxation and $pEC_{50}$ of ACh in 3rd order MRAs of 12 week and 6 month old WKY and SHR**

| | WKY | | SHR | |
|---|---|---|---|---|
| ACh | **12 weeks** | **6 months** | **12 weeks** | **6 months** |
| $E_{max}$ (g) | -0.64 ± 0.05 | -0.98 ± 0.08* | -1.07 ± 0.27 | -1.18 ± 0.10 |
| $E_{max}$ (% PE) | 97.78 ± 0.88 | 96.06 ± 1.45 | 91.23 ± 6.28 | 85.66 ± 4.39 |
| $pEC_{50}$ (% own max) | 7.62 ± 0.13 | 7.67 ± 0.11 | 7.23 ± 0.40 | 7.62 ± 0.17 |
| $pEC_{50}$ (% PE) | 7.53 ±0.09 | 7.76 ± 0.13 | 6.95 ± 0.36 | 7.51 ± 0.17 |

**Expressed as mean ± S.E.M in grams tension and as a percentage relaxation of PE-induced contraction. (12 week: WKY n=4; SHR n=2; and 6 month: WKY n=5, SHR n=6).**

***p<0.05 compared with 12 week old WKY (unpaired t-test).**

The $pEC_{50}$ of ACh was not significantly different between strains at 12 weeks of age (Table 4.2). Also, the maximum response to ACh, normalised for both strains as a percentage relaxation of the PE induced contraction, was not significantly different between the strains at 12 weeks. In terms of grams relaxation, SHR had a greater response than WKY at 12 weeks (although this was not statistically significant), most likely due to the fact that it had a far greater contractile response to PE from the outset and therefore has a greater capacity for relaxation. However, this 12 week SHR data must be interpreted with caution since the ACh data has a small sample size of only two, with the other four experiments discarded due to an unstable preconstriction to PE. This implies that the data from the two experiments analysed may not be a fair representation of the 12 week old SHR's response to ACh.

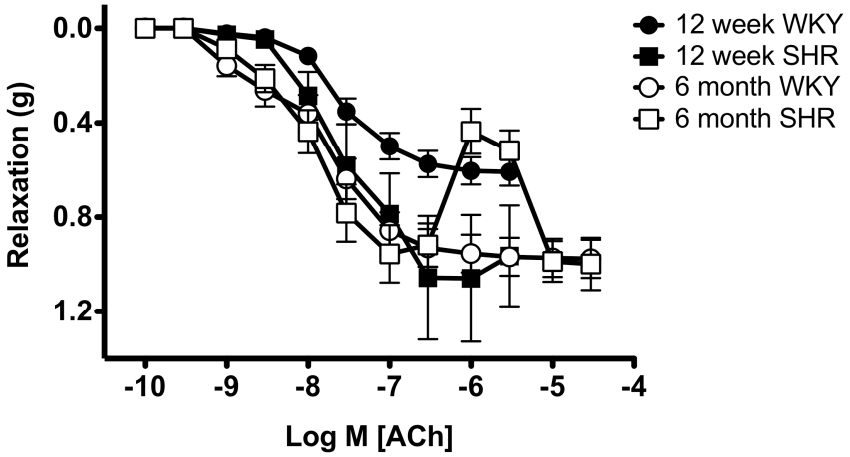


**Figure 4-7 Cumulative concentration response curves to ACh in 3rd order MRAs of WKY and SHR. (12 week: WKY n=4; SHR n=2; and 6 month: WKY n=5, SHR n=6). Expressed as mean ± S.E.M in grams tension.**

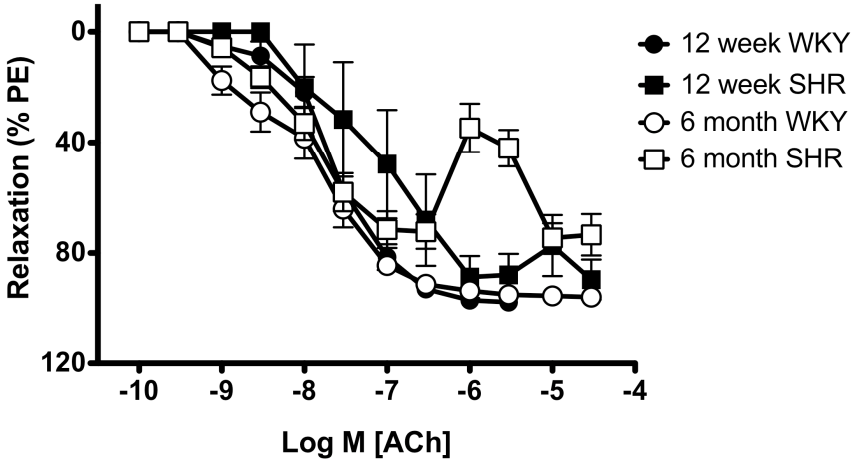


**Figure 4-8 Cumulative concentration response curves to ACh in 3rd order MRAs of WKY and SHR. (12 week: WKY n=4; SHR n=2; and 6 month: WKY n=5, SHR n=6). Expressed as mean ± S.E.M as a % of PE preconstriction.**

6 month WKY and SHR show very different profiles in their response to cumulative concentrations of ACh, although there was no significant difference in their $pEC_{50}$ values. The 6 month old WKY showed a steady decrease in tension until a maximal relaxation of near 100% was achieved, thus almost fully reversing the PE induced contraction (Table 4.2). However, the 6 month old SHR reacted very differently with an "upshoot" in the CCRC following maximal relaxation at concentrations of ACh greater than 3μM (Figures 4.7 and 4.8).

### 4.3.2.1 ACh Time Control CCRCs

Time control curves showed that there was no desensitisation of the tissue to ACh and so any differences shown on a second curve following incubation with a drug were a true effect of the drug. Time control curves for 12 week old WKY, 6

month old WKY, and 6 month old SHR strains (Figure 4.9, 4.10 and 4.11 respectively) showed that there was no significant difference between the first and second ACh curves (Tables 4.3, 4.4 and 4.5 respectively), indicating that there was no desensitisation of the tissue. Since only one time control curve was able to be performed for the 12 week old SHR it was not possible to mean the data to calculate an accurate $pEC_{50}$ or maximum relaxation for 1st and 2nd curves in this strain.

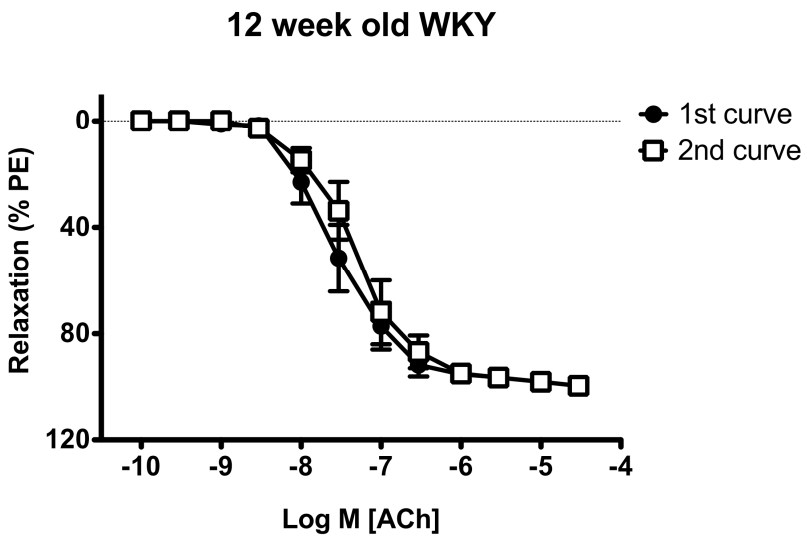


**Figure 4-9 Comparison of ACh response for control and time control CCRC in 3rd order MRAs of 12 week old WKY (n=5). Response expressed as % relaxation of PE preconstriction mean ± S.E.M.**

**Table 4-3 Comparison of ACh response for control and time control CCRCs in 3rd order MRAs of 12 week old WKY.**

| ACh | 1st curve | 2nd curve |
|---|---|---|
| $E_{max}$ (% PE) | 96.31 ± 2.47 | 96.50 ± 1.37 |
| $pEC_{50}$ (% PE) | 7.51 ± 0.18 | 7.28 ± 0.18 |

**Expressed as mean ± S.E.M as a percentage relaxation of PE-induced contraction (n=5).**

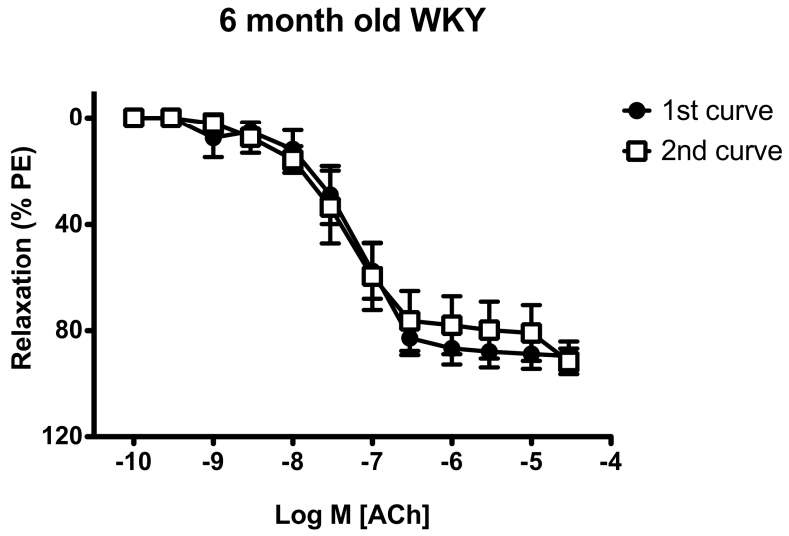


**Figure 4-10 Comparison of ACh response for control and time control CCRC in 3rd order MRAs of 12 week old WKY (n=5). Response expressed as % relaxation of PE preconstriction mean ± S.E.M.**

**Table 4-4 Comparison of ACh response for control and time control CCRCs in 3rd order MRAs of 6 month old WKY.**

| ACh | 1st curve | 2nd curve |
|---|---|---|
| $E_{max}$ (% PE) | 89.52 ± 5.43 | 81.66 ± 10.51 |
| $pEC_{50}$ (% PE) | 7.42 ± 0.15 | 6.99 ± 0.32 |

**Expressed as mean ± S.E.M as a percentage relaxation of PE-induced contraction (n=5).**

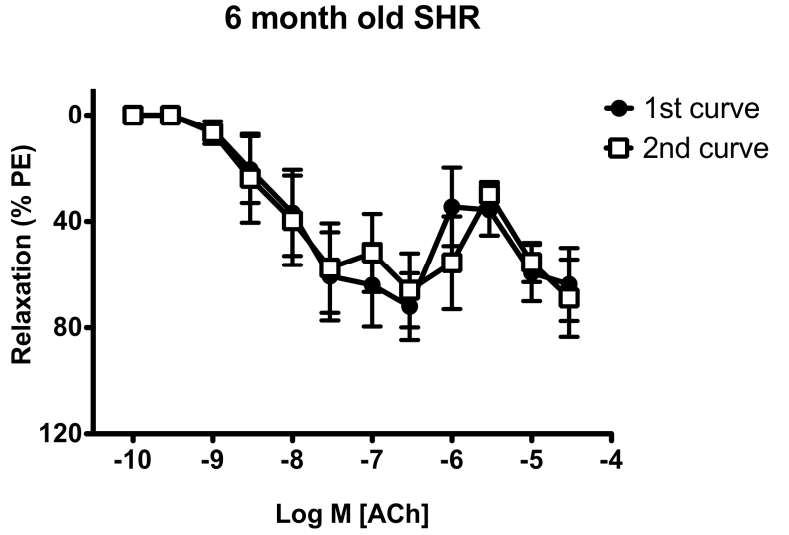


**Figure 4-11 Comparison of ACh response for control and time control CCRC in 3rd order MRAs of 6 month old SHR (n=5). Response expressed as % relaxation of PE preconstriction mean ± S.E.M.**

**Table 4-5 Comparison of ACh response for control and time control CCRCs in 3rd order MRAs of 6 month old SHR.**

| ACh | 1st curve | 2nd curve |
|---|---|---|
| $E_{max}$ (% PE) | 85.27 ± 9.34 | 82.90 ± 10.29 |
| $pEC_{50}$ (% PE) | 7.85 ± 0.32 | 7.77 ± 0.42 |

**Expressed as mean ± S.E.M as a percentage relaxation of PE-induced contraction (n=5).**

### *4.3.3 Responses to ACh following incubation with agents affecting endothelial factors*

Further ACh responses were assessed after incubation with compounds affecting various endothelium derived factors to gain a better insight into the mechanisms of the ACh response. Due to the unstable nature of the 12 week old SHR preconstrictions it was not possible to examine the effects of all the compounds on endothelial function in this strain- in the two experiments where stable preconstrictions were maintained the EDHF response was assessed.

#### 4.3.3.1 L-NAME and indomethacin incubation

ACh CCRCs were obtained in 12 week and 6 month old third order mesenteric vessels with a stable PE-induced preconstriction (Figures 4.12 and 4.13 respectively) following L-NAME and indomethacin incubation to block the production of NO and prostaglandins.

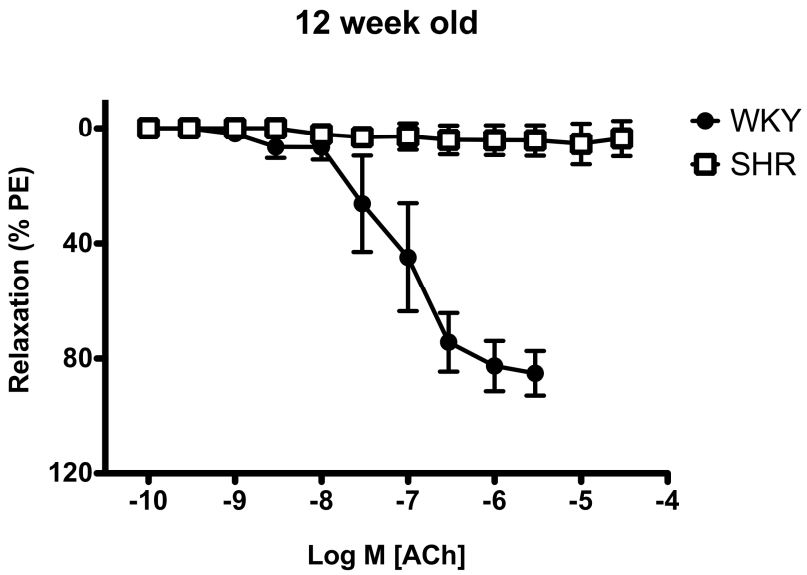


**Figure 4-12 Cumulative concentration response curves to ACh following 40 min 100μM L-NAME and 10μM indomethacin incubation in 3rd order MRAs of 12 week old male WKY (n=5) and SHR (n=2). Response expressed as % relaxation of PE preconstriction mean ± S.E.M.**

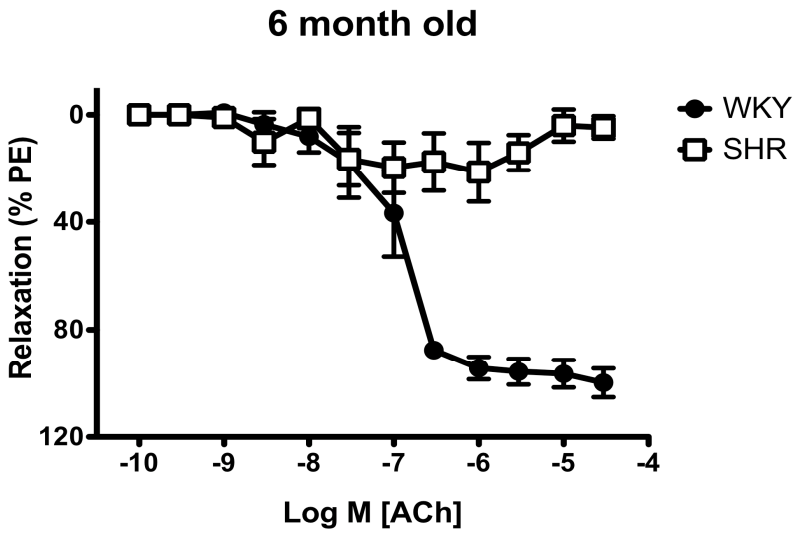


**Figure 4-13 Cumulative concentration response curves to ACh following 40 min 100μM L-NAME and 10μM indomethacin incubation in 3rd order MRAs of 6 month old male WKY (n=5) and SHR (n=6). Response expressed as % relaxation of PE preconstriction mean ± S.E.M.**

It was not possible to calculate an accurate $pEC_{50}$ for ACh in the SHR following L-NAME and indomethacin incubation at either age point since there was practically no relaxant response. Incubation with L-NAME and indomethacin significantly reduced the maximum ACh-induced relaxation in both the 12 week and 6 month old SHR compared with control data (Tables 4.6 and 4.7).

In the WKY, incubation with L-NAME and indomethacin reduced the maximum ACh-induced relaxation in the 12 week old but did not significantly alter the relaxation compared with the control data in the 6 month old (Tables 4.6 and 4.7). The $pEC_{50}$ was significantly decreased in the 12 week and 6 month old WKY (Tables 4.6 and 4.7) following incubation with L-NAME and indomethacin, thus indicating a decrease in sensitivity to ACh.

### 4.3.3.2 Indomethacin incubation

Further experiments were undertaken to assess the effects of incubating indomethacin alone in 12 week old and 6 month old rats (Figure 4.11 and 4.12 respectively). This left the NO component of relaxation intact and removed the COX-mediated component of the ACh response.

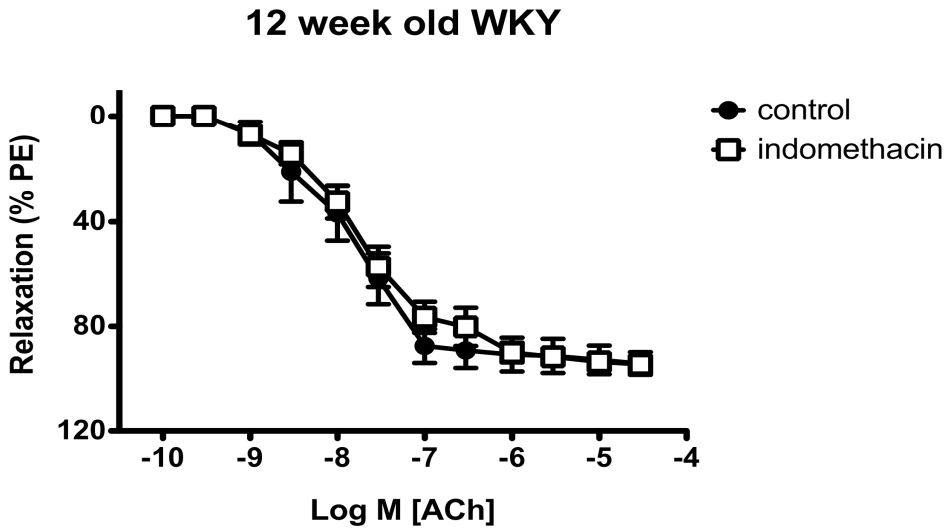


**Figure 4-14 Cumulative concentration response curve to ACh following 40 min 10μM indomethacin incubation in 3rd order MRAs of 12 week old male WKY (n=5). Response expressed as % relaxation of PE preconstriction mean ± S.E.M.**

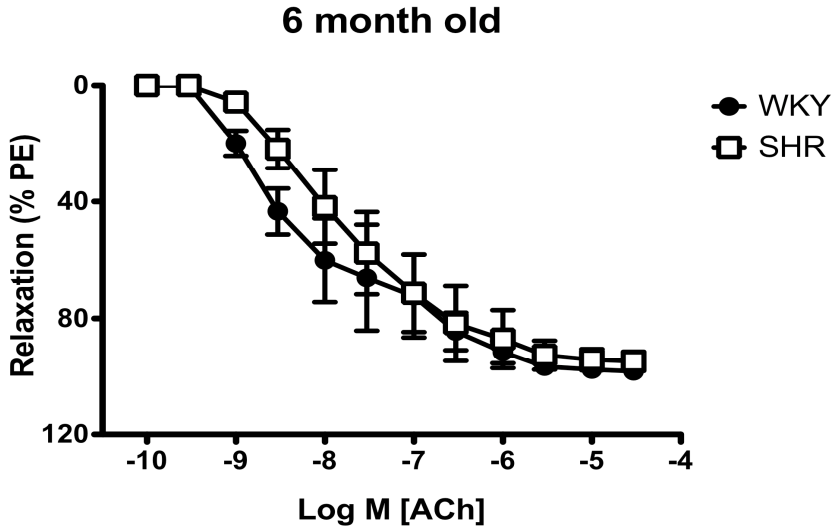


**Figure 4-15 Cumulative concentration response curves to ACh following 40 min 10μM indomethacin incubation in 3rd order MRAs of 6 month old male WKY (n=5) and SHR (n=5). Response expressed as % relaxation of PE preconstriction mean ± S.E.M.**

In the 12 week old WKY indomethacin did not significantly alter the maximum ACh-induced relaxation or the $pEC_{50}$ of ACh as compared with control data (Table 4.6). In the 6 month old animals, indomethacin incubation meant the SHR relaxation had the same profile as the WKY (Figure 4.12), and removed the secondary increase in tension to ACh seen under control conditions. However, incubation with indomethacin did not alter the sensitivity to ACh in either strain (Table 4.7).

### 4.3.3.3 Carbenoxolone incubation

The effect of carbenoxolone on ACh mediated responses in third order mesenteric vessels of 12 week and 6 month old WKY and SHR was assessed (Figures 4.13 and 4.14 respectively).

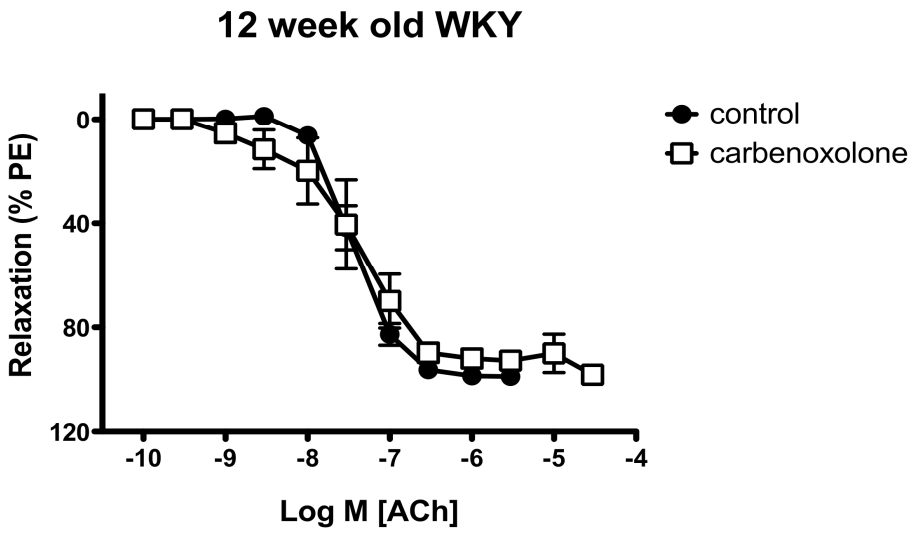


**Figure 4-16 Cumulative concentration response curves to ACh following 40 min 100μM carbenoxolone incubation in 3rd order MRAs of 12 week old male WKY (n=5). Response expressed as % relaxation of PE preconstriction mean ± S.E.M.**

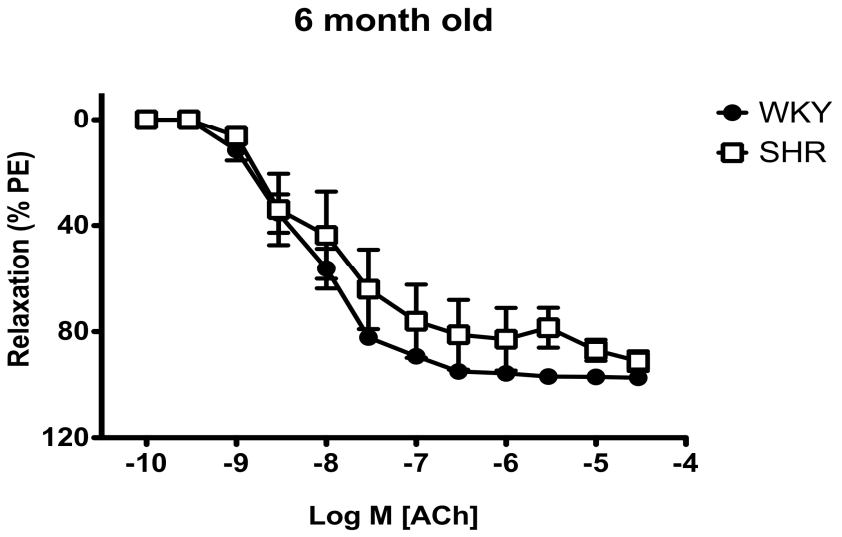


**Figure 4-17 Cumulative concentration response curves to ACh following 40 min 100μM carbenoxolone incubation in 3rd order MRAs of 6 month old male WKY (n=5) and SHR (n=5). Response expressed as % relaxation of PE preconstriction, mean ± S.E.M.**

In the 12 week old WKY and both strains at 6 months carbenoxolone did not affect the ACh-induced relaxant response in terms of efficacy or sensitivity since there was no significant difference between maximum relaxations and $pEC_{50}$s in vessels under control conditions and following incubation with carbenoxolone

(Table 4.6 and Table 4.7). Carbenoxolone incubation abolished the secondary increase in tension seen in the 6 month SHR control (Table 4.7).

### 4.3.3.4 Carbenoxolone incubation in the presence of L-NAME and indomethacin

Since carbenoxolone did not significantly alter the maximum relaxation or the sensitivity to ACh in the mesenteric arteries of either strain or age, it was tested in combination with L-NAME and indomethacin to remove the contribution of NO or prostanoids. This was only performed in the 12 week old WKY due to animal availability (Figure 4.15).

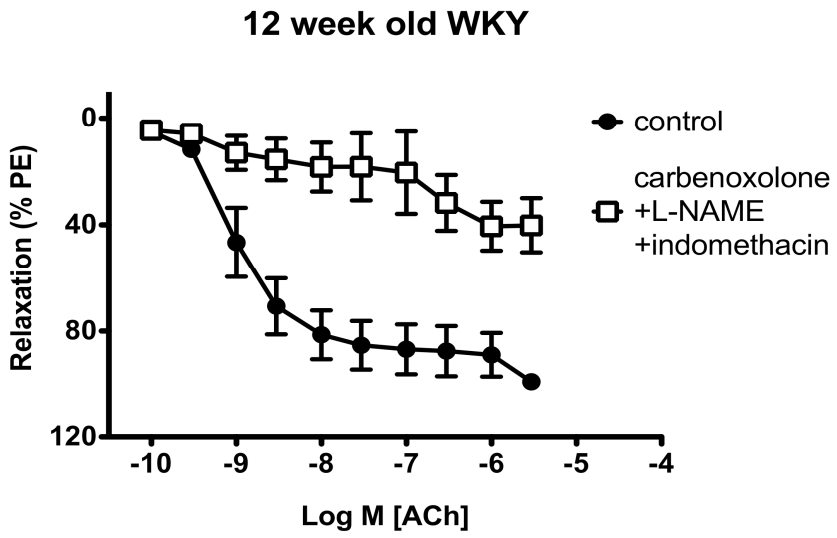


**Figure 4-18 Cumulative concentration response curves to ACh following 40 min 100μM L-NAME and 10μM indomethacin incubation in control, and +300μL carbenoxolone in 3rd order MRAs of 12 week old male WKY (n=4). Response expressed as % relaxation of PE preconstriction mean ± S.E.M.**

Carbenoxolone incubated in combination with L-NAME and indomethacin significantly reduced the maximum relaxation to ACh in the 12 week old WKY (Table 4.6).

**Table 4-6 Summary of ACh induced responses in 12 week old WKY and SHR 3rd order mesenteric arteries following incubation with agents affecting endothelium derived factors.**

| 12 week old | n | Relaxation to ACh | | Increase in tension to ACh |
|---|---|---|---|---|
| | | $E_{max}$ (% of PE) | $pEC_{50}$ | |
| WKY | | | | |
| Control | 5 | 97.82 ± 1.51 | 7.48 ± 0.25 | No |
| + L-NAME and indomethacin | 5 | 85.17 ± 7.73†† | 6.88 ± 0.31 | No |
| Control | 5 | 94.18 ± 4.28 | 7.74 ± 0.33 | No |
| + indomethacin | 5 | 94.52 ± 2.81 | 7.47 ± 0.20 | No |
| Control | 5 | 98.92 ± 0.71 | 7.43 ± 0.07 | No |
| +carbenoxolone | 5 | 93.22 ± 3.43 | 7.47 ± 0.25 | No |
| Control | 4 | 97.51 ± 1.73 | 7.84 ± 0.17 | No |
| + L-NAME, indomethacin and carbenoxolone | 4 | 42.98 ± 10.18*** | - | No |
| SHR | | | | |
| Control | 2 | 91.23 ± 6.28 | 7.23 ± 0.39 | No |
| + L-NAME and indomethacin | 2 | 5.50 ± 4.19◊◊◊ | - | No |

**Relaxations expressed as % relaxation of PE preconstriction, mean ± S.E.M in %, and $pEC_{50}$ as mean ± S.E.M.**

**††p<0.001 (unpaired t-test) compared with SHR + L-NAME and indomethacin, ◊◊◊ p<0.0001 compared with control, *** p<0.0001 compared with control (1 way-ANOVA).**

**Table 4-7 Summary of ACh induced responses in 6 month old WKY and SHR 3rd order mesenteric arteries following incubation with agents affecting endothelium derived factors.**

| 6 month old | n | Relaxation to ACh | | Increase in tension to ACh |
|---|---|---|---|---|
| | | $E_{max}$ (% of PE) | $pEC_{50}$ | |
| WKY | | | | |
| Control | 5 | 96.57 ± 2.09 | 7.87 ± 0.23 | No |
| + L-NAME and indomethacin | 5 | 96.70 ± 5.25$^{\lozenge\lozenge}$ | 7.04 ± 0.18 | No |
| Control | 5 | 99.15 ± 0.31 | 7.74 ± 0.33 | No |
| + indomethacin | 5 | 98.32 ± 0.42 | 7.86 ± 0.42 | No |
| Control | 5 | 96.43 ± 2.29 | 7.98 ± 0.26 | No |
| +carbenoxolone | 5 | 97.41 ± 0.89 | 8.22 ± 0.15 | No |
| SHR | | | | |
| Control | 6 | 88.68 ± 5.34 | 7.81 ± 0.18 | Yes |
| + L-NAME and indomethacin | 6 | 30.58 ± 9.61*** | - | No |
| Control | 5 | 93.10 ± 2.90 | 6.82 ± 0.51 | Yes |
| + indomethacin | 5 | 94.91 ± 3.39$^{\dagger\dagger\dagger}$ | 7.52 ± 0.44 | No |
| Control | 5 | 93.57 ± 3.23 | 7.62 ± 0.33 | Yes |
| +carbenoxolone | 5 | 92.79 ± 2.64$^{\$\$\$}$ | 7.64 ± 0.53 | No |

**Relaxations expressed as % relaxation of PE preconstriction, mean ± S.E.M in %, and $pEC_{50}$ as mean ± S.E.M.**

*****p<0.0001 compared with control (1 way-ANOVA).**

**$^{\dagger\dagger\dagger}$ p<0.0001 (1 way-ANOVA); $^{\$\$\$}$ p<0.0001 (1 way-ANOVA); $^{\lozenge\lozenge}$ p<0.001 (unpaired t-test) compared with SHR + L-NAME and indomethacin .**

### *4.3.4 Further examination of responses to PE in 12 week old SHR (following incubation with indomethacin or carbenoxolone)*

In order to gain a better understanding of the unstable nature of the PE response in the 12 week old SHR mesenteric vessels a series of experiments was performed to assess the effects of indomethacin and carbenoxolone individually on a CCRC to PE. Indomethacin blocks the COX enzyme which is known to be involved in the production of EDCF by acting on arachadonic acid.

Time control experiments were performed to ensure there was no desensitisation to PE on the second curve (Figure 4.15). There was no difference in sensitivity or efficacy of PE in the first and second curves (Table 4.8).

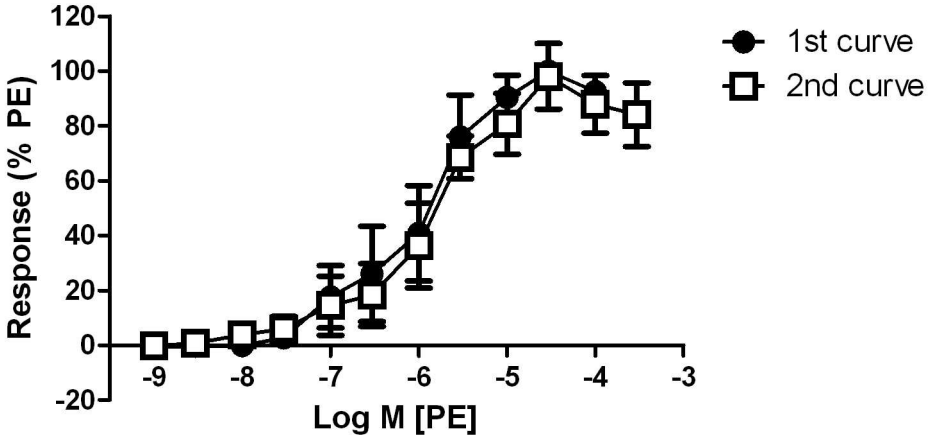


**Figure 4-19 Cumulative concentration response curves to PE in 3rd order MRAs of 12 week old SHR (n=4). Expressed as a % of maximum PE response obtained during 1st CCRC as mean ± S.E.M.**

**Table 4-8 Maximum response and $pEC_{50}$ of PE in 1st and 2nd curves of 3rd order MRAs of 12 week old SHR.**

| *PE* | *1st curve* | *2nd curve* |
|---|---|---|
| $E_{max}$ (% PE) | 100 ± 0.00 | 92.07 ± 5.737 |
| $pEC_{50}$ | 5.94 ± 0.32 | 6.07 ± 0.287 |

**Expressed as % of maximum PE response obtained during 1st CCRC as mean ± S.E.M (n=4).**

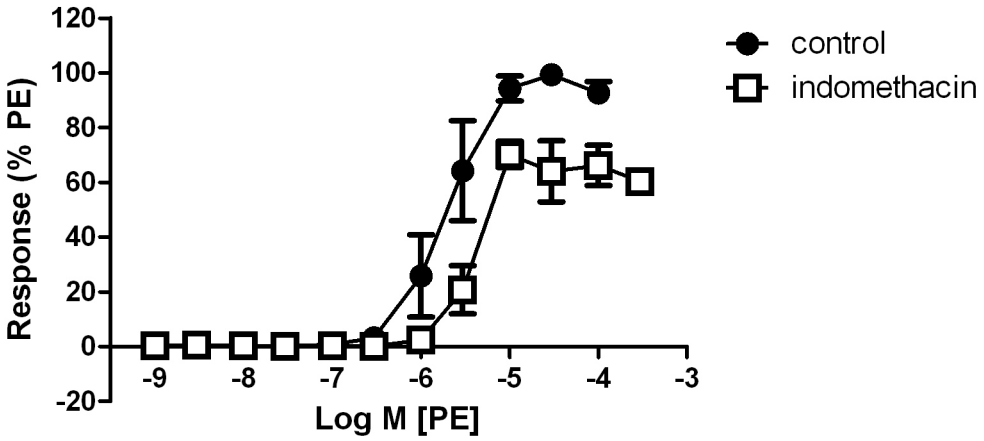


**Figure 4-20 Cumulative concentration response curves to PE following 40 min 10μM indomethacin incubation (n=4). Expressed as a % of maximum PE response obtained during control CCRC as mean ± S.E.M.**

**Table 4-9 Maximum response and $pEC_{50}$ of PE in 3rd order MRAs of 12 week old SHR.**

| PE | *Control* | *Indomethacin* |
|---|---|---|
| $E_{max}$ (% PE) | 100 ± 0.00 | 74.24 ± 5.15** |
| $pEC_{50}$ | 5.72 ± 0.18 | 5.24 ± 0.07† |

**Expressed as % of maximum PE response obtained during 1st CCRC as mean ± S.E.M (n=4).**
**† p<0.05, **p<0.001 paired t-test compared with control.**

Figure 4.17 showed that incubation with indomethacin prior to the PE CCRC caused a significant decrease in the maximum response and decreased the sensitivity of the tissue compared with the control (Table 4.9). In contrast, Figure 4.18 showed that incubation with carbenoxolone prior to the PE CCRC did not affect PE efficacy or sensitivity (Table 4.10).

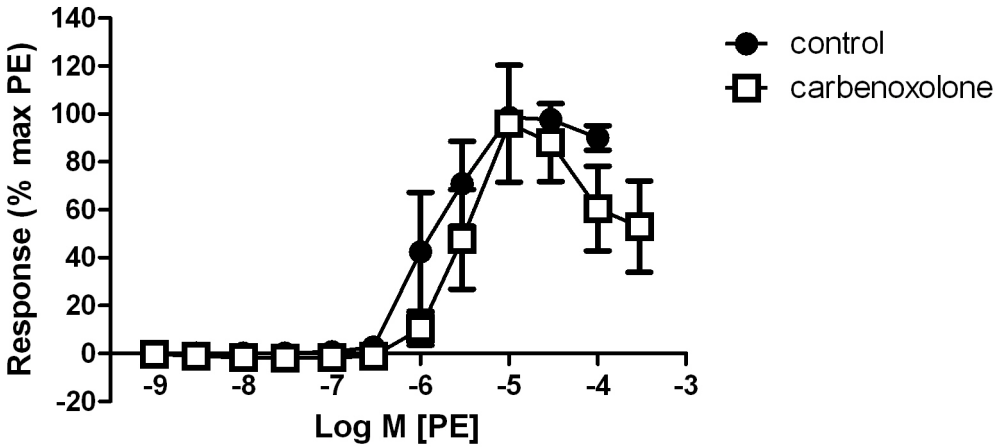


**Figure 4-21 Cumulative concentration response curves to PE following 40 min 100μM carbenoxolone incubation. Expressed as a % of maximum PE response obtained during control CCRC as mean ± S.E.M (n=4).**

**Table 4-10 Maximum response and $pEC_{50}$ of PE in 3rd order MRAs of 12 week old SHR.**

| PE | *Control* | *Carbenoxolone* |
|---|---|---|
| $E_{max}$ (% PE) | 100 ± 0.00 | 97.75 ± 23.35 |
| $pEC_{50}$ | 5.85 ± 0.22 | 5.49 ± 0.13 |

**Expressed as % of maximum PE response obtained during 1st CCRC as mean ± S.E.M (n=4).**

### *4.3.5 Hyperpolarisation of Endothelial Cells*

Since facilities were not available to measure the cell membrane potential, further experiments were performed to determine if the relaxation observed in the presence of L-NAME and indomethacin was in fact representative of an endothelial hyperpolarisation spreading to the smooth muscle cells. This was done by adding high potassium (30mM KCl) to the myograph bath and then adding cumulative concentrations of PE to achieve the same level of preconstriction as in the L-NAME and indomethacin curve. A CCRC to ACh was then performed upon this preconstriction (Figure 4.19). It was found that after the vessel was exposed to 30mM KCl there was no longer a relaxation observed in the CCRC to ACh (Figure 4.20). The addition of KCl to the preparation caused a small contraction in response to concentrations of ACh above 10 μm (Table 4.11) as opposed to the near full relaxation observed under control conditions.

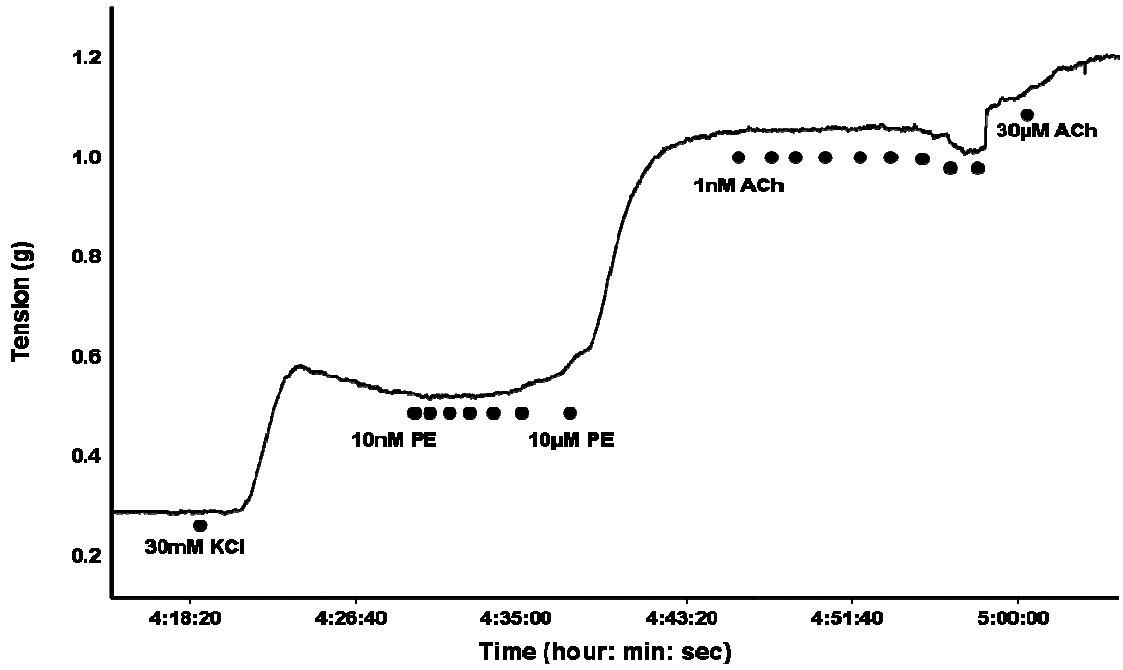


**Figure 4-22 Representative trace of mesenteric vessel from 12 week old WKY after exposure to 30mM KCl then addition of PE to preconstrict vessel prior to ACh CCRC.**

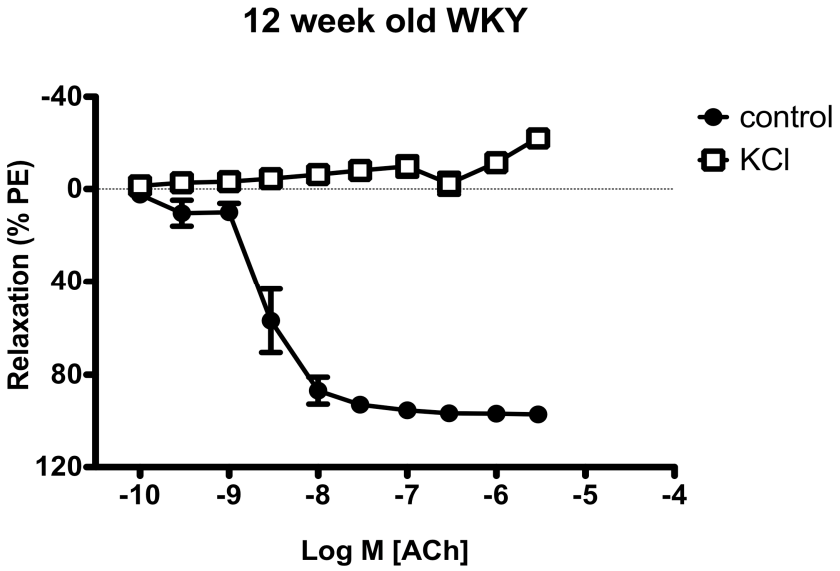


**Figure 4-23 Cumulative concentration response curves to ACh following 40 min 100µM L-NAME and 10µM indomethacin incubation: control vessels pre-constricted with 10µM PE; and vessels exposed to 30mM KCl prior to ACh CCRC (n=2)**

**Table 4-11 Maximum relaxation and $pEC_{50}$ of ACh in 3rd order MRAs of 12 week old WKY control (constricted with PE) and KCl (constricted with 30mM KCl prior to further PE pre-constriction).**

| ACh | *Control* | *KCl* |
|---|---|---|
| $E_{max}$ (% PE) | 97.04 ± 1.83 | -22.06 ± 1.70*** |
| $pEC_{50}$ | 7.54 ± 0.12 | - |

**Expressed as a % of PE preconstriction as mean ± S.E.M (n=2).**

***p<0.001 paired t-test compared with control.**

### *4.3.6 Evidence that the relaxation to ACh following incubation of L-NAME and indomethacin is an EDHF response*

It is well documented that the relaxant response persisting in the presence of L-NAME + indomethacin is an EDHF-mediated response. To confirm that this was the case in these particular experiments, blockers of the small and intermediate calcium-activated potassium channels ($SK_{Ca}$ and $IK_{Ca}$ respectively) located on the endothelium were employed to prevent the hyperpolarisation of the endothelial cells upon ACh application (Figure 4.21). The $SK_{Ca}$ and $IK_{Ca}$ channel blockers apamin and TRAM-34 used in combination significantly reduced the relaxation which persisted in the presence of L-NAME and indomethacin in the 12 week old WKY (Table 4.12). These channel blockers could not be tested in the 6 month old animals due to lack of animal availability.

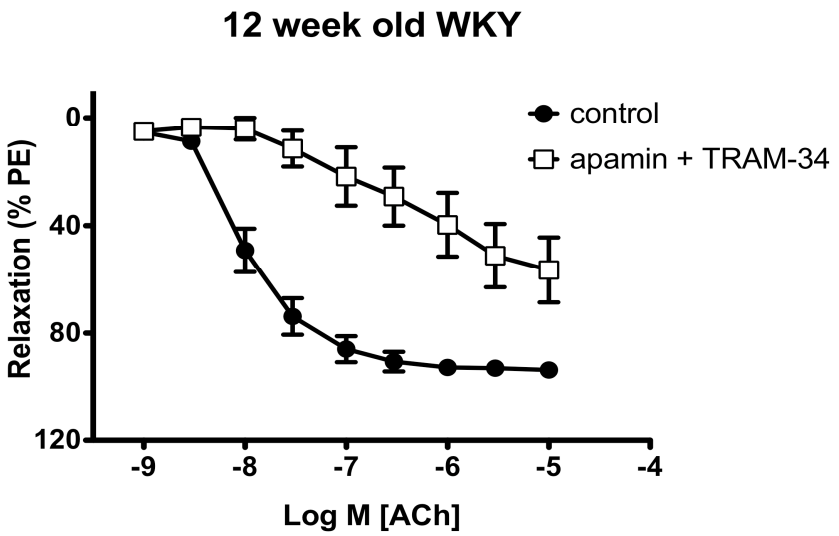


**Figure 4-24 Cumulative concentration response curves to ACh (1nM to 10mM) following 40 min 100μM L-NAME and 10μM indomethacin incubation control, and + 30μM apamin and 1μM TRAM-34 (n=4).**

**Table 4-12 Maximum relaxation and $pEC_{50}$ of ACh in 3rd order MRAs of 12 week old WKY control vessels and vessels incubated in apamin and TRAM-34. All vessels exposed to 100μM L-NAME and 10μM indomethacin for 40 minutes.**

| ACh | *Control* | *Apamin + TRAM-34* |
|---|---|---|
| $E_{max}$ (g) | 97.34 ± 0.54 | 59.01 ± 10.90** |
| $pEC_{50}$ | 7.87 ± 0.15 | 6.28 ± 0.59** |

**Expressed as a % of PE pre-constriction as mean ± S.E.M (n=4).**

****p<0.01 paired t-test compared with control.**

## 4.4 Discussion

PE had greater efficacy in SHR compared with WKY at both age points, yet there was no difference in the sensitivity to PE between any of the groups. This implied that the SHR had a greater capacity for contraction due to either: increased smooth muscle mass; release of other factors that constrict the vessel; or a decrease in compensatory relaxation. A possible candidate for this increase in contraction would be EDCF, since one mechanism of its release is an increase in intracellular calcium in the endothelial cells (Vanhoutte *et al.*, 2005). In the 12 week old SHR strain where there was difficulty in obtaining CCRCs to ACh due to an unstable preconstriction to PE, an alternative approach was attempted to examine the effects of indomethacin on the release of endothelial-derived factors. Since PE sensitivity was the same in WKY and SHR but PE still elicited a greater response in SHR, this suggested it was caused by the release of a contractile factor or a lack of compensatory relaxation against the PE response. Indomethacin was incubated before the CCRC in the SHR to determine whether this reduced the size of the PE response, bearing in mind that indomethacin abolished the secondary increase in tone to ACh in the 6 month old SHR- thought to be attributed to EDCF. EDCF is a product of arachadonic acid metabolism by COX (Vanhoutte & Tang, 2008) and in fact, inhibition of COX by indomethacin did significantly reduce the maximal PE-induced response and caused a decrease in PE sensitivity in the 12 week old SHR vessels.

A secondary contraction to ACh was observed in 6 month old SHR after maximal relaxation had been achieved. It was presumed to be an endothelium-derived contraction and not a direct effect of ACh on the SMCs since this secondary contractile response to ACh was abolished by indomethacin which blocks the COX enzyme that is involved in the production of EDCF (Vanhoutte & Tang, 2008). Therefore, this latter contraction at higher concentrations of ACh in the 6 month old SHR appears to be due to the release of EDCF which is partly responsible for the endothelial dysfunction in this strain, combined with a reduction in EDHF (Vanhoutte & Tang, 2008).

In SHR at both age points ACh elicited almost no response following incubation with L-NAME and indomethacin, indicating that EDHF was not the prevalent relaxing factor in this strain. This was in contrast to the WKY response to ACh

following L-NAME and indomethacin incubation which showed that the tissue was still capable of a full relaxation in the presence of these agents which block NO and prostaglandins. These data do not necessarily mean that the full relaxation to ACh is mediated by EDHF rather than NO in the WKY under control conditions, but they do show that when NO production was blocked EDHF was capable of fully compensating.

When indomethacin was present there was no longer a significant difference between 6 month old WKY and SHR relaxation in terms of efficacy or sensitivity. This suggested that the difference between the strains in control experiments was due to a factor produced by the COX enzyme, which was inhibited by indomethacin. These data are consistent with other data showing an increased release of EDCF in SHR mesenteric vessels compared with WKY (Jameson *et al.*, 1993); and data showing that indomethacin improved the impaired endothelium-dependent relaxations in the small mesenteric arteries of the SHR (Luscher *et al.*, 1990).

Carbenoxolone abolished the secondary increase in tension observed in the 6 month old SHR under control conditions. Also, there was no longer a significant difference between the strains at 6 months of age in terms of their relaxation to ACh following carbenoxolone incubation: vessels from the SHR no longer had an increase in tension in response to higher concentrations of ACh; and the endothelium-dependent relaxation in the SHR was now capable of almost fully reversing the PE induced preconstriction. This suggested that if the increase in tension to ACh in the SHR strain was indeed accounted for by EDCF, as was implied by its removal when the COX enzyme was blocked by indomethacin, then carbenoxolone was somehow involved in inhibiting its actions. Carbenoxolone is a putative gap junction blocker which has been shown to abolish EDHF in rat mesenteric vessels (Goto *et al.*, 2002) and so if EDCF were to be transmitted through gap junctions in a similar fashion to EDHF then it is feasible that carbenoxolone is capable of blocking EDCF also. Indeed, carbenoxolone has been shown to reduce endothelium-derived contractions to ACh in the aorta of the SHR (Tang & Vanhoutte, 2008). Further studies using the gap junction blocking peptides would be of interest to assess whether they also inhibited the secondary increase in tension to ACh in the 6 month old SHR. This was not feasible in this project due to cost, but would give a better understanding of

whether carbeoxolone's impediment of EDCF were indeed a consequence of gap junction blockade.

Incubation with carbenoxolone alone did not affect the relaxation to ACh in the 12 week or 6 month old WKY, but has been shown in publications to inhibit the EDHF component of relaxation (Goto *et al.*, 2002). Since there was still a complete relaxation to ACh following carbenoxolone incubation this suggested that if gap junctions (and hence a possible route of EDHF transmission) were blocked, then NO was capable of compensating and eliciting a full relaxation in these vessels. To clarify this point, further ACh CCRCs were performed following incubation with L-NAME and carbenoxolone in combination to assess whether a relaxation to ACh could still be achieved when the NO component of relaxation was removed and the putative gap junction blocker was present. In combination with L-NAME and indomethacin, carbenoxolone significantly reduced the maximum relaxation to ACh. This implied that carbenoxolone had some effect in blocking MEGJs, which was only apparent when the NO-mediated component of relaxation was removed.

To ensure that the relaxation to ACh which persisted in the presence of L-NAME and indomethacin was a true EDHF response (to refute the possibility that the concentration of L-NAME was not sufficient to block NOS), ACh CCRCs were performed in the presence of L-NAME, indomethacin, apamin and TRAM-34 in combination. Under these conditions the relaxations were significantly reduced from the control (L-NAME and indomethacin incubation only), however, the relaxation to ACh was not completely abolished at concentrations above 10μM. This raised the possibility of the remaining relaxation being an unknown factor, independent of NO, prostanoids and hyperpolarisation of the endothelial cells by means of opening calcium-activated potassium channels. Alternatively, this could be due to incomplete blockade of the calcium-activated potassium channels. However, the latter explanation is unlikely considering the concentrations of these toxins used in the present study are consistent with those used in the literature (Harrington *et al.*, 2007).

All functional responses were measured as changes in tension on a myograph, therefore these results alone did not prove conclusively that the relaxation to ACh in the absence of NO was a *hyperpolarising* factor. To confirm that this was

a hyperpolarising response, the relaxation to ACh was assessed following application of 30mM KCl to depolarise the vessel in the presence of L-NAME and indomethacin. KCl caused a contraction around 30% of the PE induced contraction- thereafter PE was added cumulatively to ensure the preconstriction matched that of the control. Under these conditions, ACh did not elicit a relaxation, thus suggesting that the control relaxation in the presence of L-NAME and indomethacin was caused by a hyperpolarisation of the endothelial cells. Under control conditions the concentration of potassium ions is greater in the cytoplasm than in the extracellular space, thus the opening of calcium-activated potassium channels on the endothelial cells causes an efflux of potassium ions down the electrochemical gradient, consequently hyperpolarising the endothelial cell. This hyperpolarisation by potassium ion efflux was reinforced by the decreased maximum relaxation to ACh in the presence of apamin and TRAM-34 in combination. When extracellular potassium ion concentration was increased by application of 30mM KCl, the endothelial cells were no longer capable of hyperpolarisation, and no relaxation was observed. This lack of relaxation to ACh under conditions of high potassium in the presence of L-NAME was consistent with other findings (Dora *et al.*, 2003a; Waldron & Garland, 1994).

# Chapter 5

# Functional responses of saphenous arteries from young and old WKY and SHR rats

# 5.1 Introduction

The saphenous artery has been reported as one which exhibits no EDHF response in the adult rat, proposed to be due to a lack of MEGJs (Sandow *et al.*, 2004). In this respect the saphenous artery contrasts with the mesenteric arteries which are known to have a prominent EDHF component of relaxation (Chapter 4, (Dora *et al.*, 2003a; Edwards *et al.*, 1999). Thus, the saphenous artery was chosen in this study to compare its functional responses to those of the mesenteric arteries where EDHF has a prominent role. The functional responses of saphenous arteries from normotensive and hypertensive rats at two age points: 12 week old and 6 month old, were assessed by wire myography. This was intended to elucidate whether there was an EDHF response in the young rat that became redundant during ageing owing to the reported decrease in MEGJ expression (Sandow *et al.*, 2004).

## *5.1.1 Aims*

The aims of this chapter were:

- To compare the PE contractile response of 12 week and 6 month old WKY and SHR.

- To compare the relaxation of 12 week and 6 month old WKY and SHR in response to ACh, and the contribution of EDHF, if any, in this relaxation.

- To assess the effect of the putative gap junction inhibitor carbenoxolone on the ACh relaxation in the saphenous artery.

# 5.2 Methods

Saphenous arteries were myograph mounted as detailed in the General Methods chapter. Thirty minutes after the wake up procedure CCRCs to PE were constructed. After the return to baseline from washout of the PE curve a rest period of 30 minutes elapsed before an ACh CCRC was constructed. All ACh CCRCs were performed against a stable plateau of preconstriction of the artery with 10μM PE.

In a series of experiments examining the effects of endothelial factors, L-NAME and indomethacin; indomethacin; or carbenoxolone were incubated 40 minutes prior to the ACh CCRC.

Due to some relaxations not reaching 50% of PE preconstriction, it was not possible to provide accurate $pEC_{50}$ values for saphenous arteries as a percentage of the PE-induced preconstriction. Instead, the $pEC_{50}$ was expressed as the concentration of ACh required to produce half of the maximal relaxation in grams.

Mean data for PE-induced contraction and ACh-induced responses were compared using Student's t-tests or one-way ANOVA, with the use of Bonferroni post-tests for all pairwise comparisons.

## 5.3 Results

### *5.3.1 PE-induced contraction*

Concentration dependent contractions were produced to PE in saphenous arteries from both WKY and SHR strains to assess the contractile responses (Figures 5.1 and 5.2). The response to PE in the 12 week old SHR was significantly greater than that of the other groups tested (Table 5.1), however this must be interpreted with caution since there is a small sample size of only two. There was no significant difference in the PE contraction of the 6 month old WKY and SHR rats, and the 6 month old rats of both strains had a greater PE contraction than the 12 week old WKY.

12 week old SHR had significantly greater $pEC_{50}$ value than 12 week old WKY, and the $pEC_{50}$ values of PE were significantly higher at 6 months than at 12 weeks of age in both strains. However, there was no significant difference in $pEC_{50}$ values between strains at the same age point (Figure 5.1 and Table 5.1).

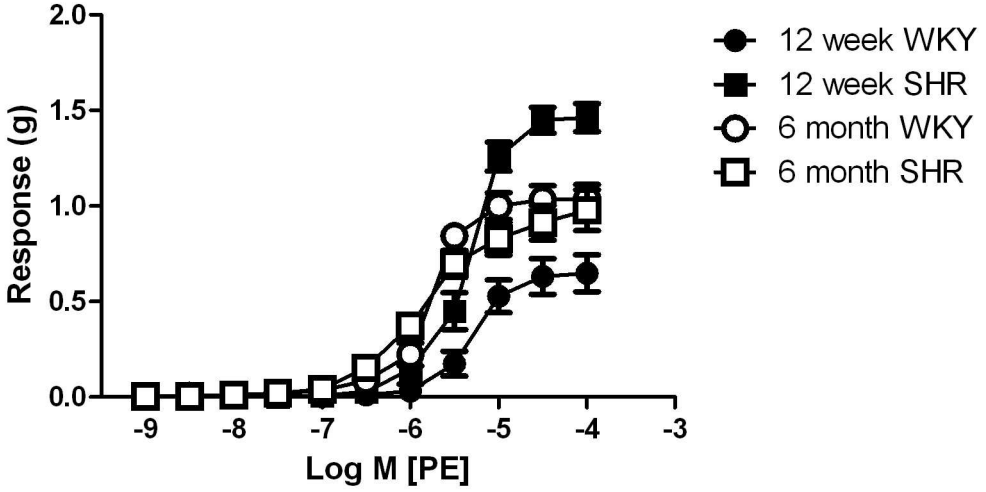


**Figure 5-1 Cumulative concentration response curves to PE in saphenous arteries of WKY and SHR (12 week: WKY n=4; SHR n=2; and 6 month: WKY n=5, SHR n=4). Expressed as mean ± S.E.M in grams tension.**

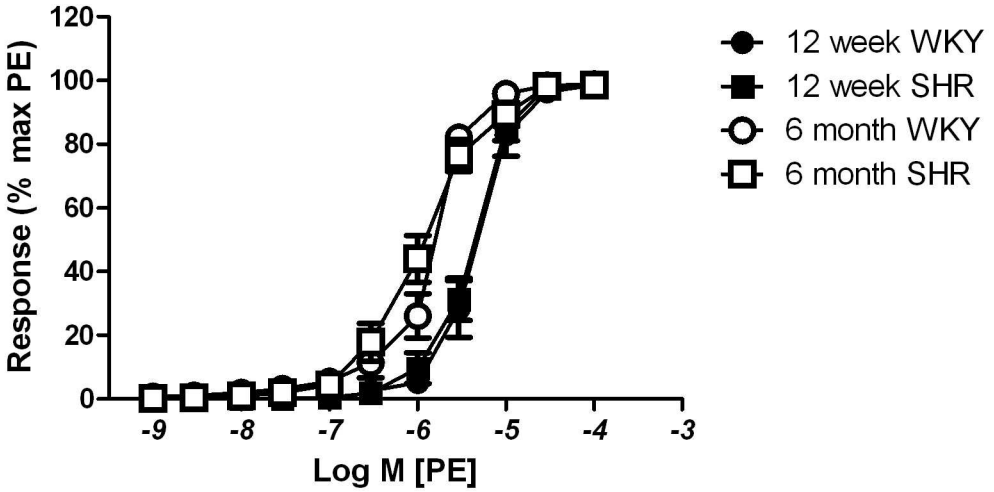


**Figure 5-2 Cumulative concentration response curves to PE in saphenous arteries of WKY and SHR (12 week: WKY n=4; SHR n=2; and 6 month: WKY n=5, SHR n=4). Expressed as a % of own maximum PE response obtained during CCRC as mean ± S.E.M.**

**Table 5-1 Maximum response and $pEC_{50}$ of PE in saphenous arteries of 12 week and 6 month old WKY and SHR.**

| | WKY | | SHR | |
|---|---|---|---|---|
| PE | ***12 week*** | ***6 month*** | ***12 week*** | ***6 month*** |
| $E_{max}$ (g) | 0.65 ± 0.10 | 1.04 ± 0.07** | 1.48 ± 0.07*** | 0.88 ± 0.09$^{\dagger\dagger\dagger}$ |
| $pEC_{50}$ | 4.94 ± 0.07 | 5.92 ± 0.09*** | 5.37 ± 0.07*** | 5.91 ± 0.12$^{\dagger\dagger}$ |

**Expressed as mean ± S.E.M. (12 week: WKY n=4; SHR n=2; and 6 month: WKY n=5, SHR n=4).**

**** p<0.01, ***p<0.001 compared with 12 week old WKY (unpaired t-test)**

**$^{\dagger\dagger}$ p<0.01, $^{\dagger\dagger\dagger}$p<0.001 compared with 12 week old SHR (unpaired t-test)**

### *5.3.2 ACh-induced responses*

Relaxations to ACh were obtained in a concentration dependent manner in both strains at both ages (Figures 5.2 and 5.3). The 12 week old SHR had a significantly greater relaxation to ACh (expressed in grams or as a percentage of PE preconstriction) than any of the other groups tested. The 12 week old WKY and 6 month old WKY and SHR had no significant difference in their relaxation to ACh (Table 5.2). The $pEC_{50}$ values were not significantly different in any of the groups (Table 5.2).

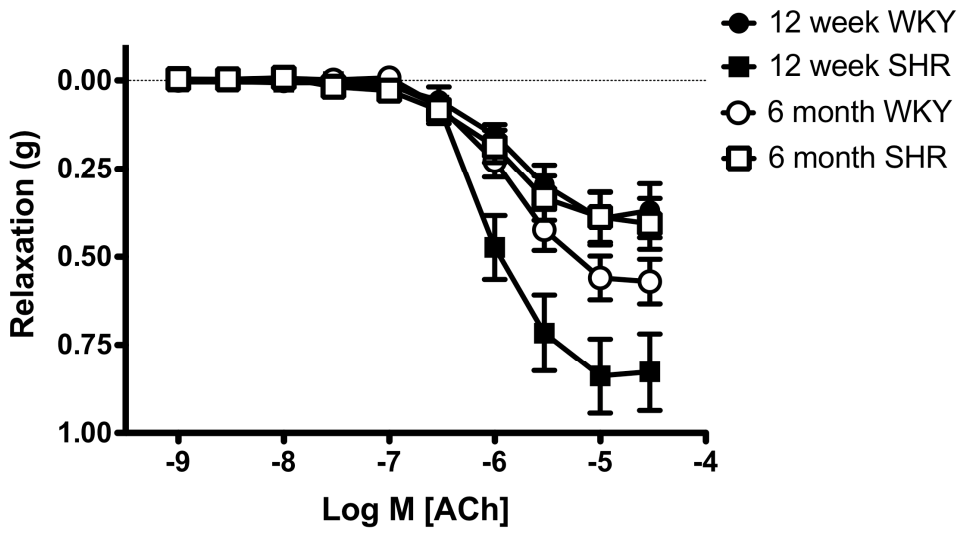


**Figure 5-3 Cumulative concentration response curves to ACh in saphenous arteries of WKY and SHR. (12 week: WKY n=4; SHR n=2; and 6 month: WKY n=5, SHR n=4). Expressed as mean ± S.E.M in grams tension.**

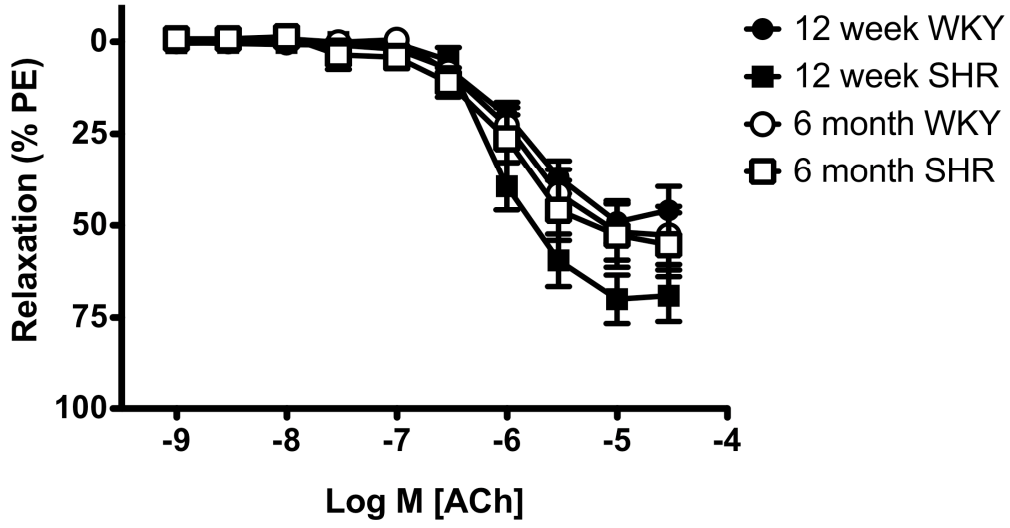


**Figure 5-4 Cumulative concentration response curves to ACh in saphenous arteries of WKY and SHR (12 week: WKY n=4; SHR n=2; and 6 month: WKY n=5, SHR n=4). Expressed as mean ± S.E.M as a % of PE preconstriction.**

**Table 5-2 Maximum relaxation and $pEC_{50}$ of ACh in saphenous arteries of 12 week and 6 month old WKY and SHR.**

| | WKY | | SHR | |
|---|---|---|---|---|
| ACh | **12 weeks** | **6 months** | **12 weeks** | **6 months** |
| $E_{max}$ (g) | 0.40 ± 0.07 | 0.58 ± 0.06 | 0.84 ± 0.11** | 0.41 ± 0.07†† |
| $E_{max}$ (% PE) | 50.67 ± 5.66 | 59.54 ± 7.53 | 70.27 ± 6.64* | 55.53 ± 8.71††† |
| $pEC_{50}$ (% own max) | 5.90 ± 0.06 | 5.90 ± 0.07 | 6.03 ± 0.06 | 5.99 ± 0.10 |

**Expressed as mean ± S.E.M in grams tension and as a percentage relaxation of PE-induced contraction (12 week: WKY n=4; SHR n=2; and 6 month: WKY n=5, SHR n=4).**

***p<0.5, **p<0.01 compared with 12 week old WKY (unpaired t-test)**

**††p<0.01, †††p<0.001 compared with 12 week old SHR (unpaired t-test)**

### *5.3.3 ACh Time Control CCRCs*

Time control curves to ACh were performed to show that there was no desensitisation of the tissue to ACh on the second curve, and so any differences observed after incubation with a drug could be considered a true effect of the drug. Time controls were performed for 12 week and 6 month old WKY and SHR (Figures 5.5, 5.6, 5.7 and 5.8), and showed no significant difference in either maximum relaxation or $pEC_{50}$ between the first and second curve (Table 5.3, 5.4, 5.5 and 5.6).

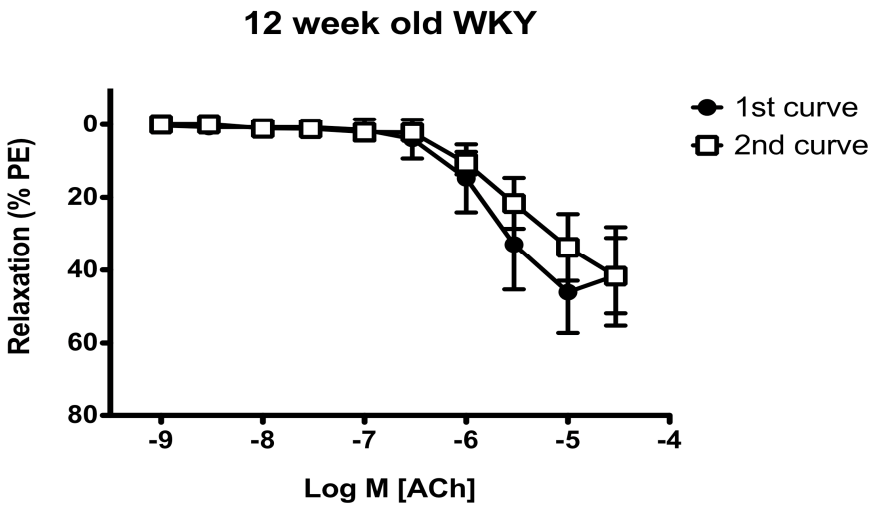


**Figure 5-5 Comparison of ACh response for control and time control CCRCs in saphenous arteries of 12 week old WKY (n=4). Response expressed as % relaxation of PE preconstriction mean ± S.E.M.**

**Table 5-3 Comparison of ACh response for control and time control CCRCs in saphenous arteries of 12 week old WKY.**

| ACh | 1st curve | 2nd curve |
|---|---|---|
| $E_{max}$ (% PE) | 41.41 ± 11.32 | 41.75 ± 13.51 |
| $E_{max}$ (g) | 0.49 ± 0.16 | 0.38 ± 0.17 |
| $pEC_{50}$ (%own max) | 6.38 ± 0.32 | 6.27 ± 0.48 |

**Expressed as mean ± S.E.M (n=4).**

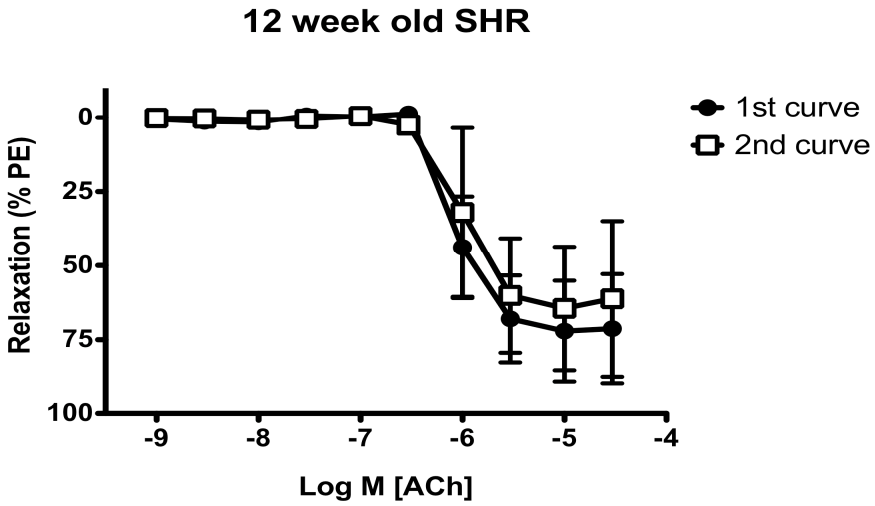


**Figure 5-6 Comparison of ACh response for control and time control CCRCs in saphenous arteries of 12 week old SHR (n=2). Response expressed as % relaxation of PE preconstriction mean ± S.E.M.**

**Table 5-4 Maximum relaxation and $pEC_{50}$ of ACh in saphenous arteries of 12 week old SHR.**

| ACh | 1st curve | 2nd curve |
|---|---|---|
| $E_{max}$ (% PE) | 72.42 ± 17.25 | 65.57 ± 21.91 |
| $E_{max}$ (g) | 0.76 ± 0.03 | 0.85 ± 0.28 |
| $pEC_{50}$ (% own max) | 6.06 ± 0.08 | 5.96 ± 0.20 |

**Expressed as mean ± S.E.M (n=2).**

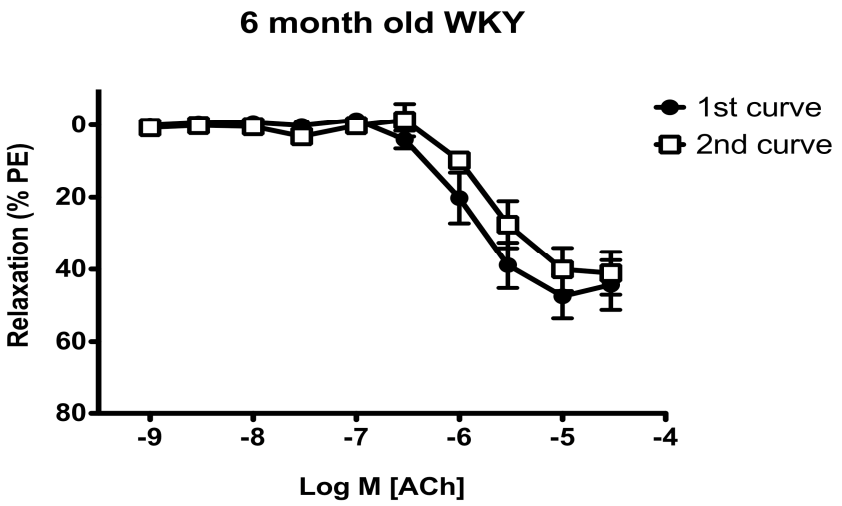


**Figure 5-7 Comparison of ACh response for control and time control CCRCs in saphenous arteries of 6 month old WKY (n=5). Response expressed as % relaxation of PE preconstriction mean ± S.E.M.**

**Table 5-5 Comparison of ACh response for control and time control CCRCs in saphenous arteries of 6 month old WKY.**

| ACh | 1st curve | 2nd curve |
|---|---|---|
| $E_{max}$ (% PE) | 47.95 ± 6.07 | 41.14 ± 5.97 |
| $E_{max}$ (g) | 0.42 ± 0.92 | 0.32 ± 0.07 |
| $pEC_{50}$ (% own max) | 5.97 ± 0.15 | 5.63 ± 0.07 |

**Expressed as mean ± S.E.M (n=5).**

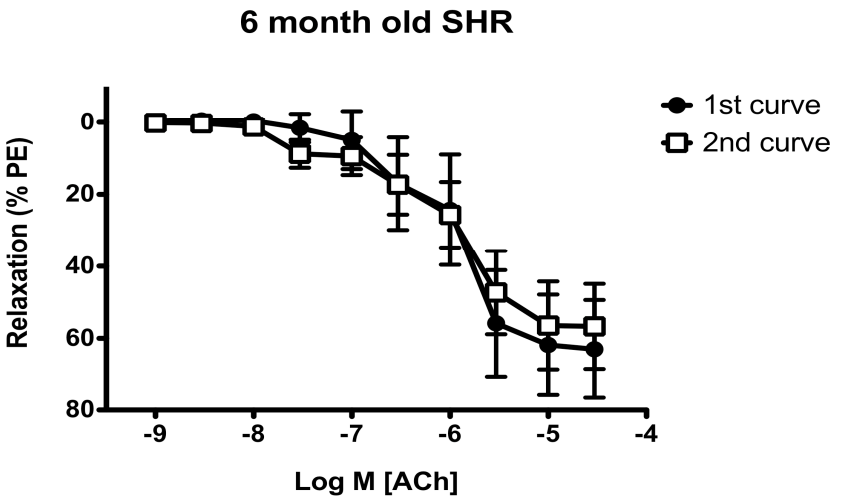


**Figure 5-8 Comparison of ACh response for control and time control CCRCs in saphenous arteries of 6 month old SHR (n=4). Response expressed as % relaxation of PE preconstriction mean ± S.E.M.**

**Table 5-6 Comparison of ACh response for control and time control CCRCs in saphenous arteries of 6 month old SHR.**

| ACh | 1st curve | 2nd curve |
|---|---|---|
| $E_{max}$ (% PE) | 63.50 ± 13.92 | 58.20 ± 11.78 |
| $E_{max}$ (g) | 0.50 ± 0.18 | 0.44 ± 0.15 |
| $pEC_{50}$ (% own max) | 5.91 ± 0.20 | 6.12 ± 0.38 |

**Expressed as mean ± S.E.M (n=4).**

### *5.3.4 Responses to ACh following incubation with agents affecting endothelial factors*

Further ACh responses were assessed after incubation with compounds affecting various endothelium derived factors to gain a better insight into the mechanisms of the ACh response.

#### 5.3.4.1 L-NAME and indomethacin incubation

ACh CCRCs were obtained in 12 week and 6 month old saphenous arteries following L-NAME and indomethacin incubation (Figure 5.9) to block the production of NO and prostaglandins respectively. The relaxation to ACh was effectively abolished in both strains at both age points (Table 5.7 and 5.8), and $pEC_{50}$ values could not be calculated due to the lack of a relaxant response.

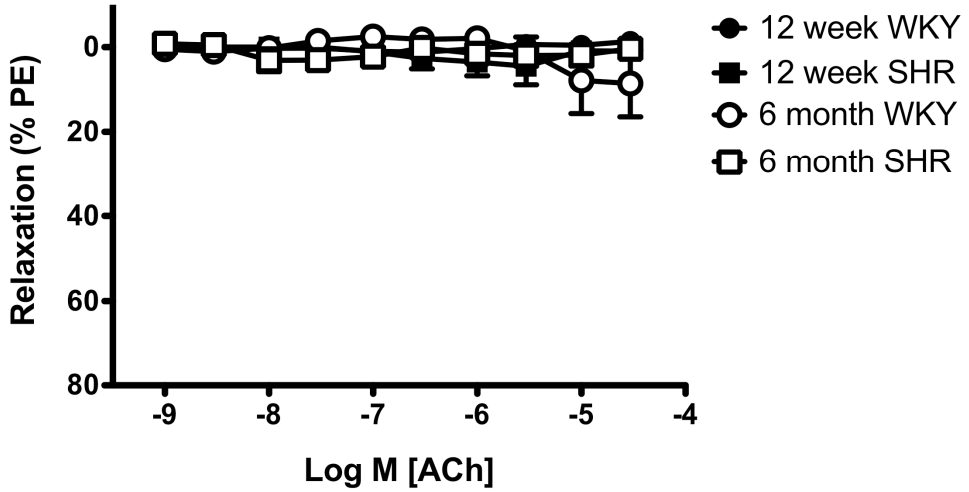


**Figure 5-9 Cumulative concentration response curves to ACh following 40 min 100μM L-NAME and 10μM indomethacin incubation in saphenous arteries of WKY and SHR (12 week: WKY n=6; SHR n=4; and 6 month: WKY n=5, SHR n=6). Expressed as mean ± S.E.M as a % of PE preconstriction.**

#### 5.3.4.2 Carbenoxolone incubation

CCRCs were performed in the presence of the putative gap junction inhibitor carbenoxolone (Figure 5.10). Carbenoxolone had no significant effect on maximum relaxations to ACh or $pEC_{50}$ values in any of the groups tested (Tables 5.7 and 5.8).

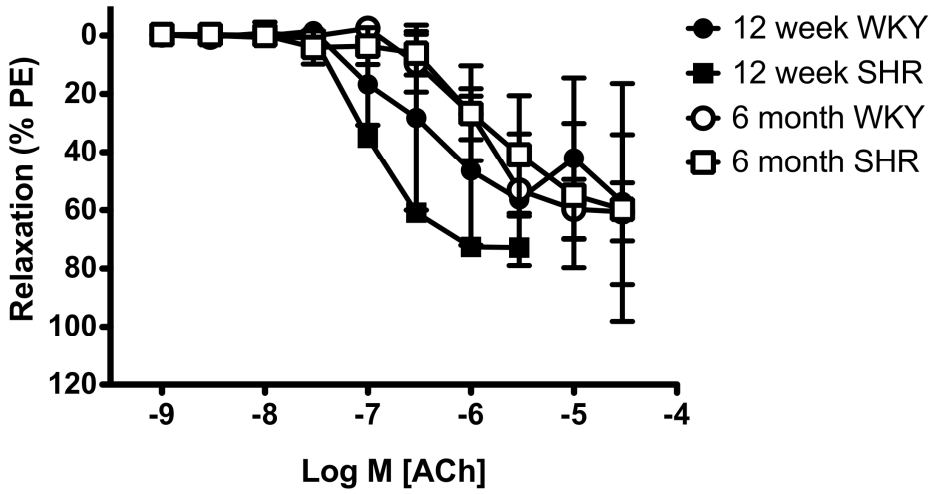


**Figure 5-10 Cumulative concentration response curves to ACh following 40 min 100μM carbenoxolone incubation in saphenous arteries of 12 week and 6 month old WKY and SHR (12 week: WKY n=4; SHR n=1; and 6 month: WKY n=5, SHR n=4). Expressed as mean ± S.E.M as a % of PE preconstriction.**

**Table 5-7 Summary of ACh induced responses in 12 week old WKY and SHR saphenous arteries following incubation with agents affecting endothelium derived factors.**

| 12 week old | n | Relaxation to ACh | |
|---|---|---|---|
| | | $E_{max}$ (% of PE) | $pEC_{50}$ |
| WKY | | | |
| Control | 6 | 38.6 ± 5.76 | 6.00 ± 0.13 |
| + L-NAME and indomethacin | 6 | 2.26 ± 1.53*** | - |
| Control | 4 | 47.18 ± 21.22 | 6.21 ± 0.15 |
| +carbenoxolone | 4 | 58.47 ± 16.25 | 6.35 ± 0.31 |
| SHR | | | |
| Control | 4 | 64.87 ± 11.29 | 6.00 ± 0.12 |
| + L-NAME and indomethacin | 4 | 5.43 ± 4.17*** | - |
| Control | 1 | 73.13 ± 0.00 | 5.48 ± 0.00 |
| +carbenoxolone | 1 | 72.90 ± 0.00 | 5.49 ± 0.00 |

***p<0.0001 compared with control (1 way-ANOVA).

**Table 5-8 Summary of ACh induced responses in 6 month old WKY and SHR saphenous arteries following incubation with agents affecting endothelium derived factors.**

| 6 month old | n | Relaxation to ACh | |
|---|---|---|---|
| | | $E_{max}$ (% of PE) | $pEC_{50}$ |
| WKY | | | |
| Control | 5 | 65.82 ± 6.62 | 5.93 ± 0.22 |
| + L-NAME and indomethacin | 5 | 10.06 ± 7.18*** | - |
| Control | 5 | 74.79 ± 20.05 | 5.75 ± 0.14 |
| +carbenoxolone | 5 | 59.87 ± 10.54 | 6.01 ± 0.21 |
| SHR | | | |
| Control | 4 | 28.99 ± 10.79 | 6.09 ± 0.19 |
| + L-NAME and indomethacin | 4 | 5.54 ± 2.88* | - |
| Control | 4 | 71.23 ± 0.53 | 5.97 ± 0.10 |
| +carbenoxolone | 4 | 84.80 ± 8.67 | 5.96 ± 0.16 |

***p<0.0001, *p<0.05 compared with control (1 way-ANOVA).

## 5.4 Discussion

The significantly higher response to PE in the 12 week old SHR compared with the other groups tested may be due to the small sample size of only two rats for the 12 week old SHR. There was no significant difference in the maximum PE-induced contraction in the 6 month old WKY and SHR rats, and the 6 month old rats of both strains had a greater PE contraction than the 12 week old WKY.

PE sensitivity increased with age in the saphenous artery, since $pEC_{50}$ values were significantly higher at 6 months than at 12 weeks of age in both strains. There was no significant difference in $pEC_{50}$ values between strains at 6 months of age, however, the SHR had a greater $pEC_{50}$ value than the WKY at 12 weeks of age.

There was almost no relaxation to ACh following L-NAME and indomethacin incubation in any of the groups tested, showing that there was no EDHF response in the 12 week or 6 month old saphenous artery. This was consistent with the findings of Sandow *et al* 2004. It would be interesting to assess the EDHF response of rats younger than 12 weeks old to determine whether the EDHF response was present during development.

These functional results in the saphenous artery contrast sharply with the mesenteric functional experiments where EDHF could compensate under conditions when the NOS enzyme was blocked by L-NAME (Chapter 4). In the saphenous artery this compensatory mechanism of EDHF relaxation was not evident. This may relate to the function of the artery in vivo: where the mesenteric is important in controlling peripheral blood pressure while the saphenous is more of a conduit artery, hence a strong relaxant response is of less importance to its function. In this respect the saphenous artery can be utilised as a control for the mesenteric artery since the contribution of EDHF was negligible and therefore could be discounted without the use of any pharmacological agents.

Carbenoxolone did not significantly alter the maximum ACh-induced relaxation or the sensitivity to ACh in any of the groups tested, implying that gap junctions played no role in the relaxant response to ACh in the rat saphenous. The effect

of carbenoxolone incubation on the ACh relaxation was not assessed in combination with L-NAME and indomethacin in the saphenous artery (as it was in the mesenteric artery) since relaxation was abolished after L-NAME and indomethacin incubation in the first instance. The incubation of indomethacin alone would have proven useful in this artery to determine if the whole relaxant response to ACh was NO mediated or if there was an additional prostanoid contribution.

# Chapter 6 Heterocellular Gap Junctional Dye Transfer in Pressurised Vessels

## 6.1 Introduction

Gap junctional communication allows the passage of current, ions and signalling molecules less than 1kDa in size between coupled cells (Evans & Martin, 2002). This property can be exploited experimentally to study cells that are thought to be in contact by gap junctions by examining dye transfer and its impediment by putative gap junction inhibitors.

Cellular projections traversing the IEL could be viewed by pressure fixing the vessels at 70mmHg and staining with the membrane dye FM4-64. Previous work in the laboratory has shown that there were less myoendothelial bridges in the SHR compared with the WKY at 6 months of age, with 73% of fenenestrae containing a bridge in the WKY and only 40% containing a bridge in the SHR (Gonzalez et al, unpublished). The existence of a bridge is only a potential site for MEGJ formation since the membranes are brought into close enough apposition for gap junction formation. Although the myoendothelial bridges could be visualised by this membrane staining method, it gave no indication as to the presence or function of MEGJs, since these can only be visualised at the electron microscope level of resolution: for this reason dye transfer experiments were undertaken.

Heterocellular dye transfer has been studied extensively in the vasculature (Dora *et al.*, 1999; Griffith *et al.*, 2002; Little *et al.*, 1995b), but it has not been considered in hypertension compared with normotensive controls. It was hoped this chapter would elucidate whether the reduction in the ACh relaxation response in the mesenteric artery in hypertension (Chapter 4) was due to a reduction in heterocellular coupling between the endothelial and smooth muscle cells. The decreased fenestrae size (Gonzalez *et al.*, 2006) together with the reduction in the proportion of fenestrae containing a myoendothelial bridge in the 6 month old SHR suggested there was less possibility for MEGJ formation in the hypertensive strain: this may be visually evident as less dye transfer (if the transfer is facilitated by MEGJs).

Early studies examined the homocellular and heterocellular passage of dye from injected cells (Little *et al.*, 1995b; Mulvany & Halpern, 1977; Dora *et al.*, 1999). This was developed further to examine the transfer of luminally loaded dyes

from the endothelial to smooth muscle cell layers in live vessels on a pressure myograph (Kansui *et al.*, 2008; Griffith *et al.*, 2002). The technique of luminally loaded dye provided a more physiological approach to studying cellular communication where the vessel was intact and pressurised.

The calcein-AM dye was selected for these purposes because it was cell permeable in the non-fluorescent state and on conversion to its fluorescent state (calcein) by intracellular esterases, it was rendered cell-impermeable (Griffith *et al.*, 2002). This feature meant that following luminal application, any fluorescence detected in the smooth muscle cells would presumably be a consequence of gap junctional transfer since the fluorescent calcein in the endothelial cells would no longer be able to diffuse through the membrane to exit. This hypothesis was tested further by examining the effects of gap junction blocking peptides on the dye transfer observed.

### *6.1.1 Aims*

The aims of this chapter were:

- To assess heterocellular dye transfer in mesenteric arteries from both the normotensive and hypertensive rats at 12 weeks and 6 months of age to compare gap junction function.

- To assess the effects of gap junction blocking peptides and carbenoxolone in mesenteric arteries from each strain to make inferences about the mode of dye transfer from the endothelial to smooth muscle cells (i.e. to test if it was gap junction mediated). These results were intended to be correlated with the EDHF function in the mesenteric vessels, such that a decrease in EDHF may be due to a reduction in MEGJs in the hypertensive strain and hence less dye transfer.

- To determine whether dye transfer occurs in an artery where there is a lack of MEGJs by studying the saphenous artery.

## 6.2 Methods

Third order mesenteric arteries and saphenous arteries were set up on the pressure myograph system as detailed in the General Methods (Chapter 2). The saphenous artery did not maintain a pressure of 70mmHg without leakage throughout the course of the experiment and so a pressure of 30mmHg was found to be optimal. Vessels exposed to the gap junction blocking peptides $^{37,43}$Gap27 100 μM and $^{40}$Gap27 100 μM were incubated with the peptides for 3 hours prior to the luminal loading of calcein-AM. The vessel was exposed to 3μM calcein-AM luminally under conditions of no flow at 70mmHg for 10 minutes and was subsequently washed at a flow 300μL/min for 10 minutes, before a 90 minute equilibration period elapsed for the dye to de-esterify. After this 90 minute period the vessel was pressure fixed at 37ºC with 4% paraformaldehyde for one hour and stored in fixative in the dark until imaged. For live imaging experiments the same protocol was followed but the vessel was imaged after the 90 minute incubation rather than pressure fixed. A control vessel was imaged under the same laser settings without calcein-AM application to assess the level of auto-fluorescent background staining from the argon laser excitation.

Fixed vessels were slide mounted in a silicone well in glycerol to ensure there was no distortion of the vessel wall. They were imaged using a x40 oil immersion objective with the argon laser at optimal iris, laser 15% and gain 10%. Z-series projections through the vessel wall were captured in 1μm steps to a depth of 50μm, with a two frame kalman for each plane.

Live vessels were imaged using a x20 ELWD objective with the argon laser at optimal iris, laser 5% and gain 10%. Z-series projections were captured identically to the fixed vessels.

Vessels were counterstained with either Alexa 633 hydrazide or SYTO 61 to stain the IEL or the nuclei respectively, and so provide a better orientation of the EC and SMC layers.

### 6.2.1 Image Analysis

In order to quantify the staining observed by eye, voxel intensities were measured from the images acquired from vessels that were fixed following calcein-AM exposure and de-esterification in the live pressurised vessel.

Three regions of interest (ROI) of 100 pixels$^2$ equating to 56.4μm$^2$ were selected at random from each 50μm Z series. This 3D ROI was separated out into endothelial and smooth muscle cell layers and the voxel intensity for each individual voxel in the endothelial or smooth muscle cell crop was recorded. This produced a readout detailing the actual number of voxels with each value of intensity ranging from 1 to 255. Due to the slight difference in depth of each EC or SMC crop, it was more informative to express the number of voxels at each intensity value as a percentage of the number of voxels in the overall volume. The intensities were then grouped in "bins" of 50 to allow comparisons to be made between strains and groups as a way of quantifying the brightness of the fluorescence observed in each cell layer crop.

Intensity values ranged from 1 to 255: with 1 being the least intense and 255 being the most intense staining. This correlated with the pseudo colour of the image on the imaging program Amira, ranging from blue being least intense to green being most intense (Figure 6.1).


**Figure 6-1 Amira intensity scale**

Live vessels were imaged using a x20 ELWD objective at Argon laser settings: laser 10%, gain 8% and optimal iris 1.2. Fixed vessel imaging produced better results than live imaging since the cells were more clearly defined when viewed on the x40 oil immersion objective. Examples of live artery imaging are provided also, but voxel intensities have not been provided because of the high variability observed. Due to the expense of the gap junction blocking peptides, carbenoxolone was used in the bath for the live imaging experiments as a putative gap junction inhibitor.

Mean data were compared using a Student's t-test or one-way ANOVA with Bonferroni post-test for all pairwise comparisons.

# 6.3 Results

## *6.3.1 Background staining and optimal conditions*

Analysis of the whole control vessel showed that almost 100% of background fluorescence from Argon laser excitation lay in the first intensity bin 1-51 (Figure 6.2). This established the first intensity bin as "background" staining which was subsequently omitted from further analysis.

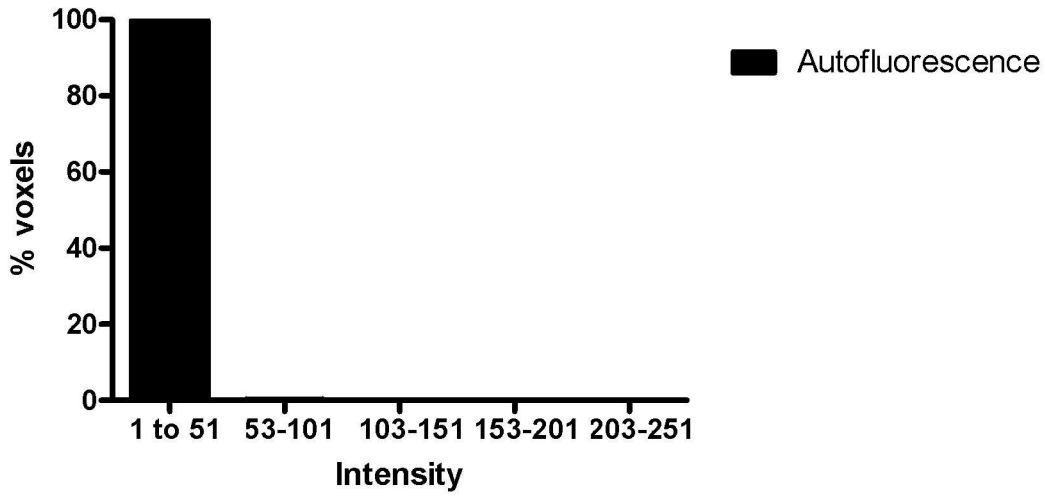


**Figure 6-2 Intensity of autofluorescence in ROI from pressure fixed vessel with no calcein-AM staining (n=2)**

To ensure optimal dye conditions were chosen, a series of different times for dye loading were tested. The smooth muscle staining intensity was measured in experiments with 5, 7 and 10 minutes luminal calcein-AM incubation (Figure 6.3).

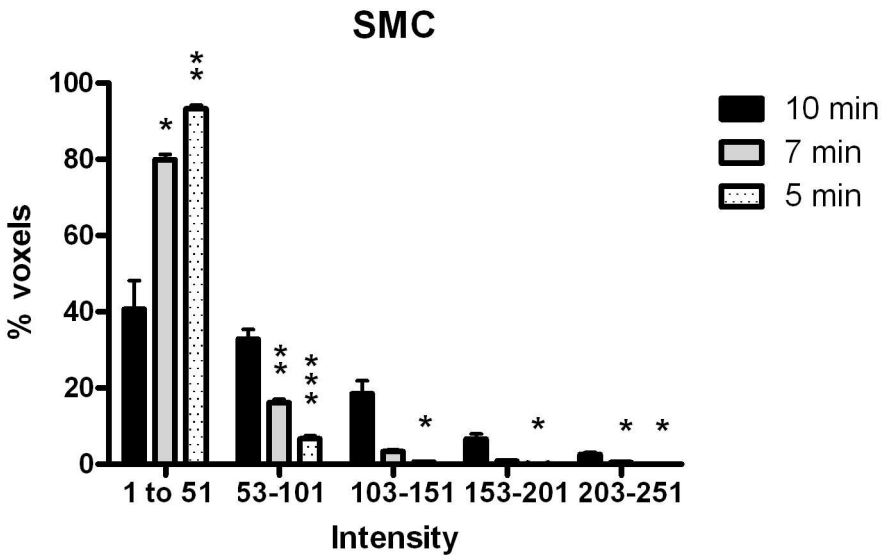


**Figure 6-3 Smooth muscle cell staining intensity in pressure fixed vessels luminally loaded with 3μM calcein-AM for 5, 7 or 10 minutes. * p<0.05, ** p<0.01, *** p<0.001 compared with fluorescence of 10 min exposure in same intensity bin (1 way ANOVA followed by Bonferroni post test)(n=2).**

10 minutes was found to be the optimal time for calcein-AM incubation, since neither 5 or 7 minutes gave sufficient SMC staining (Figure 6.3), with very little calcein staining above background levels observed in the smooth muscle cells.

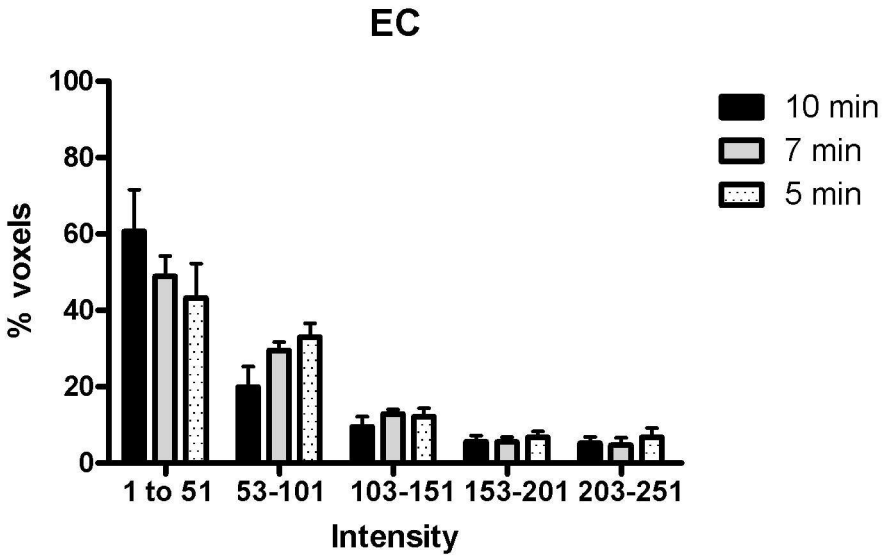


**Figure 6-4 Endothelial cell staining intensity in pressure fixed vessels luminally loaded with 3uM calcein-AM for 5, 7 or 10 minutes (n=2).**

Analysis of the endothelial cell staining by one-way ANOVA for each intensity bin showed that an increased exposure time to calcein-AM did not affect the endothelial cell voxel intensity (Figure 6.4). It should be noted that all of the above parameters were measured on pressure fixed vessels.

### *6.3.2 Fixed Vessel Image Analysis*

#### 6.3.2.1 Dye Transfer in 12 week old mesenteric arteries

Examples of the endothelial and smooth muscle cell ROI crops for the 12 week old WKY depict the distinct shape of the endothelial and smooth muscle cells and clearly show that both cellular layers were stained (Figure 6.5). This staining has been quantified by voxel intensity (Figure 6.6) and showed that there was no significant difference in the endothelial and smooth muscle cell staining in the 12 week old WKY in any of the intensity bins, with the exception of the smooth muscle cells having significantly greater staining than the endothelial cells in the 53-101 bin.

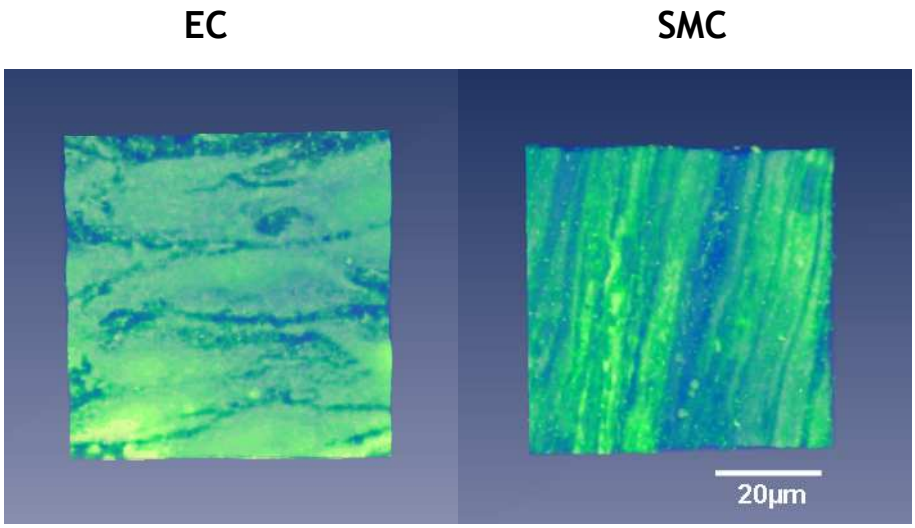


**Figure 6-5 Endothelial (left image) and smooth muscle cell (right image) calcein staining in a ROI from 12 week old WKY mesenteric artery.**

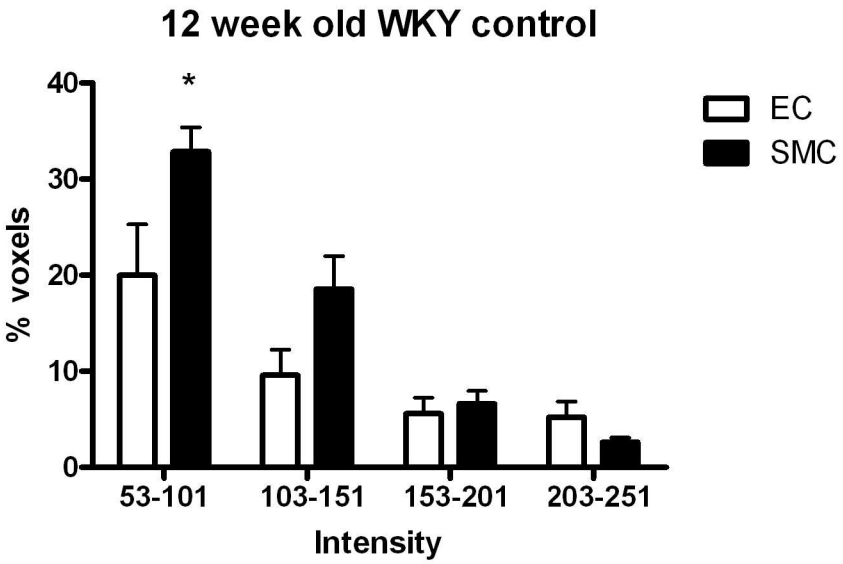


**Figure 6-6 Endothelial and smooth muscle cell staining in the 12 week old WKY mesenteric artery (n=3). * p<0.05 compared with fluorescence of EC in same intensity bin (unpaired t-test).**

Further experiments were performed in the 12 week old WKY to assess whether this calcein staining in the smooth muscle cells was a consequence of gap junctional transfer. This was done by incubating the vessels with a combination of the gap peptides $^{37,43}$Gap27 100μM and $^{40}$Gap27 100μM (GJi) prior to luminal calcein incubation. Endothelial and smooth muscle cell staining were assessed in these vessels (Figures 6.7 and 6.8 respectively).

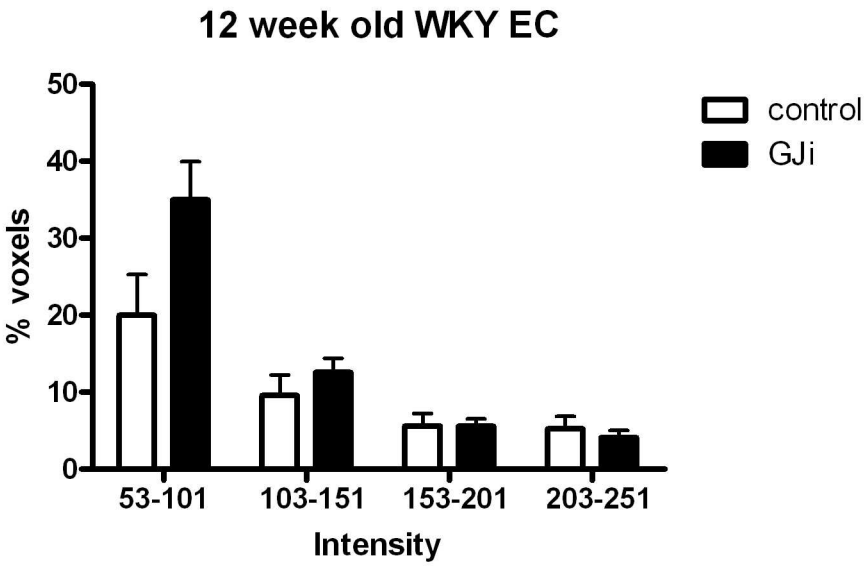


**Figure 6-7 Endothelial cell staining in 12 week old WKY mesenteric arteries with (n=3) and without (n=3) gap peptide incubation.**

Gap junction blocking peptides did not affect endothelial cell intensity since there was no significant difference from control values at any of the intensity bins (Figure 6.7). However, the gap junction blocking peptides did significantly decrease smooth muscle cell staining as compared with the control in the 12 week old WKY in all intensity bins (Figure 6.8).

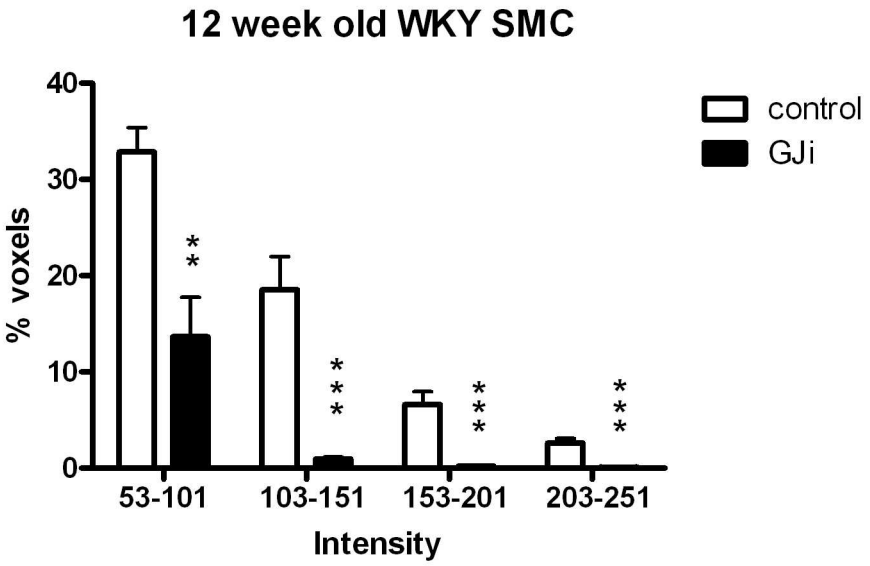


**Figure 6-8 Smooth muscle cell staining in 12 week old WKY mesenteric arteries with (n=3) and without (n=3) gap peptide incubation. * p<0.5, ** p<0.01, *** p<0.001 compared with fluorescence of control in the same intensity bin (unpaired t-test).**

Figure 6.9 shows an example of this decreased smooth muscle cell staining in vessels pre-incubated with the gap junction blocking peptides compared with control. When viewed from the adventitial side (Figure 6.9, bottom panels), the control vessel has far greater SMC staining than the vessel pre-incubated with the gap junction blocking peptides.

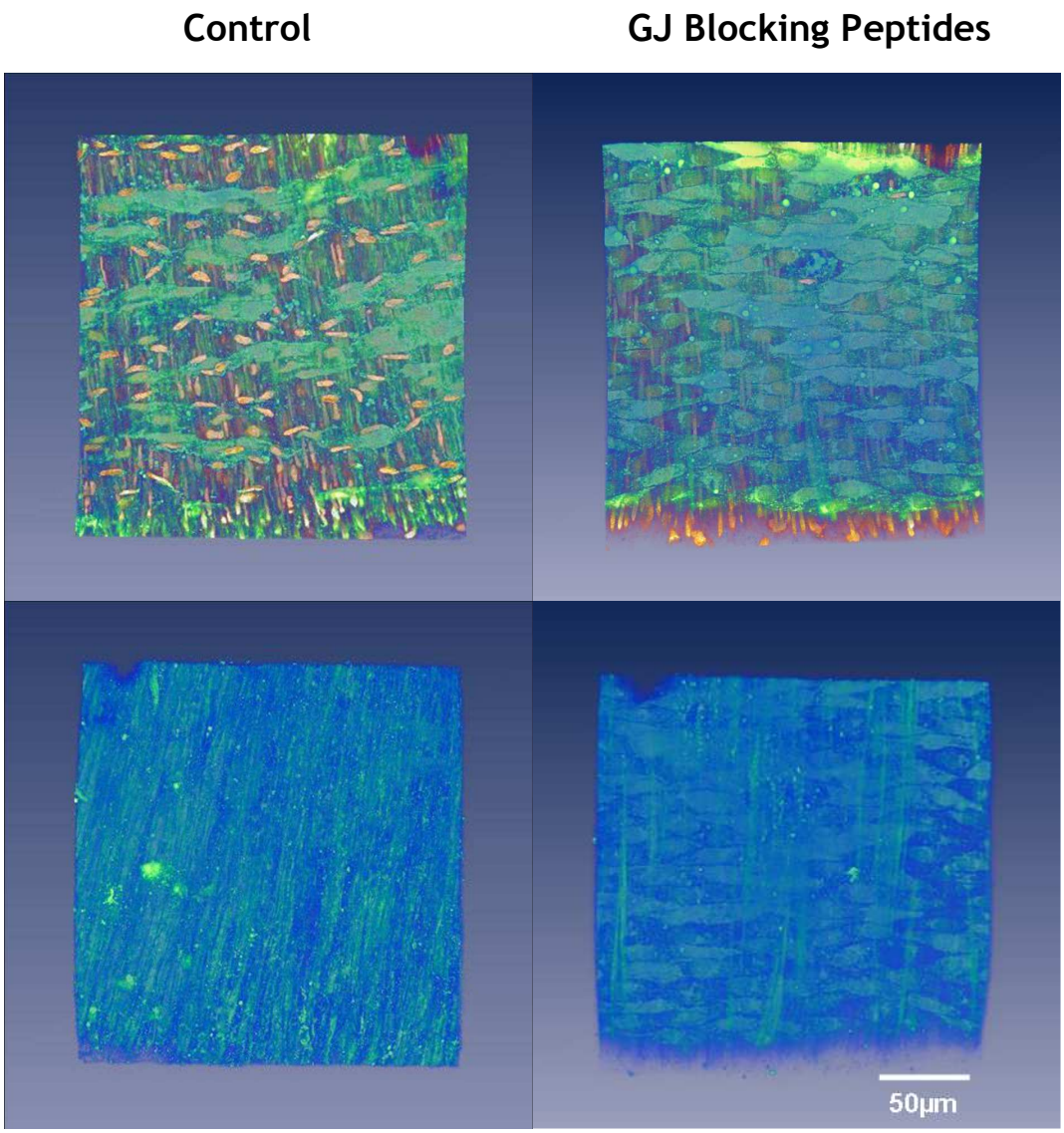


**Figure 6-9 A 50µm Z-series of calcein staining in 12 week old WKY control vessel (left image) and vessel incubated with gap junction blocking peptides (right image). Top panels are luminal view with SYTO 61 nuclear stain, bottom panels are adventitial view with SYTO 61 staining omitted for clarity.**

SHR mesenteric vessels showed significantly less staining in the smooth muscle cells compared with the endothelial cells under control conditions (Figure 6.10). In the SHR, gap junction blocking peptides did not cause endothelial or smooth muscle cell intensity to vary significantly from control values in any of the intensity bins (Figures 6.11 and 6.12 respectively).

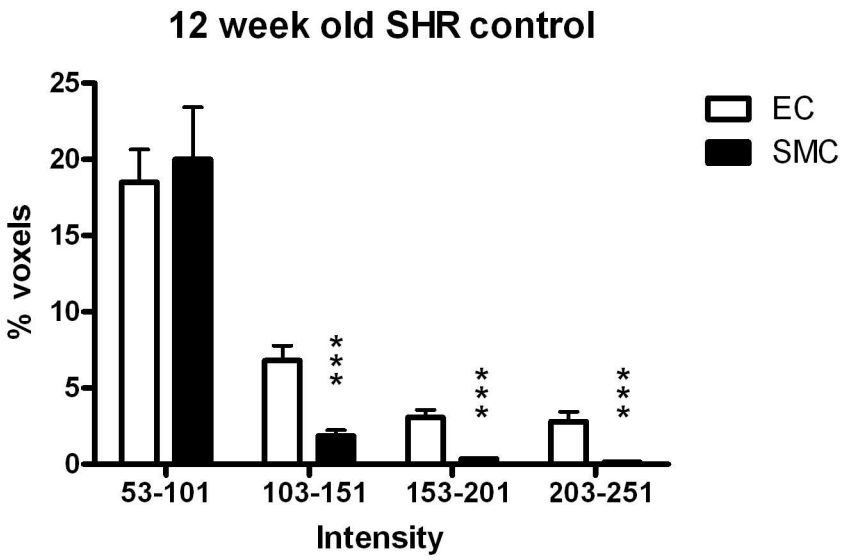


**Figure 6-10 Endothelial and smooth muscle cell staining in the 12 week old SHR mesenteric artery (n=5). *** p<0.001 compared with fluorescence of EC in the same intensity bin (unpaired t-test).**

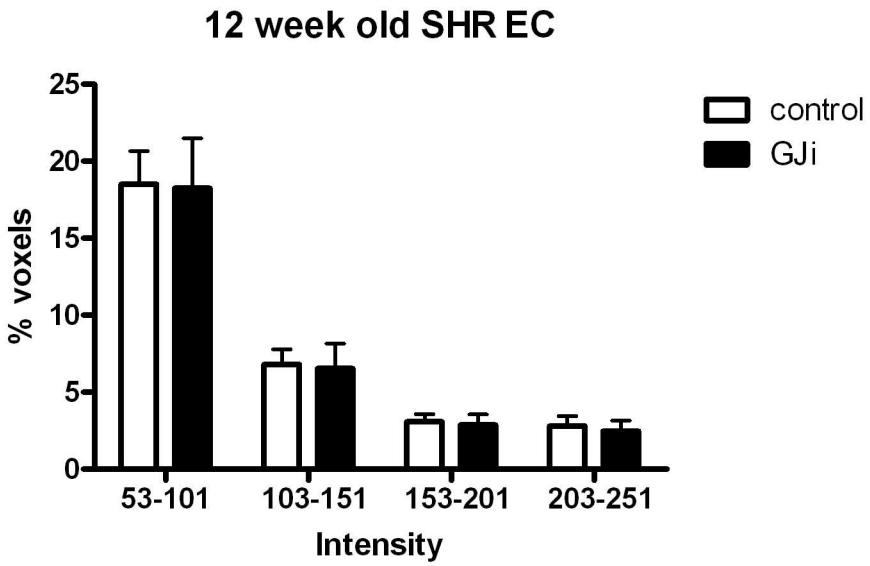


**Figure 6-11 Endothelial cell staining in 12 week old SHR mesenteric arteries with (n=5) and without (n=5) gap peptide incubation.**

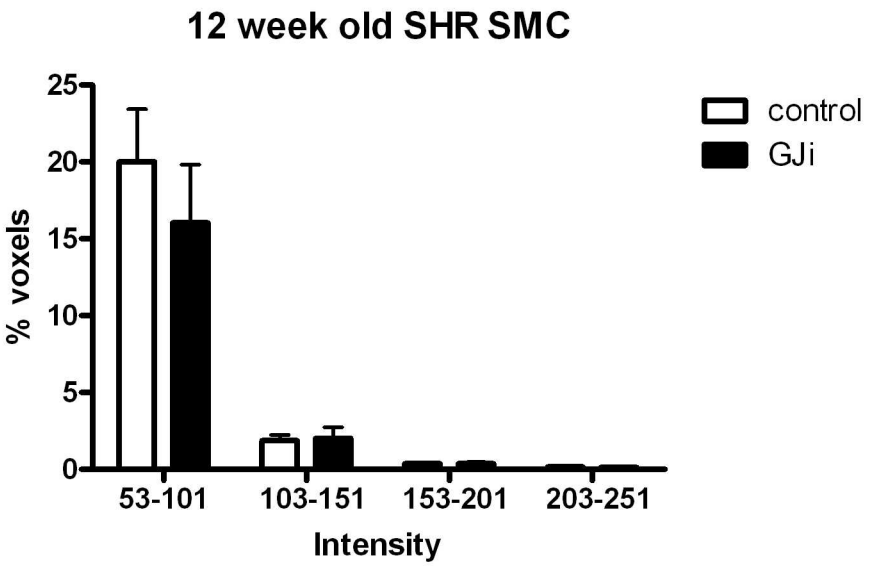


**Figure 6-12 Smooth muscle cell staining in 12 week old mesenteric arteries with (n=5) and without (n=5) gap peptide incubation.**

Comparison of WKY and SHR endothelial cell calcein staining under control conditions showed no significant difference in staining in any intensity bin (Figure 6.13). However, the smooth muscle cell staining in SHR was significantly lower in all intensity bins than WKY (Figure 6.14). Examples of the calcein staining in WKY and SHR control vessels can be seen in Figure 6.15.

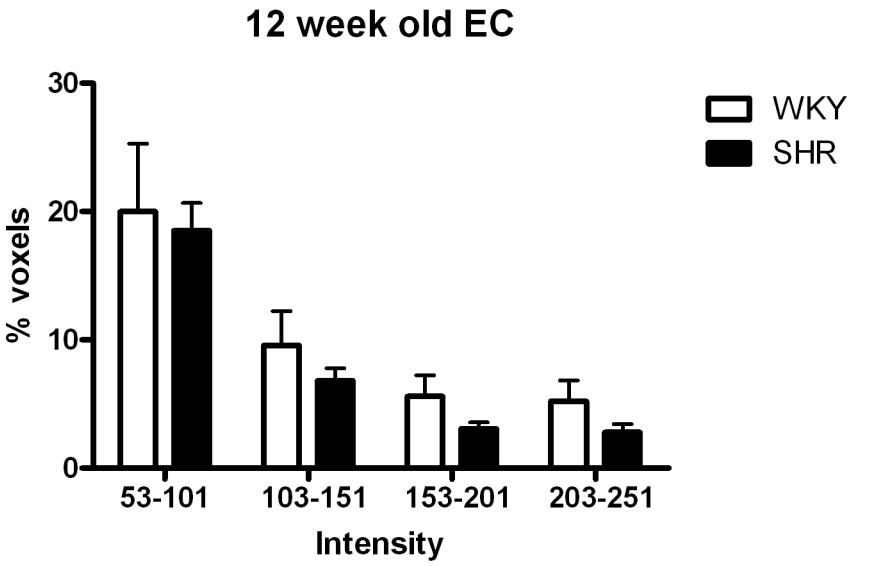


**Figure 6-13 Comparison of endothelial cell calcein staining in 12 week old WKY (n=3) and SHR (n=5) mesenteric control arteries.**

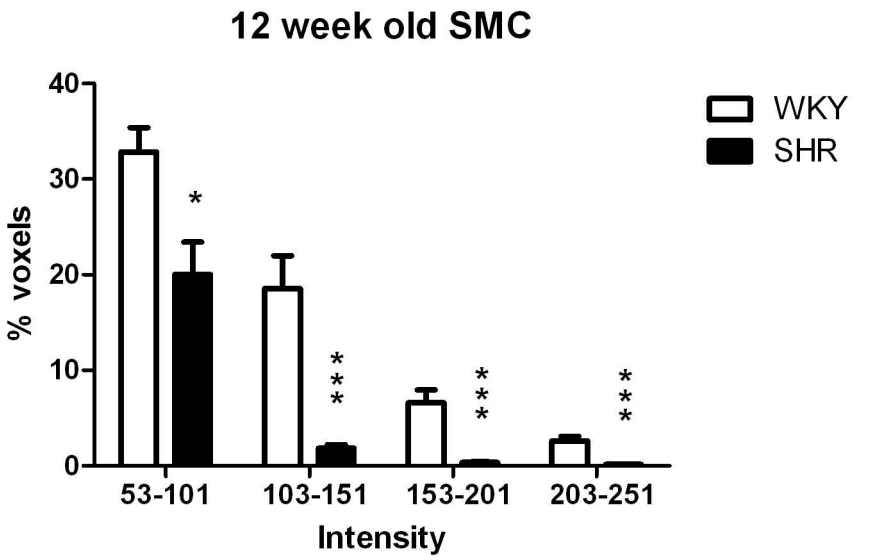


**Figure 6-14 Comparison of smooth muscle cell calcein staining in 12 week old WKY (n=3) and SHR (n=5) mesenteric control arteries. * p<0.5, *** p<0.001 compared with fluorescence of WKY in same intensity bin (unpaired t test).**

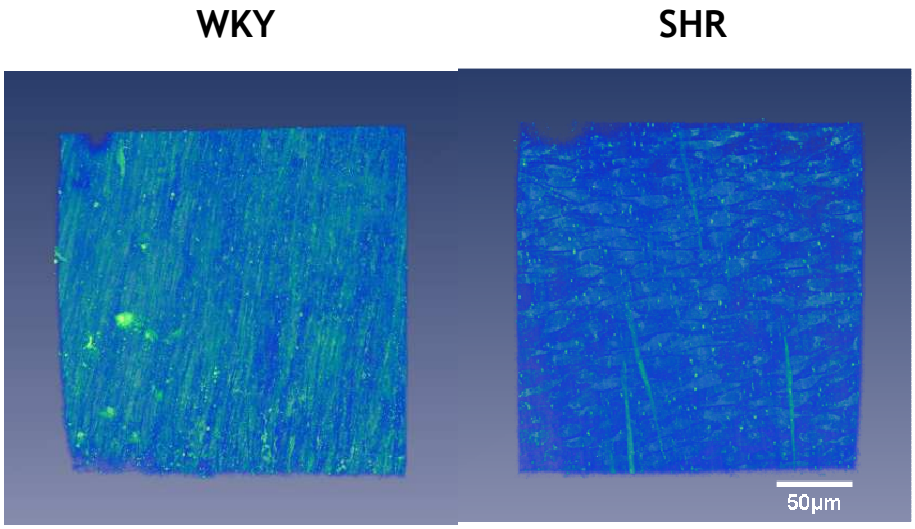


**Figure 6-15 50um Z-series of calcein staining in control vessels from 12 week old WKY (left image) and SHR (right image).**

### 6.3.2.2 Dye Transfer in 6 month old mesenteric arteries

The same experiments were performed in 6 month old animals to determine if the dye transfer varied with age. In the 6 month old WKY control vessels staining was significantly greater in the endothelial than in the smooth muscle cells in all intensity bins (Figure 6.16).

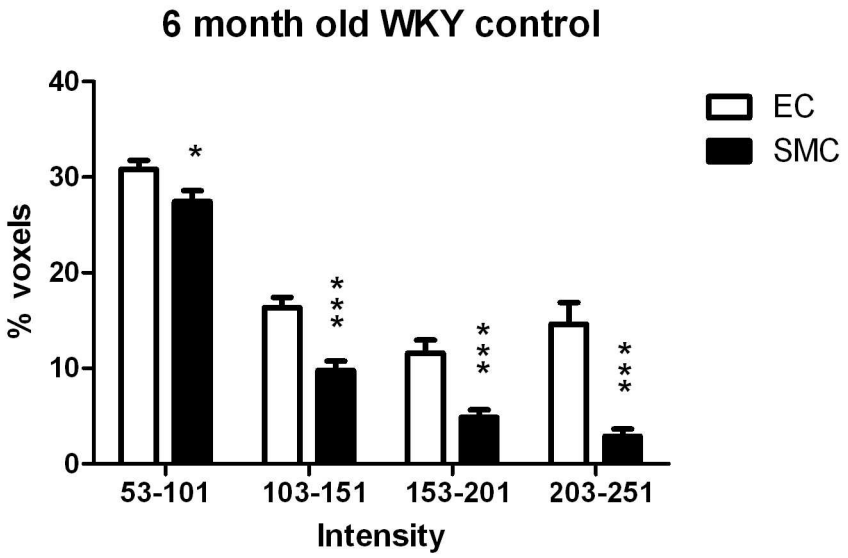


**Figure 6-16 Endothelial and smooth muscle cell staining in the 6 month old WKY mesenteric artery (n=3). * p<0.05, *** p<0.001 compared with fluorescence of EC in same intensity bin (unpaired t-test).**

The EC staining in control vessels and vessels pre-incubated with the gap peptides from the 6 month old WKY was assessed (Figure 6.17). EC staining in vessels pre-incubated with gap junction blocking peptides was not significantly different from control vessels at low intensities but was significantly lower than controls at intensity bins 153-201 and 203-251. Smooth muscle cell staining in vessels pre-incubated with the gap junction blocking peptides was significantly less than the control vessels in intensity bins 153-201 and 203-251 (Figure 6.18).

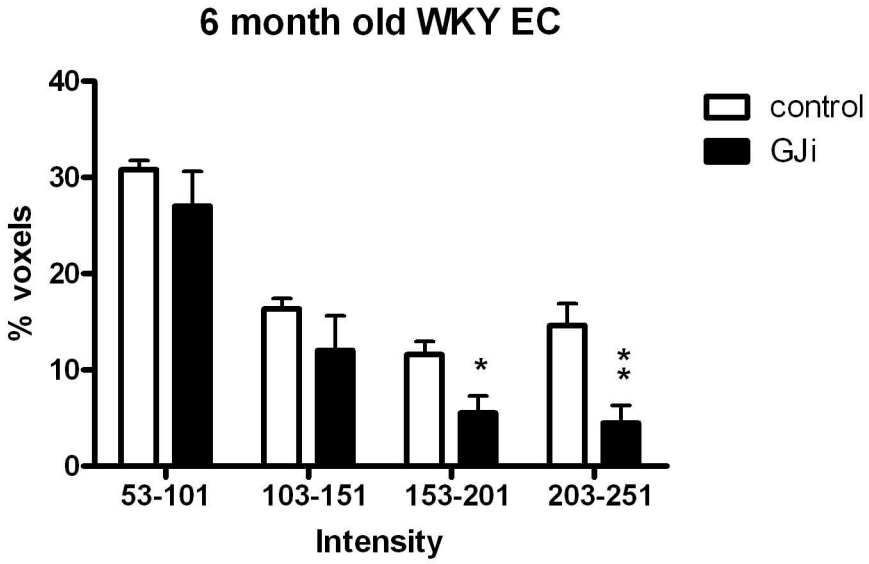


**Figure 6-17 Endothelial cell staining in 6 month old WKY mesenteric arteries with (n=2) and without (n=3) gap peptide incubation. * p<0.05, ** p<0.01 compared with fluorescence of control in the same intensity bin (unpaired t-test).**

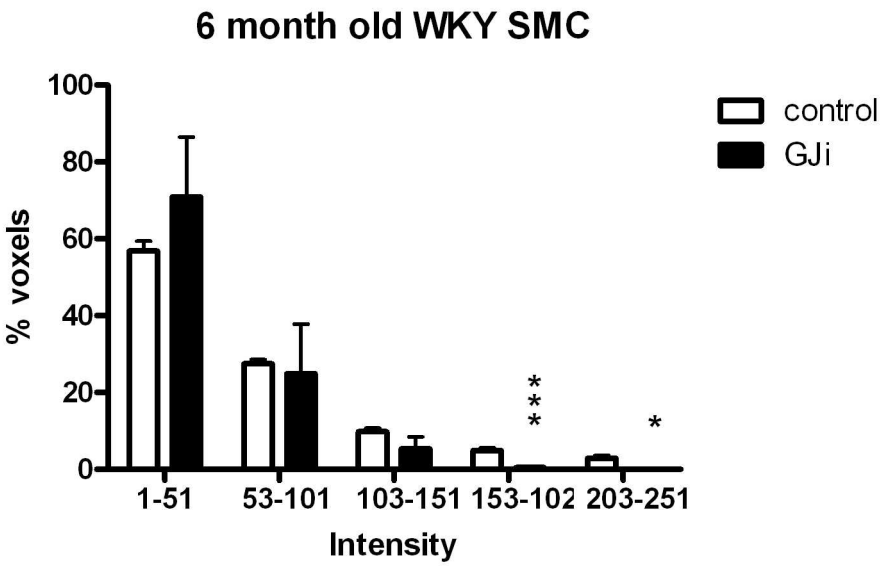


**Figure 6-18 Smooth muscle cell staining in 6 month old WKY mesenteric arteries with (n=2) and without (n=3) gap peptide incubation. * p<0.05, *** p<0.001 compared with fluorescence of control in the same intensity bin (unpaired t-test).**

SHR control vessels showed significantly less SMC staining than EC staining in all intensity bins above 53-101 (Figure 6.19). The gap junction blocking peptides did not significantly alter EC or SMC staining compared with the control in the 6 month old SHR (Figures 6.20 and 6.21 respectively).

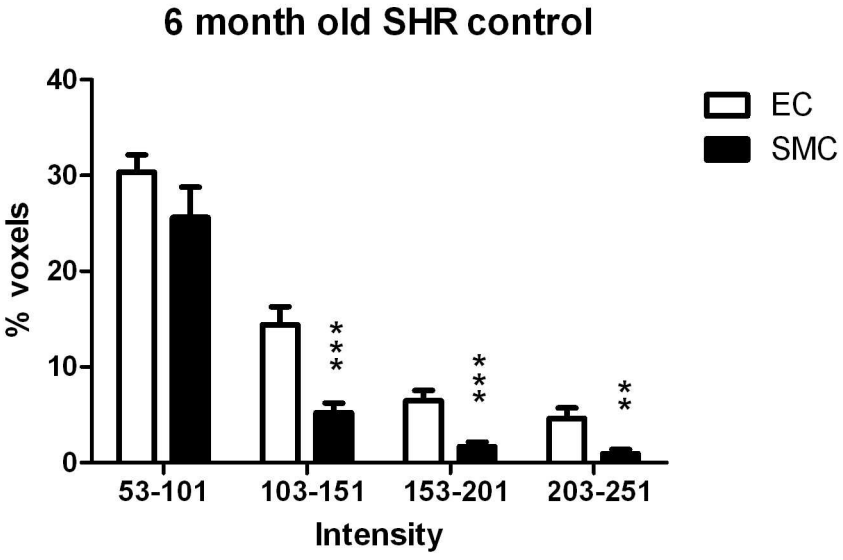


**Figure 6-19 Endothelial and smooth muscle cell staining in the 6 month old SHR mesenteric artery (n=4).** p<0.01, *** p<0.001 compared with fluorescence of control in the same intensity bin (unpaired t-test).**

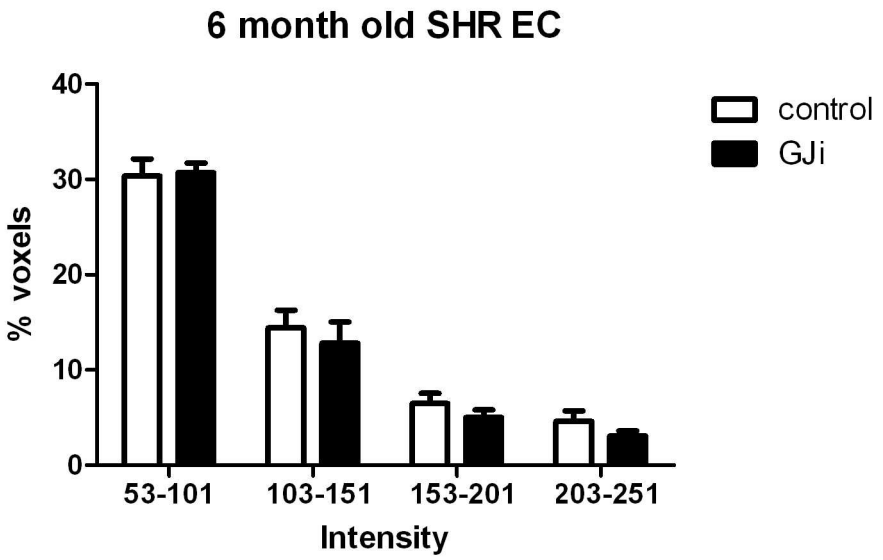


**Figure 6-20 Endothelial cell staining in 6 month old SHR mesenteric arteries with (n=4) and without (n=4) gap peptide incubation.**

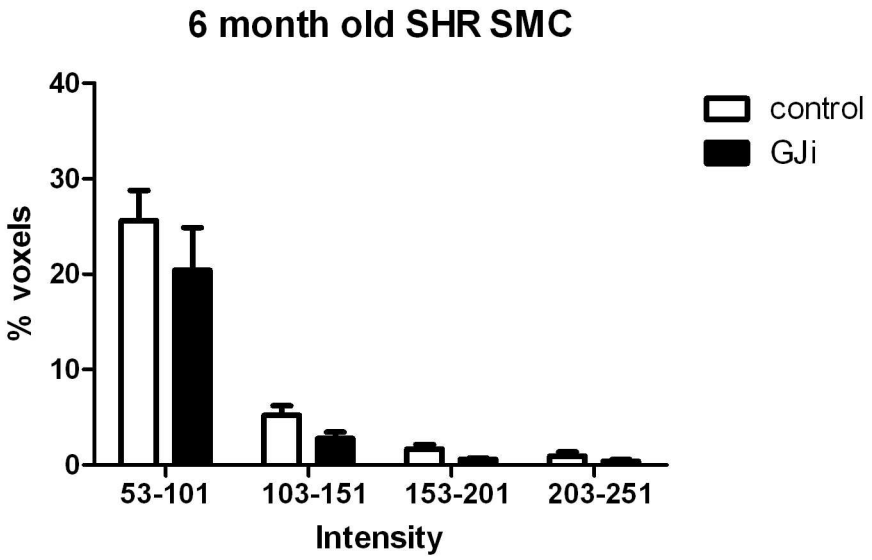


**Figure 6-21 Smooth muscle cell staining in 6 month old SHR mesenteric arteries with (n=4) and without (n=4) gap peptide incubation.**

In comparing the two strains at 6 months of age it was found that the SHR had significantly less EC staining than the WKY at intensity bins 153-210 and 203-251 (Figure 6.22). Also, the SHR had significantly less SMC staining than the WKY in all intensity bins above 53-101 (Figure 6.23).

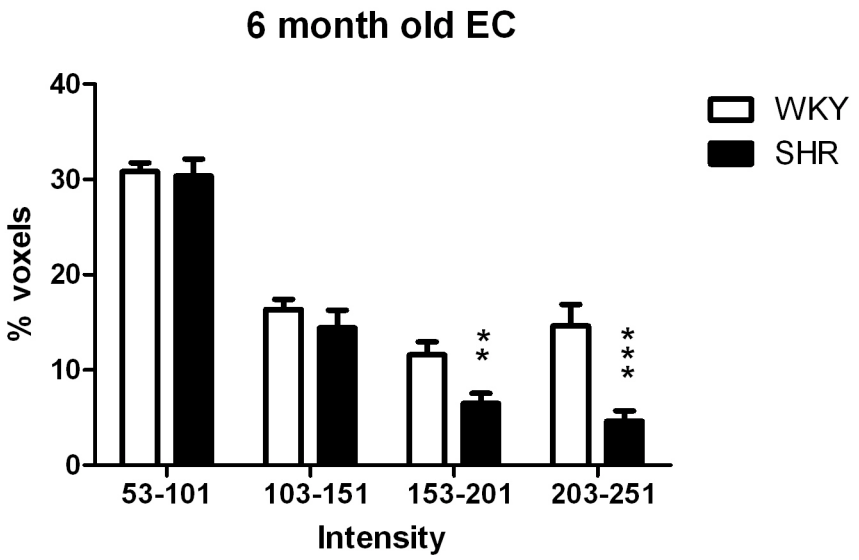


**Figure 6-22 Comparison of endothelial cell calcein staining in 6 month old WKY (n=2) and SHR (n=4) mesenteric control arteries. ** p<0.01, *** p<0.001 compared with fluorescence of WKY in the same intensity bin (unpaired t-test).**

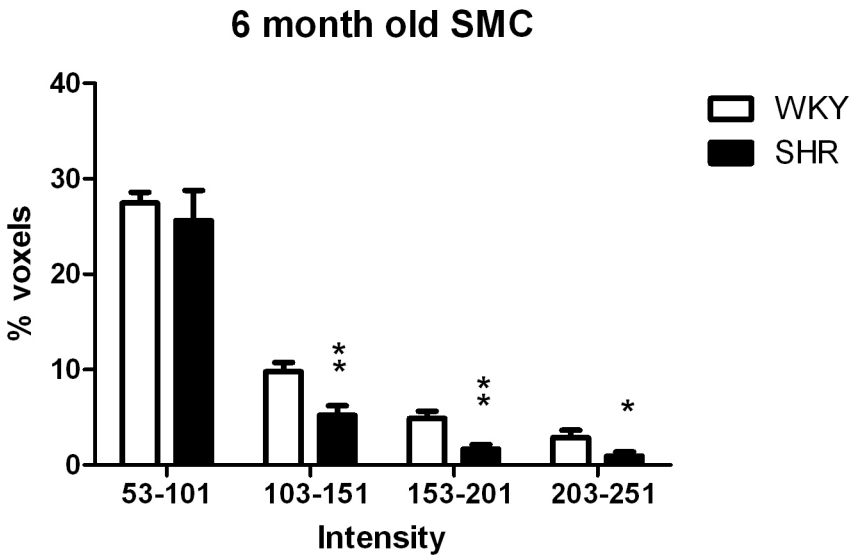


**Figure 6-23 Comparison of smooth muscle cell calcein staining in 12 week old WKY (n=2) and SHR (n=4) mesenteric control arteries . * p<0.5, ** p<0.01 compared with fluorescence of control in the same intensity bin (unpaired t-test).**

### *6.3.3 Live vessel image analysis*

Following the purchase of extra long working distance objectives for the confocal microscope it was possible to image the vessels live on the pressure system. This was a more physiological approach than imaging the vessels after they were pressure fixed.

The staining on the live mesenteric vessels was found to be variable, with no consistent profile of staining seen in the controls of 12 week old WKY, 12 week old SHR, or 6 month old WKY (Figures 6.25, 6.26 and 6.27 respectively) (no 6 month old SHR were imaged live due to lack of animal availability). For this reason the voxel intensities were not quantified, but the Z series projections of the vessels imaged were provided. This technique was first tested on murine vessels in preliminary experiments to test the dye staining (Figure 6.24). The same experiments were performed on vessels pre-incubated in the putative gap junction inhibitor carbenoxolone 100μM in the bath for 40 minutes prior to luminal calcein-AM exposure (Figures 6.25, 6.26 and 6.27). Images of the calcein staining in live saphenous arteries are provided (Figure 6.28).

The live murine vessel (Figure 6.24) shows both endothelial and smooth muscle cell calcein staining following the luminal application of calcein-AM. In the live 12 week old WKY this same pattern of endothelial and smooth muscle cell calcein staining was also observed in control experiments, although the brightness of staining varied considerably between preparations imaged under the same conditions (Figure 6.25, left hand pane). Incubation with carbenoxolone in the live 12 week old WKY vessels appeared to decrease the brightness of smooth muscle cell calcein staining on some occasions (Figure 6.25, upper two panels), but not on others (Figure 6.25, lower panel). In the live 12 week old SHR control vessels the smooth muscle cell calcein staining was not consistent between preparations (Figure 6.26, left hand pane), but it did appear less bright than in the live 12 week old WKY controls (Figure 6.25, left hand pane). Incubation with carbenoxolone did not seem to alter staining compared with the controls in the live 12 week old SHR. In the live 6 month old WKY, carbenoxolone incubation appeared to decrease the smooth muscle cell calcein staining compared with the control (Figure 6.27). The live saphenous artery showed calcein staining in the smooth muscle and adventitia (Figure 6.27), however the endothelial cells could not be clearly seen in this artery due to the thickness of the adventitia.

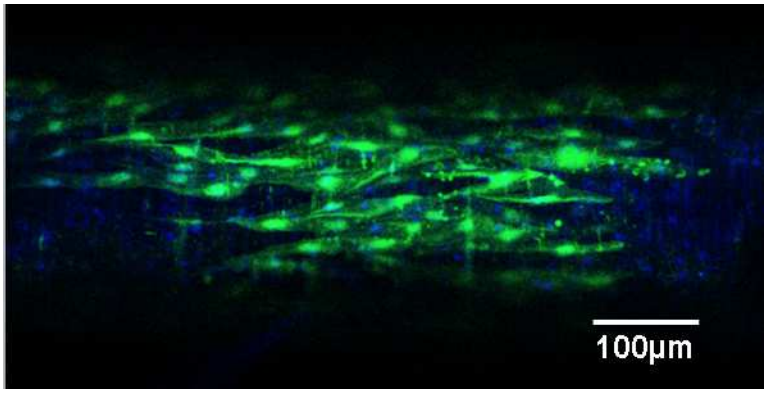


**Figure 6-24 Live pressurized 1st order murine mesenteric artery stained with luminally loaded calcein-AM 30µM.**

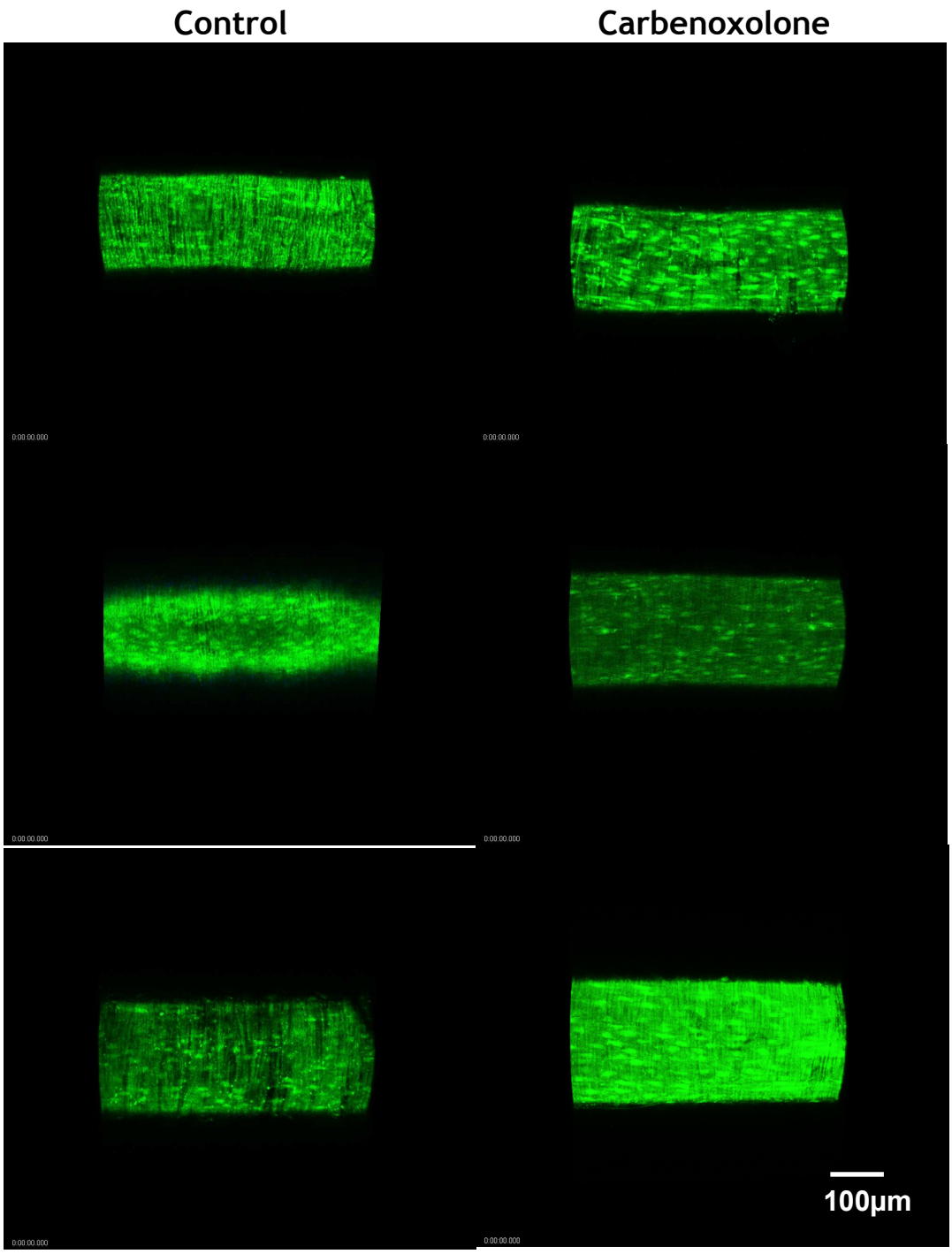


**Figure 6-25 Live pressurised (70mmHg) 3rd order MRA of 12 week old WKY stained with luminally-loaded calcein-AM, with (right hand pane, n=3) and without (left hand pane, n=3) 100µM carbenoxolone incubation.**

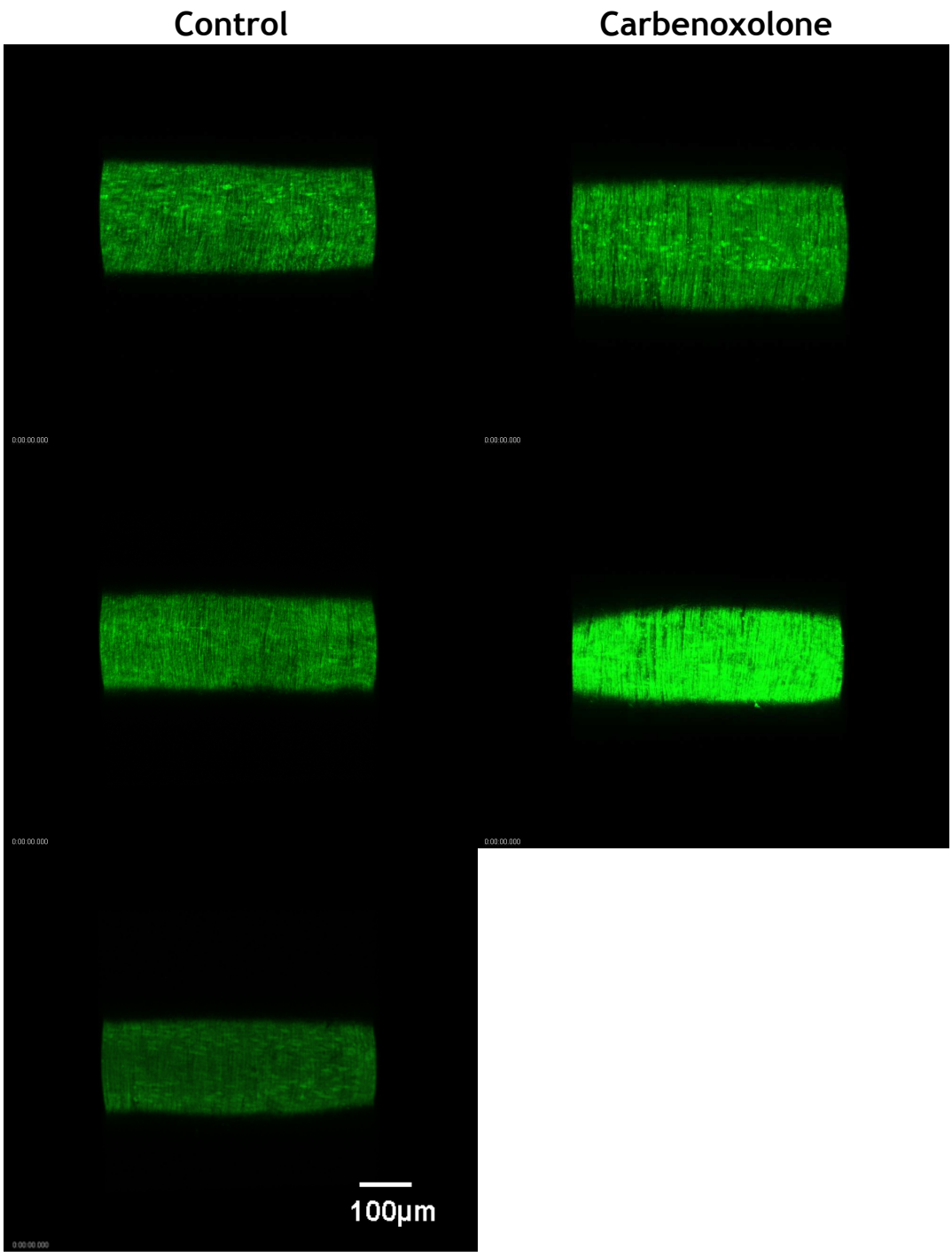


**Figure 6-26 Live pressurised (70mmHg) 3rd order MRA of 12 week old SHR stained with luminally-loaded calcein-AM, with (right hand pane, n=2) and without (left hand pane, n=3) 100µM carbenoxolone incubation.**

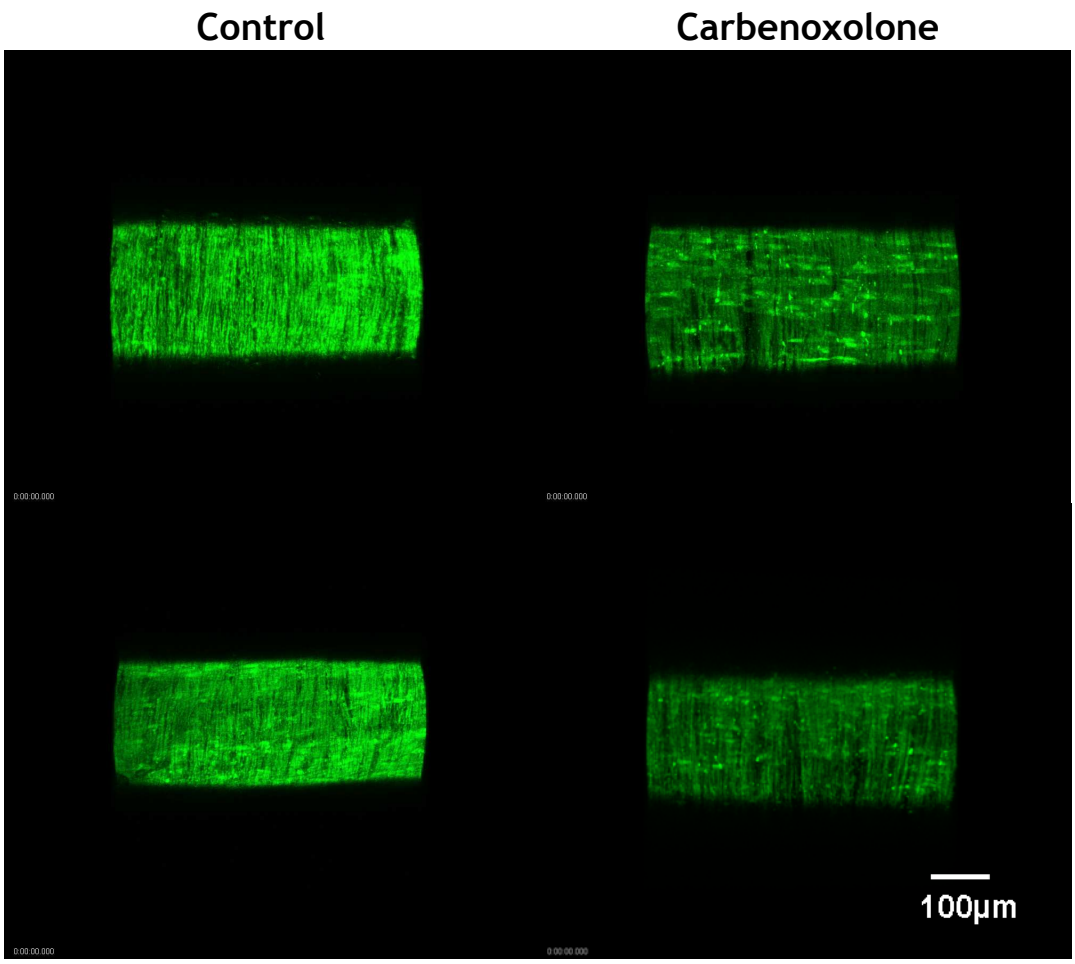


**Figure 6-27 Live pressurised (70mmHg) 3rd order MRA of 6 month old WKY stained with luminally-loaded calcein-AM, with (right hand pane, n=2) and without (left hand pane, n=2) 100µM carbenoxolone incubation.**

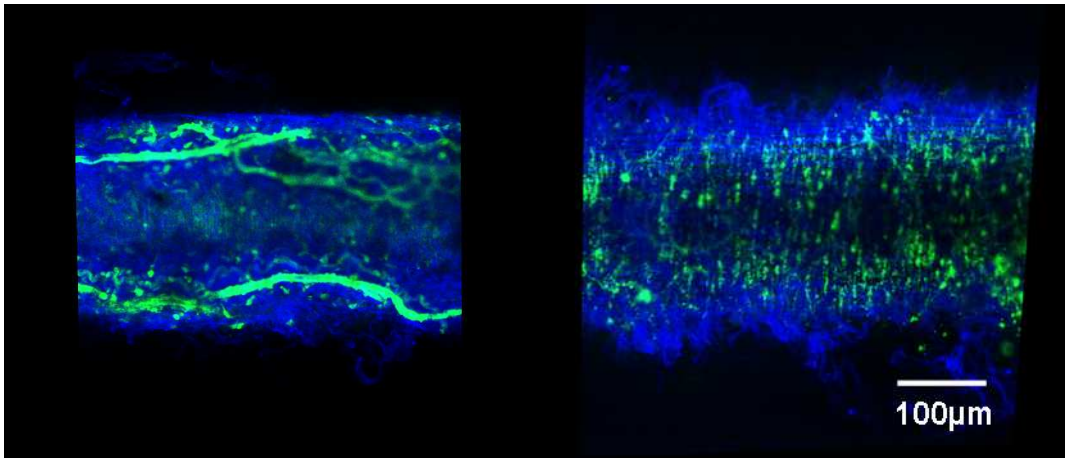


**Figure 6-28 Live pressurised (30mmHg) saphenous artery from 12 week old WKY (n=2, images from different animals)**

## 6.4 Discussion

### *6.4.1 Fixed Mesenteric Artery Staining*

Calcein-AM incubation was assessed at 5, 7 and 10 minutes luminal exposure and endothelial cell staining intensity did not vary significantly between these time points. However, neither 5 nor 7 minutes exposure to calcein-AM gave sufficient smooth muscle cell staining above background levels. Consequently a 10 minute exposure time was chosen for all subsequent experiments.

In the 12 week old WKY the endothelial and smooth muscle cell staining was not significantly different in any of the intensity bins, with the exception of bin 53-101, showing that calcein was transferred to the smooth muscle cells from the endothelium following luminal application of the calcein-AM. In order to establish if this smooth muscle cell staining was a consequence of gap junctional transfer, the same experiments were performed on vessels pre-incubated in a cocktail of the gap junction blocking peptides. The gap junction inhibitors did not affect endothelial cell staining in the 12 week old WKY, showing that they did not affect the uptake of the calcein-AM. However, the smooth muscle cell staining was significantly reduced in the 12 week old WKY after incubation with the gap junction inhibitors.

In contrast to the 12 week old WKY, the 12 week old SHR mesenteric vessels showed significantly less staining in the smooth muscle cells compared with the endothelial cells under control conditions. The gap peptides did not significantly alter either endothelial or smooth muscle cell staining from the control in 12 week old SHR. This suggested that the small amount of smooth muscle cell staining observed in the 12 week old SHR was not a consequence of gap junctional transfer and could represent calcein-AM that diffused across the endothelial layer escaping de-esterification (thus enabling it to enter the smooth muscle cells through the membrane, overriding the need for gap junctional transfer).

Comparison of both strains at 12 weeks of age showed that the endothelial fluorescence was not significantly different in any of the intensity bins. This demonstrated that endothelial cell uptake of calcein-AM was independent of

strain. However, comparison of the WKY and SHR smooth muscle cell staining at 12 weeks of age showed that the SHR had significantly less voxels in all of the intensity bins above background. This implied that the WKY had greater communication between the endothelial and smooth muscle cell layers, since in the SHR there was less dye transfer from the endothelium to the smooth muscle.

In the 6 month old WKY control there was significantly less staining in the smooth muscle cells than in the endothelial layer in all intensity bins. This implied that the endothelial and smooth muscle cell communication had deteriorated with age from 12 week old animals, where there was no significant difference between the fluorescence of the two cell layers. The gap junction inhibitors cause a decrease in endothelial cell staining at high intensities in the 153-201 and 203-251 intensity bins. This difference may be accounted for by the low sample number in these experiments rather than a direct effect of the gap junction inhibitors. The gap junction inhibitors caused a significant decrease in smooth muscle cell staining at the high intensity bins 153-201 and 203-251, which would suggest that some of the smooth muscle cell staining observed in the 6 month old WKY control is a result of gap junctional transfer.

The 6 month old SHR mesenteric vessels showed significantly less staining in the smooth muscle cells compared with the endothelial cells at all intensities above 101. The gap junction blocking peptides did not significantly affect either endothelial or smooth muscle cell intensities in the 6 month old SHR, as was the case in the 12 week old SHR. This implied that there were less functional gap junctions in the SHR as compared with the WKY since the gap junction blocking peptides had an effect in the WKY at both age points but not at either age point of the SHR.

### *6.4.2 Live Mesenteric Artery staining*

Progressing from the fixed experiments, live vessel imaging was undertaken using the newly purchased ELWD objectives. In contrast to the fixed vessels which showed consistent staining among preparations of the same group, the live imaging was found to have variable results- with strong staining observed some days and poor staining others, under the same experimental conditions. Analysis of results from these experiments showed high variability from

preparation to preparation and no consistent patterns in staining could be established.

Due to the variable nature of the control vessels in the live imaging experiments, no conclusions could be reached from the experiments with carbenoxolone incubation. A steady level of fluorescence was not observed in vessels without carbenoxolone incubation therefore inferences could not be made about the effect of carbenoxolone, even thought it did appear to decrease fluorescence in some cases. Also, on occasion, the vessels pre-incubated in carbenoxolone appeared to have punctate calcein staining at sites which may potentially be MEGJs. Experiments with carbenoxolone pre-incubation may have been more conclusive if a concentration of 300μM were used.

These live imaging results were unexpected after the success of the fixed image analysis, since there appeared to be no obvious visual difference between the WKY and SHR mesenteric staining at either age point.

It may be the case that the experimental conditions in the live experiments were not suitable to detect subtle differences between the preparations. Some vessels were more brightly stained than others but this was not due to the imaging parameters which were kept constant. The reason for the variation was unknown, but perhaps the live vessel was not as resilient to imaging as the fixed vessel, making it is more difficult to obtain clear images, especially on a Z-series where multiple layers were scanned.

### *6.4.3 Live Saphenous Artery Staining*

Dye transfer was studied in the saphenous artery to assess whether luminally loaded dye would transfer to the smooth muscle cells in an artery in which an absence of EDHF has been established (Sandow *et al.*, 2004). The saphenous artery proved difficult to image on the pressure system due to the thickness of the adventitia and the problems encountered getting the vessel to maintain pressure. Although the imaging through the saphenous was more difficult than the mesentery due to its dense adventitia it was possible on several occasions. Smooth muscle cell staining was evident in the saphenous artery where it was expected there would be no staining since a functional EDHF response was not

obtained in myography experiments (Chapter 4). Due to the problems maintaining pressure in the saphenous artery there may have been calcein-AM leakage into the bath, causing its uptake from the adventitial side of the vessel.

To conclude, these results suggest that the fixed image analysis gave more consistent patterns of staining between strains than the live imaging. The reasons for this are unclear, but it may be that the fixing process halts any further progression of dye, whereas the live vessel is still capable of facilitating further dye transfer between cell layers.

# Chapter 7 Vascular Connexin Immunohistochemistry

## 7.1 Introduction

Gap junctions are formed by the docking of two connexon subunits, each of which are composed of 6 connexin proteins (Segretain & Falk, 2004). Four connexin subtypes have been found in the vasculature, namely: Cx37, Cx40, Cx43 and Cx45. The distribution of connexins has been shown to vary between different vessel types and between layers of the same vessel.

Connexin expression was studied in normotensive and hypertensive rats to determine if there was a difference in expression between the strains, and make comparisons with the literature. Cx37 and Cx40 expression is reported to be decreased in the endothelial cells of mesenteric arteries of SHR compared with WKY at 8 months of age (Kansui *et al.*, 2004).

Mesenteric and saphenous vessels were chosen as examples of resistance and conduit arteries respectively. The saphenous artery was of particular interest due to its apparent absence of MEGJs in the adult rat shown by electron microscopy (Sandow *et al.*, 2004) thereby implying that there would be no connexin staining at the myoendothelial border.

## 7.2 Aims

The aims of this chapter were:

- To establish Cx37 and Cx43 distribution in the third order mesenteric artery and saphenous artery of 6 month old WKY and SHR.

- To compare Cx37 and Cx43 profiles between strains.

## 7.3 Methods

### *7.3.1 Tissue Preparation*

The mesenteric arcade was removed from the rat and spread flat with the gut wall outermost. The gut wall was then cut away from the preparation leaving the blood vessels and surrounding fat intact. The superior branch and surrounding fat was tied with string and the remaining arterial braches were gathered and tied at the distal end so that all vessels in the mesenteric arcade

were arranged in parallel. This mesenteric bundle was pinned out taut on dental wax before emersion in fixative. The saphenous artery and adjoining nerve and vein were pinned out at either end under tension before emersion in PBS.

Tissues were washed in 0.1M PB and dehydrated through the series: 70% alcohol (2 hours), 90% alcohol (2 hours), absolute alcohol (2 hours) x3, amyl acetate (2 hours) x3, paraffin wax (4 hours) x2. Tissue embedded in wax was then cryostat sectioned at 5µm.

### *7.3.2 Immunohistochemistry*

The 5µm cryosections of transverse rings of the fixed tissue were mounted on poly-L-lysine-coated slides (Surgipath) and air-dried. Slides were incubated in Hydroclear for 15 minutes and dehydrated in decreasing concentrations of alcohol. Slides were then heated at 100°C for 10 minutes to remove cross-linkages and rinsed twice in fresh PBS. Sections were blocked with PBS containing 1% goat serum with 0.3% Triton for one hour at room temperature.

Samples were exposed to Cx37 (Cx37 mouse polyclonal, Alpha Diagnostics, dilution 1:200) or Cx43 (Cx43 rabbit monoclonal, Millipore, dilution 1:100) antibodies at 4°C overnight. Secondary antibodies of goat anti-mouse conjugated Alexa 488 (Molecular Probes; 1:400 dilution) or goat anti-rabbit conjugated Alexa 546 (Molecular Probes; 1:400 dilution) were applied to the Cx37 and Cx43 samples respectively and incubated for 3 hours at room temperature in a dark humidity box. They were then washed twice with PBS and finally with distilled water. Control slides were incubated with primary antibody but secondary antibody incubation was omitted. Sections were mounted with Fluorsave (Calbiochem) and imaged using confocal microscopy.

In the presence of a peroxidase conjugated secondary antibody, 3,3'-diaminobenzidine (DAB) produces a brown insoluble precipitate in that is insoluble in alcohol in the area of the section where the antibody has bound antigen. This process was attempted to see if similar results to the fluorescent secondary antibody were obtained.

## 7.4 Results

The SHR sections cut were of a poor quality compared with the WKY, and have been excluded from the study.

Control vessels for 6 month WKY (with no secondary antibody for Cx37) were imaged at the same laser settings as the vessels incubated in the secondary antibody. Control vessels have no punctuate staining, but indicate the level of background autofluorescence (Figures 7.1 (a), (b)).

Immunostaining of Cx37 in the WKY mesenteric arteries was confirmed by DAB and fluorescence staining, and revealed expression in the endothelial and medial layers (Figure 7.1 (c), (d), (e)). The Cx37 staining was prominent on endothelial cells, smooth muscle cells, and at the endothelial smooth muscle cell border (Figure 7.1 (c)). Control vessels for Cx37 were imaged at the same laser settings and have no punctuate staining, but indicate the level of background autofluorescence (Figures 7.1 (a), (b)).

In contrast to the mesenteric arteries, the saphenous artery did not show prominent staining for Cx37 in the media, but did exhibit punctuate staining on the luminal border of the endothelial cells, and staining at the adventitia (Figure 7.2).

Cx43 staining was not present in the mesenteric (Figure 7.3 (c)) or saphenous arteries, even after the trial of several other secondary antibodies, and a higher dilution (1 in 50) of the Cx43 primary antibody. To confirm that the Cx43 antibody staining could be detected in other tissues, it was tested on transverse sections of the gut (Figure 7.3 (a), (b)), and there appeared to be some punctuate staining in these cells.

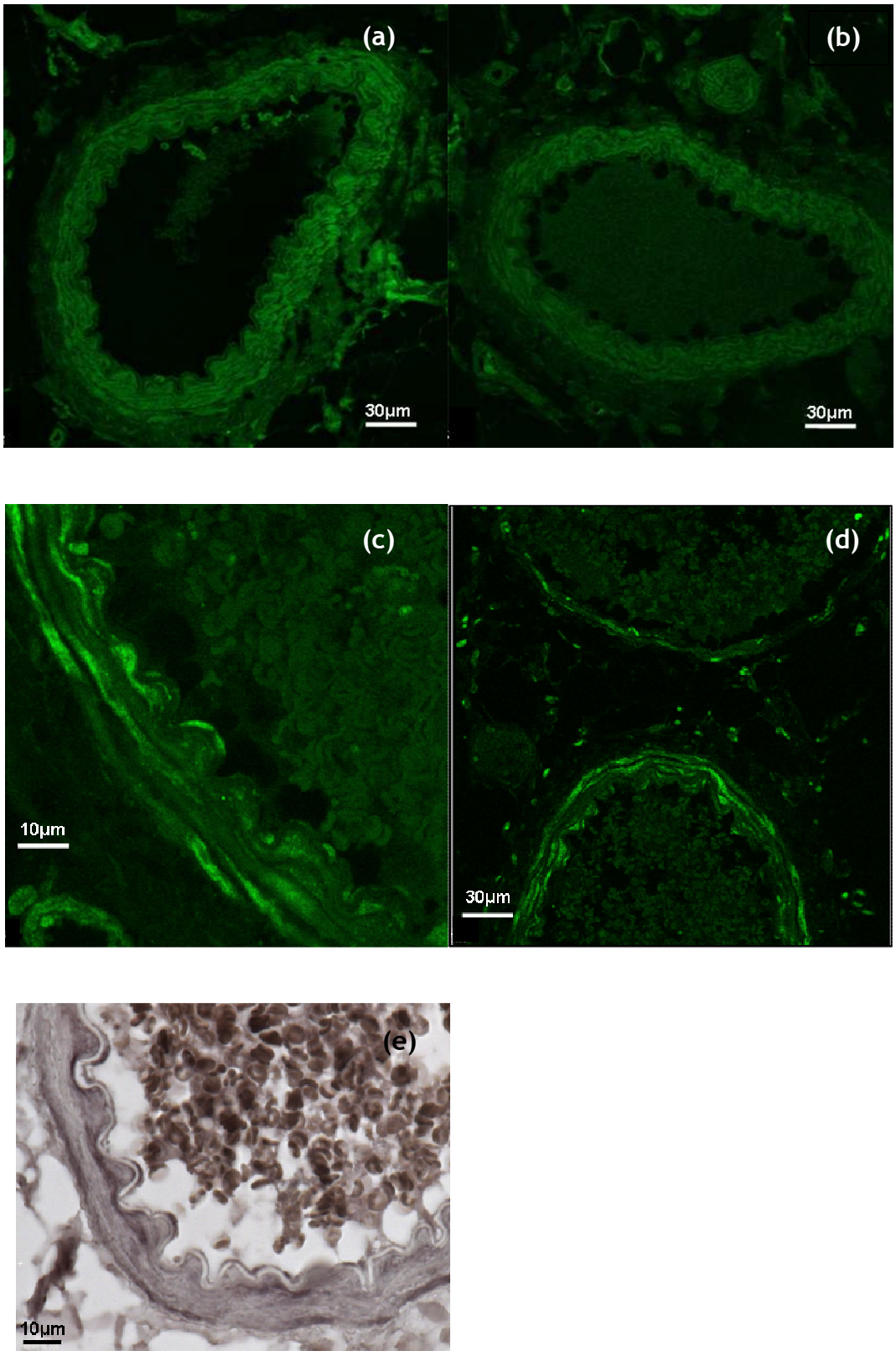


**Figure 7-1 Cx37 staining in mesenteric vessels of 6 month old WKY rat: (a) and (b) control sections lacking the secondary antibody, (c) high power confocal image of artery wall, (d) high power confocal image of vein and artery wall, (e) DAB staining of artery wall.**

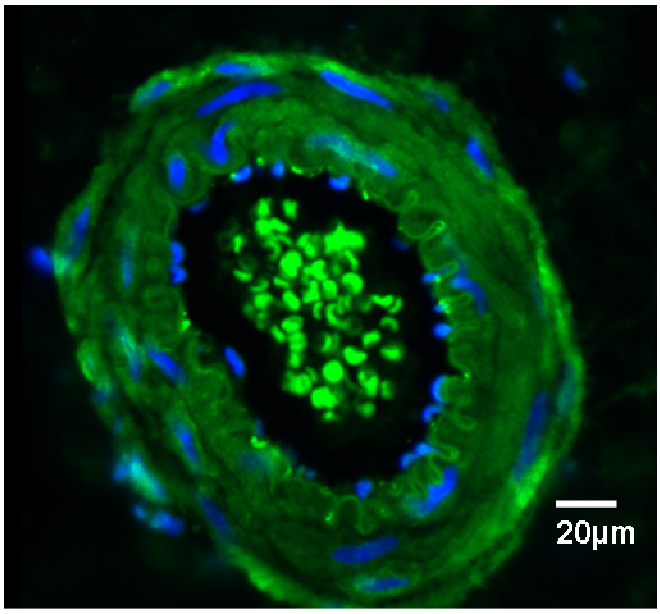


**Figure 7-2 Staining of Cx37 in saphenous artery of 6 month old WKY rat. Counterstained with DAPI nuclear stain.**

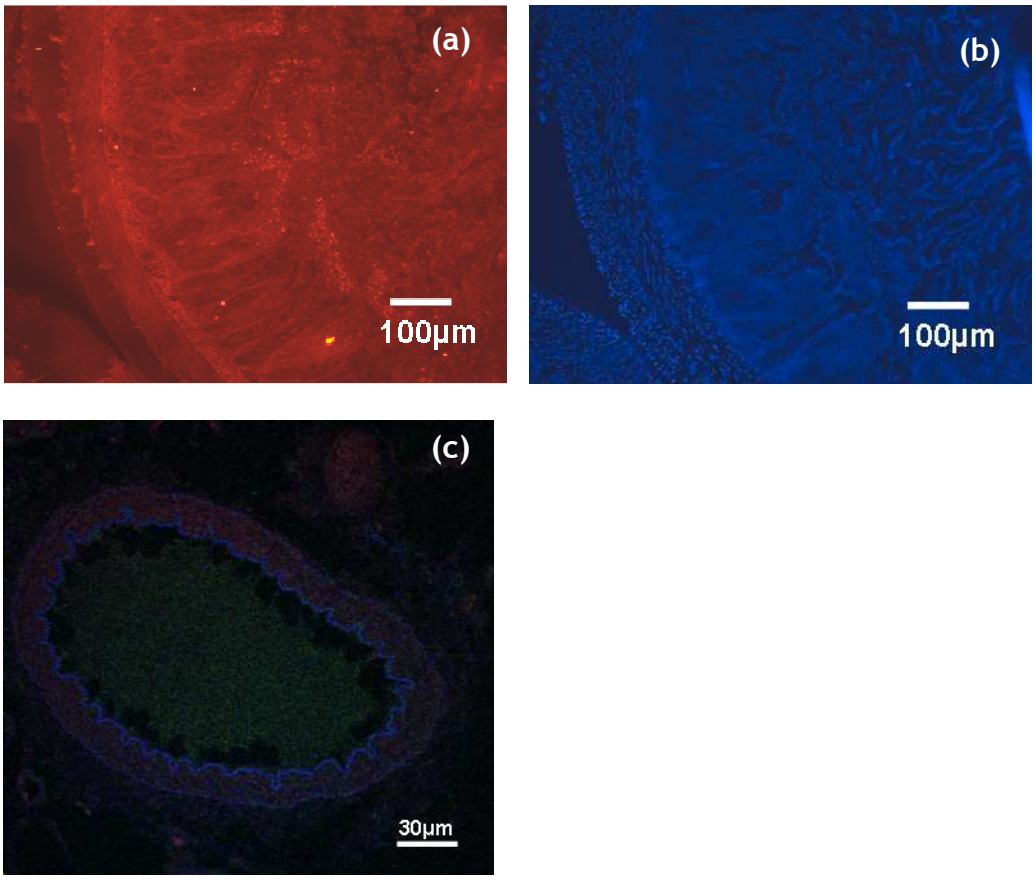


**Figure 7-3 Cx43 staining (a), and DAPI nuclear counterstain (b), in a transverse section of the gut, and absence of Cx43 staining in the mesenteric artery (c).**

## 7.5 Discussion

The results from this chapter are by no means conclusive due to the difficulties in obtaining good sections for staining. It was not possible to assess Cx40 distribution due to time limitations but this would be a subject of further interest. Unfortunately the SHR sections were of a poor quality, and staining could not be analysed due to only a partial adhesion of the sections to the slides. It would possibly have been more informative to use whole-mount arteries, or to perfusion fix the animals, but this was out with the consent of our Home Office Licence.

Cx37 showed strong staining in the endothelial and smooth muscle cell layers in the mesenteric artery. The profile of Cx37 staining differed in the saphenous artery, where punctate staining was observed on the luminal border of the endothelial cells and at the adventitia. This is suggestive of a lack of connexins, hence gap junctions at the endothelial smooth muscle cell border in the saphenous artery. However, these results must be interpreted with caution since Cx40 staining has not been assessed.

Due to an absence of control data, the Cx43 staining seen in the gut could not be ruled out as autofluorescence, however, the staining is far brighter than that observed in the mesenteric artery at the same laser settings. The lack of Cx43 staining in the mesenteric arteries is consistent with other studies (Earley *et al.*, 2004; Hong & Hill, 1998). Hong at al. (1998) found that expression of Cx43 was restricted to elastic arteries in the rat, following investigation of 11 different artery types.

# Chapter 8 General Discussion

Hypertension is a medical condition in which blood pressure is chronically elevated. Around 95% of hypertension is essential or idiopathic hypertension, that is, it has no known cause. The remaining 5% of cases are secondary hypertension, whereby the high blood pressure is a consequence of another condition such as kidney disease or an adrenal medulla tumor. As yet, treatment for hypertension is symptomatic; therefore drug treatment is aimed at restoring blood pressure to normal levels but does not treat the cause of the hypertension. Hypertension has been shown to be associated with an impairment of endothelium-dependent relaxation in humans (Panza *et al.*, 1990; Linder *et al.*, 1990; Treasure *et al.*, 1992) and in animal models (Luscher & Vanhoutte, 1986; Clozel *et al.*, 1990). Consequently, the differences in endothelial function of normotensive and hypertensive resistance arteries, which are the vessels important in determining peripheral blood pressure, are the subject of much study. SHR cannot directly replicate the condition of human hypertension, but due to difficulty in obtaining human tissue biopsies with appropriate controls, SHR and WKY controls are widely used in assessing the effects of elevated blood pressure on the vasculature.

In functional experiments (Chapters 4 and 5), there was almost a full reversal of the PE preconstriction by ACh in the SHR, similar to that of the WKY, provided the NO component of relaxation was intact. However, if NO production was blocked, the relaxation to ACh was very poor in the SHR, owing to a blunted EDHF response. The transmission of NO does not require gap junctions since sandwich preparations have shown that if smooth muscle was opposed with endothelium from another vessel then the smooth muscle was still capable of relaxation (Chaytor *et al.*, 1998a). This, coupled with the ability of carbenoxolone to reduce the EDHF response in the WKY in the present study, would suggest that the decreased EDHF response in the SHR is at least partly due to a reduction in MEGJs. The idea that EDHF is dependent on gap junctions correlates well with dye transfer experiments (Chapter 6), in which SHR showed little smooth muscle cell staining in control experiments. No EDHF response was obtained in the saphenous arteries in this study (Chapter 5). This is consistent with the theory that EDHF is most important in small resistance arteries compared with conduit arteries (Berman *et al.*, 2002; Shimokawa *et al.*, 1996b). This most likely relates to the physiological roles of the saphenous and

mesenteric vessels: where the mesenteric arteries are fundamental to blood pressure control and therefore require the additional mechanism of EDHF to backup NO; and where the saphenous artery is capable of dilation by NO release, but its dilation does not have an intervening effect on blood pressure, therefore EDHF is not an essential functional component.

The use of a non-adrenergic contractile agonist would have determined whether the increased contractility in the SHR was an adrenergic effect or if it was due to a general increase in contractility. Similarly, it would have been useful to assess responses to the endothelium-independent vasodilator levcromakalim (a direct opener of ATP-sensitive $K^+$ channels) to ensure that the WKY and SHR were capable of similar levels of relaxation, independent of the release of endothelial factors. However, no significant difference in the levcromakalim response was found between the WKY and SHR mesenteric arteries (Onaka *et al.*, 1998).

The compound Rotigapeptide (ZP123) is reported to increase gap junctional communication (Clarke *et al.*, 2006), thereby raising the possibility that the reduced EDHF response in the SHR could be restored. The mechanism of action of Rotigapeptide is unclear but it has been shown to increase dye transfer in myocytes and atrial HL-1 cells where Cx43 is the dominant connexin, without modifying the overall level of Cx43 or the phosphorylation status of the protein (Clarke *et al.*, 2006). As Cx43 is the dominant connexin expressed in the mammalian heart this was a very exciting finding. Acidosis causes conduction slowing in Langendorff-perfused guinea pig hearts due to intercellular uncoupling, and ZP123 was found to inhibit this conduction slowing during acidosis by approximately 60%. However, ZP123 had no effect on conduction velocity in the absence of acidosis, suggesting that only gap junctions under metabolic stress were targeted. In addition, ZP123 did not affect $Na^+$ current in isolated myocytes, suggesting that the activity of the drug was due to an action at gap junctions (Eloff *et al.*, 2003). Rotigapeptide is in Phase II clinical trials for ventricular arrhythmias, but has the practical limitation of poor oral availability due to enzymatic degradation (Mazzini & Monahan, 2008). In another study, Rotigapeptide was found to have no effect on forearm blood flow in man when NO production and COX were blocked (Lang *et al.*, 2008), showing that it did not enhance the EDHF response *in-vivo*. It would be interesting to assess

Rotigapeptide in functional myography experiments to determine if it was effective in restoring the diminished EDHF response in the SHR *in-vitro*. Also, dye transfer experiments following Rotigapeptide incubation could be performed to assess if calcein transfer was increased in the SHR.

Another potential therapeutic target for the restoration of EDHF in hypertension is to selectively target the endothelial $IK_{Ca}$ channels which are involved in the initial hyperpolarisation of the endothelial cells which is transmitted to the smooth muscle as EDHF. This may be a promising field of research, with the drug SKA-31 documented to have a half life of 12 hours and low plasma binding. SKA-31 was shown to potentiate the dilations of carotid arteries from KCa3.1 (+/+) mice but not from KCa3.1 (-/-) mice, thus affirming it acted on KCa3.1 channels. *In-vivo* SKA-31 lowered the mean arterial blood pressure by 6mmHg in normotensive mice, and by 12mmHg in angiotensin-II-induced hypertensive mice (Sankaranarayanan *et al.*, 2009). On the other hand, activation of $IK_{Ca}$ channels must be treated with caution due to their role of in the proliferation of endothelial cells (Grgic *et al.*, 2005) and cancerous cells (Wang *et al.*, 2007). It was also found that in mice, administration of TRAM-34 for two weeks significantly suppressed angiogenesis by around 85% (Grgic *et al.*, 2005). Similarly, in endometrial cancer cells from human specimens, clotrimazole and TRAM-34, two inhibitors of $IK_{Ca}$ channels, suppressed the proliferation of the cancer cells (Wang *et al.*, 2007).

A further hopeful approach to the treatment of endothelial dysfunction was to target the transient receptor potential vanilloid subtype 4 (TRPV4) channel, which is involved in $Ca^{2+}$ entry following endothelial stimulation. Indeed, mice deficient for the TRPV4 channel exhibit impaired endothelium dependent relaxation to ACh *in-vitro* and *in-vivo* (Zhang *et al.*, 2009). A novel activator of TRPV4, GSK1016790A, caused a profound decrease in blood pressure in the three species tested (mouse, rat and dog), but this was followed by a profound circulatory collapse and death (Willette *et al.*, 2008). The GSK compound had no effect on TRPV4 deficient mice, thus affirming its action at TRPV4.

A class of drugs in common therapeutic use, blockers of the renin-angiotensin-system, has been shown to have actions improving EDHF in the mesenteric arteries of SHR. Enalapril, an inhibitor of the angiotensin-converting enzyme (ACE inhibitor) improved the EDHF function in mesenteric arteries of the SHR, but NO-mediated relaxation was not altered by this drug therapy (Onaka *et al.*, 1998). A subsequent

study demonstrated that the angiotensin 1 ($AT_1$) receptor antagonist TCV-116 could also improve the EDHF response in SHR treated from 8 to 11 months (Goto *et al.*, 2000). Chronic treatment with the $AT_1$ receptor antagonist candesartan was reported to increase Cx37 and Cx40 expression in mesenteric arteries of the SHR, where Cx37 and Cx40 expression was significantly decreased in SHR compared with WKY (Kansui *et al.*, 2004). Hyperpolarisations to ACh were 30% smaller in the SHR than in WKY, but this was restored by enalapril (Ellis *et al.*, 2009). There were also fewer MEGJs per endothelial cell in the mesenteric resistance arteries of SHR than WKY and fewer of the holes in the IEL had endothelial projections, but neither of these parameters were altered by enalapril treatment (Ellis *et al.*, 2009).

In this study, Cx43 could not be detected in the mesenteric or saphenous arteries of the WKY or SHR (Chapter 7). This is consistent with the findings of Hong and Hill (1998), where Cx43 was only present in larger elastic arteries such as aorta. The immunohistochemical findings in this study were by no means conclusive but do give an indication of Cx37 presence in both the endothelium and smooth muscle in the mesenteric artery; and the restriction of Cx37 to the endothelium and parts of the adventitial-SMC border in the saphenous artery.

The mesenteric imaging data (Chapter 6) revealed a relationship between EDHF function and dye transfer in the mesenteric arteries. Smooth muscle cell staining was significantly greater in WKY compared with SHR at both age points, whilst endothelial cell staining remained consistent between strains. There was a functional EDHF response in the mesenteric arteries at both age points, whereas no EDHF response was detected in the SHR at either age. The smooth muscle cell staining in the WKY was reduced following incubation with the gap peptides, and these gap peptides had no significant effect on the SHR smooth muscle cell staining. Dye transfer experiments in the saphenous artery were unsuccessful since the dense adventitia made this artery difficult to image. A suitable alternative may have been to try another artery documented to be lacking an EDHF response, with a thinner wall than the saphenous, such as the renal artery, to assess dye transfer. The saphenous artery was chosen in this study due to the publication by Sandow's group detailing the EDHF functional response and presence of MEGJs by electron microscopy (Sandow *et al.*, 2004). Renal arteries have been reported to have a loss of the EDHF response with ageing from 8 weeks to 22 months (Bussemaker *et al.*, 2003), therefore dye transfer

experiments in this artery at these two age points would test the robustness of the theory that calcein staining is correlated with the EDHF function of the vessel.

It has been demonstrated that different connexin subunits in a gap junction affect the channel permeability. Cx26 gap junctions are more permeable to lower molecular weight dyes such as Lucifer yellow (MW 457), but are impermeable to larger dyes such as Alexa 594 (MW 780) (Nicholson *et al.*, 2000). This is likely to have implications for dye transfer studies where the composition of the gap junctions has not been considered, such that dye transfer did not occur due to the size selectivity of the connexins in the gap junctional pore rather than due to an absence of gap junctions. Calcein-AM used in this study had a molecular weight of 995, which is narrowly within the limit of gap junctional transfer of less than 1kDa. When de-esterified to calcein the molecular weight is reduced to 622.5. It would be useful to test another dye and assess if it was transferred in a similar fashion. However, the property of calcein-AM being converted to its cell impermeable fluorescent form calcein made this dye ideally suited to the purposes of this study.

Gap junctions in the cardiovascular system are formed by connexins 37, 40, 43 and 45. Cx40 has been localised to endothelial cell borders and to small regions at the end of endothelial cell projections passing through the IEL in mesenteric arteries of the rat (Mather *et al.*, 2005). Rat aortic endothelia have been shown to express Cx40, Cx37 and Cx43; and coronary artery endothelia expressed Cx40 and Cx37, but lacked Cx43 (Yeh *et al.*, 1998). In microvessels from the brain and cremaster of the rat, and arterioles of the hamster cheek pouch, Cx43 and Cx40 have been found in both the endothelial and smooth muscle cell layers (Little *et al.*, 1995a). Cx37 has been found in both the endothelial and smooth muscle cells of the rat mesenteric arteries, but Cx43 was not detected in this study (Earley *et al.*, 2004). In the rat it has been shown that Cx43 staining was observed in the endothelium and media of larger elastic arteries, but in smaller muscular arteries such as the mesenteric, hepatic, and tail, Cx43 expression was high in the endothelium but absent from the media (Hong & Hill, 1998).

Recently gap peptides have been developed which are small peptides designed to interfere with a specific extracellular region of the appropriate connexin. Gap

peptides cannot be selectively targeted to *myoendothelial* connexins, since the inhibitor is selective only for the connexin subunit, therefore will act on any gap junctions where this connexin is present. This has therapeutic implications if a viable gap junction inhibitor were to be given systemically, since it would have a multitude of undesirable effects on gap junctions in the heart and elsewhere.

There is some ambiguity about the mode of action of gap peptides and whether they are truly specific, so another approach to studying the function of a specific connexin in the vasculature is to use transgenic connexin knockout mice. Cx45 deficient mice die during embryonic development due to severe abnormalities in vascular development (Kruger *et al.*, 2000). Cx43 knockout mice die perinatally caused by a failure in pulmonary gas exchange due to the obstruction of the right ventricular outflow tract from the heart (Reaume *et al.*, 1995). Together these studies suggest that Cx45 and Cx43 play an essential role in the development of the vasculature and the heart respectively. Cell-specific deletion of these connexins rather than a full knockout would perhaps permit their functional study. Cx40 knockout mice are viable, and study of these animals revealed them to be hypertensive in both anaesthetised and awake states, without an alteration in heart rate compared with control mice (de Wit *et al.*, 2000; de Wit *et al.*, 2003). In addition to this, a polymorphism within the Cx40 promoter has been demonstrated to be associated with an increased risk of hypertension in men (Firouzi *et al.*, 2006), thus implying that connexins are involved in blood pressure regulation in the human vasculature. The use of connexin knockout mice would have aided this study in assessing the EDHF response and dye transfer in the absence of a particular connexin.

It was found that there were significantly more fenestrae in the 12 week old WKY compared with the 12 week old SHR, but at 6 months of age there was no significant difference in fenestrae number between the strains. This coupled with an increase in fenestrae area with age in the WKY is suggestive of the fusing of adjacent fenestrae in the SHR. Since there are no genetic differences in the amount of elastin between WKY and SHR (Briones *et al.*, 2003), then the smaller fenestrae in the 6 month old SHR appears to be a protective mechanism against the elevated blood pressure in this strain. It would be interesting to assess the fenestrae in SHR given antihypertensive treatment from an early age to see if the fenestrae develop in the same way as the WKY if blood pressure was not

excessively high, that is, to determine whether the smaller fenestrae are a result of strain (SHR) or pressure.

In summary, although a unifying hypothesis regarding the relationship between EDHF and myoendothelial coupling could not be reached, a number of conclusions can be drawn from the studies presented. EDHF function in third order mesenteric arteries was shown to be reduced in the SHR compared with the WKY, and non-existent in the saphenous artery of either strain. The transfer of luminally loaded dye was reduced in the WKY following incubation with the gap peptides; and in the SHR compared with the WKY control. These results are suggestive of dye transfer, representative of gap junctional transfer, being related to the functional EDHF response of an artery. The reduced fenestrae area in the SHR mesenteric artery may contribute towards this reduction in EDHF and dye transfer, since it provides less opportunity for endothelial and smooth muscle cell communication, be it via MEGJs or by diffusion.

# Reference List

ARRIBAS, SM, HILLIER, C, GONZALEZ, C, MCGRORY, S, DOMINICZAK, AF & MCGRATH, JC. (1997). Cellular aspects of vascular remodeling in hypertension revealed by confocal microscopy. *Hypertension*, **30**, 1455-1464.

BERMAN, RS, MARTIN, PEM, EVANS, WH & GRIFFITH, TM. (2002). Relative contributions of NO and gap junctional communication to endothelium-dependent relaxations of rabbit resistance arteries vary with vessel size. *Microvascular Research*, **63**, 115-128.

BOLTON, TB, LANG, RJ & TAKEWAKI, T. (1984). Mechanisms of action of noradrenaline and carbachol on smooth muscle of guinea-pig anterior mesenteric artery. *The Journal of Physiology*, **351**, 549-572.

BRANDES, RP, SCHMITZ-WINNENTHAL, FH, FELETOU, M, GODECKE, A, HUANG, PL, VANHOUTTE, PM, FLEMMING, I & BUSSE, R. (2000). An endothelium-derived hyperpolarising factor distinct from NO and prostacyclin is a major endothelium-dependent vasodilator in resistance vessels of wild type and endothelial NO synthase knowckout mice. *Proceedings of the National Academy of Sciences of the United States of America*, **97**, 9747-9752.

BRINK, PR. (1998). Gap junctions in vascular smooth muscle. *Acta Physiologica Scandinavica*, **164**, 349-356.

BRIONES, AM, GONZALEZ, JM, SOMOZA, B, GIRALDO, J, DALY, CJ, VILA, E, GONZALEZ, MC, MCGRATH, JC & ARRIBAS, SM. (2003). Role of elastin in spontaneously hypertensive rat small mesenteric artery remodelling. *The Journal of Physiology*, **552**, 185-195.

BUNTING, S, GRYGLEWSKI, R, MONCADA, S & VANE, JR. (1976). Arterial walls generate from prostaglandin endoperoxidases a substance (prostaglandin X) which relaxes strips of mesentery and coeliac arteries and inhibits platelet aggregation. *Prostaglandins*, **12**, 897-913.

BUSSE, R & MULSCH, A. (1990). Calcium-dependent nitric oxide synthesis in endothelial cytosol is mediated by calmodulin. *Federation of European Biochemical Societies Letters*, **265**, 133-136.

BUSSE, R, EDWARDS, G, FÉLÉTOU, M, FLEMING, I, VANHOUTTE, PM & WESTON, AH. (2002). EDHF: bringing the concepts together. *Trends in Pharmacological Sciences*, **23**, 374-380.

BUSSEMAKER, E, POPP, R, FISSLTHALER, B, LARSON, CM, FLEMING, I, BUSSE, R & BRANDES, RP. (2003). Aged spontaneously hypertensive rats exhibit a selective loss of EDHF-mediated relaxation in the renal artery. *Hypertension*, **42**, 562-568.

CAMPBELL, WB, GEBREMEDHIM, D, PRATT, PF & HARDER, DR. (1996). Identification of epoxyeicosatrienoic acids as endothelium-derived hyperpolarising factors. *Circulation Research*, **78**, 415-423.

CARVAJAL, JA, GERMAIN, AM, HUIDOBRO-TORO, JP & WEINER, CP. (2000). Molecular mechanism of cGMP-mediated smooth muscle relaxation. *Journal of Cellular Physiology*, **184**, 409-420.

CHAYTOR, AT, EVANS, WH & GRIFFITH, TM. (1998). Central role of heterocellular gap junctional communication in endothelium-dependent relaxations of rabbit arteries. *The Journal of Physiology*, **508**, 561-573.

CHAYTOR, AT, MARTIN, PEM, EDWARDS, DH & GRIFFITH, TM. (2001). Gap junctional communication underpins EDHF-type relaxations evoked by ACh in the rat hepatic artery. *American Journal of Physiology - Heart and Circulatory Physiology*, **280**, H2441-H2450.

CHEN, G, SUZUKI, H & WESTON, AH. (1988). Acetylcholine releases endothelium-derived hyperpolarizing factor and EDRF from rat blood vessels. *British Journal of Pharmacology*, **95**, 1165-1174.

CHOBANIAN, AV, BAKRIS, GL, BLACK, HR, CUSHMAN, WC, GREEN, LA, IZZO, JL, JONES, DW, MATERSON, BJ, OPARIL, S, WRIGHT, JL & ROCELLA, EJ. (2003). Seventh report of the joint national comitte on prevention, detection, evaluation and treatment of high blood pressure. *Hypertension*, **42**, 1206-1252.

CLARKE, TC, THOMAS, D, PETERSEN, JS, EVANS, WH & MARTIN, PEM. (2006). The antiarrhythmic peptide rotigaptide (ZP123) increases gap junction intercellular communication in cardiac myocytes and HeLa cells expressing connexin 43. *British Journal of Pharmacology*, **147**, 486-495.

CLOZEL, M, KUHN, H & HEFTI, F. (1990). Effects of angiotensin converting enzyme inhibitors and of hydralazine on endothelial function in hypertensive rats. *Hypertension*, **16**, 532-540.

DAGA-GORDINI, D, BRESSAN, GM, CASTELLANI, I & VOLPIN, D. (1987). Fine mapping of tropoelastin-derived components in the aorta of developing chick embryo. *Histochemical Journal*, **19**, 623-632.

DAVIES, PF, GANZ, P & DIEHL, PS. (1985). Reversible microcarrier-mediated junctional communication between endothelial and smooth muscle cell monolayers: an in vitro model of vascular cell interactions. *Laboratory Investigation*, **53**, 710-718.

DAVIS, EC. (1995). Elastic lamina growth in the developing mouse aorta. *Journal of Histochemistry and Cytochemistry*, **43**, 1115-1123.

DE MEY, JG & VANHOUTTE, PM. (1982). Heterogeneous behavior of the canine arterial and venous wall. Importance of the endothelium. *Circulation Research*, **51**, 439-447.

DE WIT, C, HOEPFL, B & WOLFLE, SE. (2006). Endothelial mediators and communication through vascular gap junctions. *Biological Chemistry*, **387**, 3-9.

DE WIT, C, ROOS, F, BOLZ, SS & POHL, U. (2003). Lack of vascular connexin 40 is associated with hypertension and irregular arteriolar vasomotion. *Physiological Genomics*, **13**, 169-177.

DE WIT, C, ROOS, F, BOLZ, SS, KIRCHHOFF, S, KRUGER, O, WILLECKE, K & POHL, U. (2000). Impaired Conduction of Vasodilation Along Arterioles in Connexin40-Deficient Mice. *Circulation Research*, **86**, 649-655.

DORA, KA, GALLAGHER, NT, TAKANO, H, RUMMERY, NM, HILL, CE, GARLAND, CJ & SANDOW, SL. (2003a). Myoendothelial gap junctions may provide the pathway for EDHF in mouse mesenteric artery. *Journal of Vascular Research*, **40**, 480-490.

DORA, KA, GALLAGHER, NT, MCNEISH, A & GARLAND, CJ. (2008). Modulation of endothelial cell KCa3.1 channels during endothelium-derived hyperpolarizing factor signaling in mesenteric resistance arteries. *Circulation Research*, **102**, 1247-1255.

DORA, KA, MARTIN, PEM, CHAYTOR, AT, EVANS, WH, GARLAND, CJ & GRIFFITH, TM. (1999). Role of heterocellular gap junctional communication in endothelium-dependent smooth muscle hyperpolarization: inhibition by a connexin-mimetic peptide. *Biochemical and Biophysical Research Communications*, **254**, 27-31.

DORA, KA, XIA, J & DULING, BR. (2003b). Endothelial cell signaling during conducted vasomotor responses. *American Journal of Physiology - Heart and Circulatory Physiology*, **285**, H119-H126.

DULING, BR & BERNE, RM. (1970). Propagated Vasodilation in the Microcirculation of the Hamster Cheek Pouch. *Circulation Research*, **26**, 163-170.

DUSTING, GJ, MONCADA, S & VANE, JR. (1977). Prostacyclin (PGX) is the endogenous metabolite responsible for relaxation of coronary arteries induced by arachadonic acid. *Prostaglandins*, **13**, 3-15.

EARLEY, S, RESTA, TC & WALKER, BR. (2004). Disruption of smooth muscle gap junctions attenuates myogenic vasoconstriction of mesenteric resistance arteries. *American Journal of Physiology - Heart and Circulatory Physiology*, **287**, H2677-H2686.

EDWARDS, G, DORA, KA, GARDENER, MJ, GARLAND, CJ & WESTON, AH. (1998). K+ is an endothelium-derived hyperpolarizing factor in rat arteries. *Nature*, **396**, 269-272.

EDWARDS, G, FÉLÉTOU, M, GARDENER, MJ, THOLLON, C, VANHOUTTE, PM & WESTON, AH. (1999). Role of gap junctions in the responses to EDHF in rat and guinea-pig small arteries. *British Journal of Pharmacology*, **128**, 1788-1794.

ELLIS, A, GOTO, K, CHASTON, DJ, BRACKENBURY, TD, MEANEY, KR, FALCK, JR, WOJCIKIEWICZ, RJH & HILL, CE. (2009). Enalapril treatment alters the contribution of epoxyeicosatrienoic qcids but not gap junctions to endothelium-derived hyperpolarizing factor activity in mesenteric arteries of spontaneously hypertensive rats. *Journal of Pharmacology And Experimental Therapeutics*, **330**, 413-422.

ELOFF, BC, GILAT, E, WAN, X & ROSENBAUM, DS. (2003). Pharmacological modulation of cardiac gap junctions to enhance cardiac conduction: evidence

supporting a novel target for antiarrhythmic therapy. *Circulation*, **108**, 3157-3163.

EMERSON, GG & SEGAL, SS. (2000). Electrical coupling between endothelial cells and smooth muscle cells in hamster feed arteries : Role in Vasomotor Control. *Circulation Research*, **87**, 474-479.

EVANS, WH & MARTIN, PEM. (2002). Gap junctions: structure and function. *Molecular Membrane Biology*, **19**, 121-136.

FARACI, FM & DIDION, SP. (2004). Vascular protection:superoxide dismutase isoforms in the vessel wall. *Arteriosclerosis, Thrombosis and Vascular Biology*, **24**, 1367-1373.

FIGUEROA, XF & DULING, BR. (2009). Gap Junctions in the control of vascular function. *Antioxidants & Redox Signaling*, **11**, 251-266.

FIROUZI, M, KOK, B, SPIERING, W, BUSJAHN, A, BEZZINA, CR, RUIJTER, JM, KOELEMAN, BP, SCHIPPER, M, GROENEWEGEN, WA, JONGSMA, HJ & DE LEEUW, PW. (2006). Polymorphisms in human connexin40 gene promoter are associated with increased risk of hypertension in men. *Journal of Hypertension*, **24**, 325-330.

FLEMMING, I & BUSSE, R. (2006). Endothelium-derived epoxyeicosatrienoic acids and vascular function. *Hypertension*, **47**, 629-633.

FUJII, K, OHMORI, S, TOMINAGA, M, ABE, I, TAKATA, Y, OHYA, Y, KOBAYASHI, K & FUJISHIMA, M. (1993). Age-related changes in endothelium-dependent hyperpolarization in the rat mesenteric artery. *American Journal of Physiology - Heart and Circulatory Physiology*, **265**, H509-H516.

FUJII, K, TOMINAGA, M, OHMORI, S, KOBAYASHI, K, KOGA, T, TAKATA, Y & FUJISHIMA, M. (1992). Decreased endothelium-dependent hyperpolarization to acetylcholine in smooth muscle of the mesenteric artery of spontaneously hypertensive rats. *Circulation Research*, **70**, 660-669.

FURCHGOTT, RF & ZAWADZKI, JV. (1980). The obligatory role of endothelial cells in the relaxation of arterial smooth muscle by acetylcholine. *Nature*, **288**, 373-376.

GARCIA, ML, GAO, YD, MCMANUS, OB & KACZOROWSKI, GJ. (2001). Potassium channels: from scorpion venoms to high resolution. *Toxicon*, **39**, 739-748.

GARLAND, CJ & MCPHERSON, GA. (1992). Evidence that nitric oxide does not mediate the hyperpolarization and relaxation to acetylcholine in the rat small mesenteric artery. *British Journal of Pharmacology*, **105**, 429-435.

GERRITY, RG & CLIFF, WJ. (1975). The aortic tunica media of the developing rat. I. Quantitative stereologic and biochemical analysis. *Laboratory Investigation*, **32**, 585-600.

GLUAIS, P, EDWARDS, G, WESTON, AH, VANHOUTTE, PM & FELETOU, M. (2005). Hydrogen peroxide and endothelium-dependent hyperpolarisation in the guinea-pig carotid artery. *European Journal of Pharmacology*, **513**, 219-224.

GONZALEZ, JM, BRIONES, AM, SOMOZA, B, DALY, CJ, VILA, E, STARCHER, B, MCGRATH, JC, GONZALEZ, MC & ARRIBAS, SM. (2006). Postnatal alterations in elastic fiber organization precede resistance artery narrowing in SHR. *American Journal of Physiology - Heart and Circulatory Physiology*, **291**, H804-H812.

GONZALEZ, JM, BRIONES, AM, STARCHER, B, CONDE, MV, SOMOZA, B, DALY, C, VILA, E, MCGRATH, I, GONZALEZ, MC & ARRIBAS, SM. (2005). Influence of elastin on rat small artery mechanical properties. *Experimental Physiology*, **90**, 463-468.

GOTO, K, FUJII, K, KANSUI, Y, ABE, I & IIDA, M. (2002). Critical role of gap junctions in endothelium-dependent hyperpolarization in rat mesenteric arteries. *Clinical and Experimental Pharmacology and Physiology*, **29**, 595-602.

GOTO, K, FUJII, K, ONAKA, U, ABE, I & FUJISHIMA, M. (2000). Renin-angiotensin system blockade improves endothelial dysfunction in hypertension. *Hypertension*, **36**, 575-580.

GRGIC, I, EICHLER, I, HEINAU, P, SI, H, BRAKEMEIER, S, HOYER, J & KOHLER, R. (2005). Selective blockade of the intermediate-conductance Ca2+-activated K+ channel suppresses proliferation of microvascular and macrovascular endothelial cells and angiogenesis in vivo. *Arteriosclerosis, Thrombosis, and Vascular Biology*, **25**, 704-709.

GRIFFITH, TM, CHAYTOR, AT, TAYLOR, HJ, GIDDINGS, BD & EDWARDS, DH. (2002). cAMP facilitates EDHF-type relaxations in conduit arteries by enhancing electrotonic conduction via gap junctions. *Proceedings of the National Academy of Sciences of the United States of America*, **99**, 6392-6397.

HABERMANN, E. (1984). Apamin. *Pharmacology and Therapeutics*, **25**, 255-270.

HARRINGTON, LS, CARRIER, MJ, GALLAGHER, N, GILROY, D, GARLAND, CJ & MITCHELL, JA. (2007). Elucidation of the temporal relationship between endothelial-derived NO and EDHF in mesenteric vessels. *American Journal of Physiology - Heart and Circulatory Physiology*, **293**, H1682-H1688.

HEAGERTY, AM, AALKJAER, C, BUND, SJ, KORSGAARD, N & MULVANY, MJ. (1993). Small artery structure in hypertension. Dual processes of remodeling and growth. *Hypertension*, **21**, 391-397.

HILL, CE, RUMMERY, N, HICKEY, H & SANDOW, SL. (2002). Heterogeneity in the distribution of vascular gap junctions and connexins: implications for function. *Clinical and Experimental Pharmacology and Physiology*, **29**, 620-625.

HONG, T & HILL, CE. (1998). Restricted expression of the gap junctional protein connexin 43 in the arterial system of the rat. *Journal of Anatomy*, **192**, 583-593.

HUANG, PL, HUANG, Z, MASHIMO, H, BLOCH, KD, MOSKOWITZ, MA, BEVAN, JA & FISHMAN, MC. (1995). Hypertension in mice lacking the gene for endothelial nitric oxide synthase. *Nature*, **377**, 239-242.

HUTCHESON, IR, CHAYTOR, AT, EVANS, WH & GRIFFITH, TM. (1999). Nitric oxide independent relaxations to acetylcholine and A23187 involve different routes of

heterocellular communication : role of gap junctions and phospholipase A2. *Circulation Research*, **84**, 53-63.

JAMESON, M, DAI, FX, LUSCHER, T, SKOPEC, J, DIEDERICH, A & DIEDERICH, D. (1993). Endothelium-derived contracting factors in resistance arteries of young spontaneously hypertensive rats before development of overt hypertension. *Hypertension*, **21**, 280-288.

JORDAN, K, CHODOCK, R, HAND, AR & LAIRD, DW. (2001). The origin of annular junctions: A mechanism of gap junction internalization. *Journal of Cell Science*, **114**, 763-773.

KANSUI, Y, FUJII, K, NAKAMURA, K, GOTO, K, ONIKI, H, ABE, I, SHIBATA, Y & IIDA, M. (2004). Angiotensin II receptor blockade corrects altered expression of gap junctions in vascular endothelial cells from hypertensive rats. *American Journal of Physiology - Heart and Circulatory Physiology*, **287**, H216-H224.

KANSUI, Y, GARLAND, CJ & DORA, KA. (2008). Enhanced spontaneous Ca2+ events in endothelial cells reflect signalling through myoendothelial gap junctions in pressurized mesenteric arteries. *Cell Calcium*, **44**, 135-146.

KRISTEK, F & GEROVA, M. (1997). Dynamics of endothelium-muscle cell contacts in the coronary artery of the dog in ontogeny. *Acta Anatomica (Basel)*, **158**, 166-171.

KRUGER, O, PLUM, A, KIM, JS, WINTERHAGER, E, MAXEINER, S, HALLAS, G, KIRCHHOFF, S, TRAUB, O, LAMERS, WH & WILLECKE, K. (2000). Defective vascular development in connexin 45-deficient mice. *Development*, **127**, 4179-4193.

KÜHBERGER, E, GROSCHNER, K, KUKOVETZ, WR & BRUNNER, F. (1994). The role of myoendothelial cell contact in non-nitric oxide-, non-prostanoid-mediated endothelium-dependent relaxation of porcine coronary artery. *British Journal of Pharmacology*, **113**, 1289-1294.

KUMAR, NM & GILULA, NB. (1996). The gap junction communication channel. *Cell*, **84**, 381-388.

LANG, NN, LUKSHA, L, NEWBY, DE & KUBLICKIENE, K. (2007). Connexin 43 mediates endothelium-derived hyperpolarizing factor-induced vasodilatation in subcutaneous resistance arteries from healthy pregnant women. *American Journal of Physiology - Heart and Circulatory Physiology*, **292**, H1026-H1032.

LANG, NN, MYLES, RC, BURTON, FL, HALL, DP, CHIN, YZ, BOON, NA & NEWBY, DE. (2008). The vascular effects of rotigaptide in vivo in man. *Biochemical Pharmacology*, **76**, 1194-1200.

LESSON, TS. (1979). Rat retinal blood vessels. *Canadian Journal of Opthamology*, **14**, 21-28.

LI, J, CAO, YX, LIU, H & XU, CB. (2007). Enhanced G-protein coupled receptors-mediated contraction and reduced endothelium-dependent relaxation in hypertension. *European Journal of Pharmacology*, **557**, 186-194.

LINDER, L, KIOWSKI, W, BUHLER, FR & LUSCHER, TF. (1990). Indirect evidence for release of endothelium-derived relaxing factor in human forearm circulation in vivo. Blunted response in essential hypertension. *Circulation*, **81**, 1762-1767.

LITTLE, TL, BEYER, EC & DULING, BR. (1995a). Cx43 and Cx40 gap junctional proteins are present in arteriolar smooth muscle and endothelium in vivo. *American Journal of Physiology*, **268**, 729-739.

LITTLE, TL, XIA, J & DULING, BR. (1995b). Dye tracers define differential endothelial and smooth muscle coupling patterns within the arteriolar wall. *Circulation Research*, **76**, 498-504.

LUSCHER, T, AARHUS, LL & VANHOUTTE, PM. (1990). Indomethacin improves the impaired endothelium-dependent relaxations in small mesenteric arteries of the spontaneously hypertensive rat. *American Journal of Hypertension*, **3**, 55-58.

LUSCHER, TF. (1990). Imbalance of endothelium-derived relaxing and contracting factors. A new concept in hypertension? *American Journal of Hypertension*, **3**, 317-330.

LUSCHER, TF & VANHOUTTE, PM. (1986). Endothelium-dependent contractions to acetylcholine in the aorta of the spontaneously hypertensive rat. *Hypertension*, **8**, 344-348.

MARRIENCHECK, MC, DAVIS, EC, ZHANG, H, RAMIREZ, F, ROSENBLOOM, J, GIBSON, MA, PARKS, WC & MERCHAM, RP. (1995). Fibrillin-1 and fibrillin-2 show temporal and tissue-specific regulation of expression in developing elastic tissues. *Connective Tissue Research*, **31**, 87-97.

MARTIN, W, FURCHGOTT, RF, VILLANI, GM & JOTHIANANDAN, D. (1986). Depression of contractile responses in rat aorta by spontaneously released endothelium-derived relaxing factor. *Journal of Pharmacology And Experimental Therapeutics*, **237**, 529-538.

MATCHKOV, VV, RAHMAN, A, PENG, H, NILSSON, H & AALKJAER, C. (2004). Junctional and nonjunctional effects of heptanol and glycyrrhetinic acid derivatives in rat mesenteric small arteries. *British Journal of Pharmacology*, **142**, 961-972.

MATHER, S, DORA, KA, SANDOW, SL, WINTER, P & GARLAND, CJ. (2005). Rapid endothelial cell-selective loading of connexin 40 antibody blocks endothelium-derived hyperpolarizing factor dilation in rat small mesenteric arteries. *Circulation Research*, **97**, 399-407.

MATOBA, H, SHIMOKAWA, H, NAKASHIMA, M, HIRAKAWA, Y, MUKAI, Y & HIRANO, K. (2000). Hydrogen peroxide is an endothelium-derived hyperpolarising factor in mice. *Journal of Clinical Investigation*, **106**, 1521-1530.

MAZZINI, MJ & MONAHAN, KM. (2008). Pharmacotherapy for atrial arrhythmias: Present and future. *Heart Rhythm*, **5**, S26-S31.

MONCADA, S, GRYGLEWSKI, R, BUNTING, S & VANE, JR. (1976). An enzyme isolated from arteries transforms prostaglandin endoperoxides to an unstable substance that inhibits platelet aggregation. *Nature*, **263**, 663-665.

MORIKAWA, K, SHIMOKAWA, H, MATOBA, T, KUBOTA, H, AKAIKE, T & TALUKDER, MA. (2003). Pivotal role of Cu,Zn-dismutase in endothelium-dependent hyperpolarisation. *Journal of Clinical Investigation*, **112**, 1871-1879.

MULVANY, MJ, BAANDRUP, U & GUNDERSEN, HJ. (1985). Evidence for hyperplasia in mesenteric resistance vessels of spontaneously hypertensive rats using a three-dimensional disector. *Circulation Research*, **57**, 794-800.

MULVANY, MJ, BAUMBACH, GL, AALKJAER, C, HEAGERTY, AM, KORSGAARD, N, SCHIFFRIN, EL & HEISTAD, DD. (1996). Vascular remodeling. *Hypertension*, **28**, 505-506.

MULVANY, MJ & HALPERN, W. (1977). Contractile properties of small arterial resistance vessels in spontaneously hypertensive and normotensive rats. *Circulation Research*, **41**, 19-26.

NAKAMURA, H. (1995). Electron microscopic study of the prenatal development of the thoracic aorta in the rat. *American Journal of Anatomy*, **181**, 406-418.

NELSON, MT, PATLAK, JB, WORLEY, JF & STANDEN, NB. (1990). Calcium channels, potassium channels and voltage dependence of arterial smooth muscle tone. *American Journal of Physiology*, **259**, 3-18.

NEYLON, CB. (1999). Vascular biology of endothelin signal transduction. *Clinical and Experimental Pharmacology and Physiology*, **26**, 149-153.

NICHOLSON, BJ, WEBER, PA, CAO, F, CHANG, HC, LAMPE, P & GOLDBERG, G. (2000). The molecular basis of selective permeability of connexins is complex and includes both size and charge. *Brazilian Journal of Medical and Biological Research*, **34**, 369-378.

ONAKA, U, FUJII, K, ABE, I & FUJISHIMA, M. (1998). Antihypertensive treatment improves endothelium-dependent hyperpolarization in the mesenteric artery of spontaneously hypertensive rats. *Circulation*, **98**, 175-182.

PALMER, RM, ASHTON, DS & MONCADA, S. (1988a). Vascular endothelial cells synthesize nitric oxide from L-arginine. *Nature*, **333**, 664-666.

PALMER, RMJ, FERRIGE, AG & MONCADA, S. (1987). Nitric oxide release accounts for the biological activity of endothelium-derived relaxing factor. *Nature*, **327**, 524-526.

PALMER, RMJ, REES, DD, ASHTON, DS & MONCADA, S. (1988b). L-arginine is the physiological precursor for the formation of nitric oxide in endothelium-dependent relaxation. *Biochemical and Biophysical Research Communications*, **153**, 1251-1256.

PANZA, JA, QUYYUMI, AA, BRUSH, JE & EPSTEIN, SE. (1990). Abnormal endothelium-dependent vascular relaxation in patients with essential hypertension. *New England Journal of Medicine*, **323**, 22-27.

PEACH, MJ, SINGER, HA, IZZO, NR & LOEB, AL. (1987). Role of calcium in endothelium-dependent relaxation of arterial smooth muscle. *American Journal of Cardiology*, **59**, 35-43.

QIU, HY, VALTIER, B, STRUYKER-BOUDIER, HAJ & LEVY, BI. (1995). Mechanical and contractile properties of in situ localized mesenteric arteries in normotensive and spontaneously hypertensive rats. *Journal of Pharmacological and Toxicological Methods*, **33**, 159-170.

QUIGNARD, JF, FÉLÉTOU, M, THOLLON, C, VILAINE, JP, DUHAULT, J & VANHOUTTE, PM. (1999). Potassium ions and endothelium-derived hyperpolarizing factor in guinea-pig carotid and porcine coronary arteries. *British Journal of Pharmacology*, **127**, 27-34.

RAMOS-VARA, JA. (2005). Technical aspects of immunohistochemistry. *Vetinary Pathology*, **42**, 405-426.

RAPOPORT, RM & WILLIAMS, SP. (1996). Role of prostaglandins in acetylcholine-induced contraction of aorta from spontaneously hypertensive and Wistar-Kyoto rats. *Hypertension*, **28**, 64-75.

RAPPORT, RM & MURAD, F. (1983). Agonist-induced endothelium-dependent relaxation may be mediated through cyclic GMP. *Circulation Research*, **52**, 352-357.

REAUME, AG, DE SOUSA, PA, KULKARNI, S, LANGILLE, BL, ZHU, D, DAVIES, TC, JUNGA, SC, KIDDER, GM & ROSSANT, J. (1995). Cardiac malformation in neonatal mice lacking connexin43. *Science*, **267**, 1831-1834.

REES, DD, PALMER, RM, SCHULZ, R, HODSON, HF & MONCADA, S. (1990). Characterization of three inhibitors of endothelial nitric oxide synthase in vitro and in vivo. *British Journal of Pharmacology*, **101**, 746-752.

REES, DD, PALMER, RM, HODSON, HF & MONCADA, S. (1989). A specific inhibitor of nitric oxide formation from L-arginine attenuates endothelium-dependent relaxation. *British Journal of Pharmacology*, **96**, 418-424.

RUMMERY, NM & HILL, CE. (2004). Vascular gap junctions and implications for hypertension. *Clinical and Experimental Pharmacology and Physiology*, **31**, 659-667.

RUMMERY, NM & HILL, CE. (2009). Vascular gap junctions and implications for hypertension. *Clinical and Experimental Pharmacology and Physiology*, **31**, 659-667.

SANDOW, SL, GZIK, DJ & LEE, R. (2009). Arterial internal elastic lamina holes: relationship to function? *Journal of Anatomy*, **214**, 258-266.

SANDOW, SL, NEYLON, CB, CHEN, MX & GARLAND, CJ. (2006). Spatial separation of endothelial small- and intermediate-conductance calcium-activated potassium channels ($K_{Ca}$) and connexins:possible relationship to vasodilator function? *Journal of Anatomy*, **209**, 689-698.

SANDOW, SL, GOTO, K, RUMMERY, NM & HILL, CE. (2004). Developmental changes in myoendothelial gap junction mediated vasodilator activity in the rat saphenous artery. *The Journal of Physiology*, **556**, 875-886.

SANDOW, SL, LOOFT-WILSON, R, DORAN, B, GRAYSON, TH, SEGAL, SS & HILL, CE. (2003). Expression of homocellular and heterocellular gap junctions in hamster arterioles and feed arteries. *Cardiovascular Research*, **60**, 643-653.

SANDOW, SL, TARE, M, COLEMAN, HA, HILL, CE & PARKINGTON, HC. (2002). Involvement of myoendothelial gap junctions in the actions of endothelium-derived hyperpolarizing factor. *Circulation Research*, **90**, 1108-1113.

SANKARANARAYANAN, A, RAMAN, G, BUSCH, C, SCHULTZ, T, ZIMIN, PI, HOYER, J, KOHLER, R & WULFF, H. (2009). Naphtho[1,2-d]thiazol-2-ylamine (SKA-31), a new activator of KCa2 and KCa3.1 potassium channels, potentiates the endothelium-derived hyperpolarizing factor response and lowers blood pressure. *Molecular Pharmacology*, **75**, 281-295.

SEGRETAIN, D & FALK, MM. (2004). Regulation of connexin biosynthesis, assembly, gap junction formation, and removal. *Biochimica et Biophysica Acta (BBA) - Biomembranes*, **1662**, 3-21.

SHIMOKAWA, H, YASUTAKE, H, FUJII, K, OWADA, MK, NAKAIKE, R, FUKUMOTO, Y, TAKAYANAGI, T, NAGAO, T, EGASHIRA, K, FUJISHIMA, M & TAKESHITA, A. (1996a). The Importance of the hyperpolarizing mechanism increases as the vessel size decreases in endothelium-dependent relaxations in rat mesenteric circulation. *Journal of Cardiovascular Pharmacology*, **28**.

SHIMOKAWA, H, YASUTAKE, H, FUJII, K, OWADA, MK, NAKAIKE, R, FUKUMOTO, Y, TAKAYANAGI, T, NAGAO, T, EGASHIRA, K, FUJISHIMA, M & TAKESHITA, A. (1996b). The importance of the hyperpolarizing mechanism increases as the vessel size decreases in endothelium-dependent relaxations in rat mesenteric circulation. *Journal of Cardiovascular Pharmacology*, **28**.

SI, H, HEYKEN, WT, WOLFLE, SE, TYSAIC, M, SCHUBERT, R, GRIGIC, I, VILIANOVICH, L, GIEBING, G, MAIER, T, GROSS, V, BADER, M, DE WIT, C, HOYER, J & KOHLER, R. (2006). Impaired endothelium derived hyperpolarising factor-mediated dilations and increased blood pressure in mice deficient of the intermediate-conductance $Ca^{2+}$-activated $K^+$ channel. *Circulation Research*, **99**, 537-544.

SOKOYA, EM, BURNS, AR, SETIAWAN, CT, COLEMAN, HA, PARKINGTON, HC & TARE, M. (2006). Evidence for the involvement of myoendothelial gap junctions in EDHF-mediated relaxation in the rat middle cerebral artery. *American Journal of Physiology - Heart and Circulatory Physiology*, **291**, H385-H393.

SPAGNOLI, LG, VILLASCHI, S, NERI, L & PALMIERI, G. (1982). Gap junctions in myo-endothelial bridges of rabbit carotid arteries . *Cellular and Molecular Life Sciences*, **38**, 124-125.

STANDEN, NB, QUAYLE, JM, DAVIS, NW, BRAYDEN, JE, HUANG, Y & NELSON, TM. (1989). Hyperpolarising vasodilators activate ATP-sensitive $K^+$ channels in arterial smooth muscle. *Science*, **245**, 177-180.

TAKANO, H, DORA, KA, SPITALER, MM & GARLAND, CJ. (2004). Spreading dilatation in rat mesenteric arteries associated with calcium-independent endothelial cell hyperpolarization. *The Journal of Physiology*, **556**, 887-903.

TAKATA, Y & KATO, H. (1995). Adrenoceptors in SHR: Alterations in binding characteristics and intracellular signal transduction pathways. *Life Sciences*, **58**, 91-106.

TANG, EHC & VANHOUTTE, PM. (2008). Gap junction inhibitors reduce endothelium-dependent contractions in the aorta of spontaneously hypertensive rats. *Journal of Pharmacology And Experimental Therapeutics*, **327**, 148-153.

TARE, M, PARKINGTON, HC, COLEMAN, HA, NEILD, TO & DUSTING, GJ. (1990). Hyperpolarisation and relaxation of arterial smooth muscle caused by nitric oxide derived from the endothelium. *Nature*, **346**, 69-71.

TAUGNER, R, KIRCHHEIM, H & FORSSMANN, WG. (1984). Myoendothelial contacts in glomerular arterioles and in renal interlobular arteries of rat, mouse and Tupaia belangeri. *Cell Tissue Research*, **253**, 319-325.

TAYLOR, HJ, CHAYTOR, AT & EVANS, WH. (1998). Inhibition of the gap junctional component of endothelium-dependent relaxations in rabbit iliac artery by 18-glycyrrhetinic acid. *British Journal of Pharmacology*, **125**, 1-3.

TAYLOR, MS, BONEV, AD, GROSS, TP, ECKMAN, DM, BRAYDEN, JE, BOND, CT, ADELMAN, JP & NELSON, MT. (2003). Altered expression of small-conductance $Ca^{2+}$-activated $K^{+}$ (SK3) channels modulates arterial tone and blood pressure. *Circulation Research*, **93**, 124-131.

TAYLOR, SG & WESTON, AH. (1988). Endothelium-derived hyperpolarizing factor: a new endogenous inhibitor from the vascular endothelium. *Trends in Pharmacological Sciences*, **9**, 272-274.

THOMA, R. (1921) *Virchows Arch path Anat*, **230**, 1.

TREASURE, CB, MANOUKIAN, SV, KLEIN, JL, VITA, JA, NABEL, EG, RENWICK, GH, SELWYN, AP, ALEXANDER, RW & GANZ, P. (1992). Epicardial coronary artery responses to acetylcholine are impaired in hypertensive patients. *Circulation Research*, **71**, 776-781.

VANHOUTTE, PM. (1996). Endothelial dysfunction in hypertension. *Journal of Hypertension*, **14**, 583-593.

VANHOUTTE, PM, FELETOU, M & TADDEI, S. (2005). Endothelium-dependent contractions in hypertension. *British Journal of Pharmacology*, **144**, 449-458.

VANHOUTTE, PM & TANG, EHC. (2008). Endothelium-dependent contractions: when a good guy turns bad! *The Journal of Physiology*, **586**, 5295-5304.

WALDRON, GJ & GARLAND, CJ. (1994). Contribution of both nitric oxide and a change in membrane potential to acetylcholine-induced relaxation in the rat small mesenteric artery. *British Journal of Pharmacology*, **112**, 831-836.

WANG, ZH, SHEN, B, YAO, HL, JIA, YC, REN, J, FENG, YJ & WANG, YZ. (2007). Blockage of intermediate-conductance-Ca2+-activated K+ channels inhibits progression of human endometrial cancer. *Oncogene*, **26**, 5107-5114.

WILLETTE, RN, BAO, W, NERURKAR, S, YUE, TL, DOE, CP, STANKUS, G, TURNER, GH, JU, H, THOMAS, H, FISHMAN, CE, SULPIZIO, A, BEHM, DJ, HOFFMAN, S, LIN,

Z, LOZINSKAYA, I, CASILLAS, LN, LIN, M, TROUT, REL, VOTTA, BJ, THORNELOE, K, LASHINGER, ESR, FIGUEROA, DJ, MARQUIS, R & XU, X. (2008). Systemic activation of the transient receptor potential vanilloid subtype 4 channel causes endothelial failure and circulatory collapse: Part 2. *Journal of Pharmacology And Experimental Therapeutics*, **326**, 443-452.

WONG, LCY & LANGILLE, BL. (1996). Developmental remodeling of the internal elastic lamina of rabbit arteries : effect of blood flow. *Circulation Research*, **78**, 799-805.

WULFF, H, MILLER, MJ, HANSEL, W, GRISSMER, S, CAHALAN, MD & CHANDY, KG. (2000). Design of a potent and selective inhibitor of the intermediate conductance Ca2+-activated K+ channel, IKCa1: a potential immunosuppressant. *Proceedings of the National Academy of Sciences of the United States of America*, **97**, 8151-8156.

YEH, HI, ROTHERY, S, DUPONT, E, COPPEN, SR & SEVERS, NJ. (1998). Individual gap junction plaques contain multiple connexins in arterial endothelium. *Circulation Research*, **83**, 1248-1263.

ZHANG, DX, MENDOZA, SA, BUBOLZ, AH, MIZUNO, A, GE, ZD, LI, R, WARLTIER, DC, SUZUKI, M & GUTTERMAN, DD. (2009). Transient receptor potential vanilloid type 4-deficient mice exhibit impaired endothelium-dependent relaxation induced by acetylcholine in vitro and in vivo. *Hypertension*, **53**, 532-538.

ZIMMERMANN, K, HEIN, A, HAGER, U, KACZMAREK, JS, TURNQUIST, BP, CLAPHAM, DE & REEH, PW. (2009). Phenotyping sensory nerve endings in vitro in the mouse. *Nature Protocols*, **4**, 174-196.

ZYGMUNT, PM, EDWARDS, G, WESTON, AH & DAVIS, SC. (1996). Effects of cytochrome P450 inhibitors on EDHF-mediated relaxation in the rat hepatic artery. *British Journal of Pharmacology*, **1180**, 1147-1152.